A WATERSHED INFORMATION SYSTEM

by

Anton G. Thomsen and William D. Striffler

Colorado Water

Resources Research Institute

Completion Report No. 100

Colorado State University

A WATERSHED INFORMATION SYSTEM

Completion Report
OWRT Project No. B-160-COLO
Part II

by

Anton G. Thomsen

and

William D. Striffler

Department of Earth Resources
Colorado State University
Fort Collins, Colorado 80523

Submitted to

Office of Water Research and Technology
U. S. Department of Interior
Washington, D. C. 20240

September 1980

COLORADO WATER RESOURCES RESEARCH INSTITUTE
Colorado State University
Fort Collins, Colorado

Norman A. Evans, Director

A WATERSHED INFORMATION SYSTEM

ABSTRACT

Planning the efficient use of water in the western states requires accurate timely information on available suppplies. In states such as Colorado, where much of the water originates from melting snowpack, snowmelt runoff forecasts become extremely important in planning seasonal water use. This report presents a watershed information system which simulates snowpack processes and utilizes remote sensing data to provide periodic updates in the simulation processes.

A watershed information system for the analysis and simulation of mountain watersheds is described. Watershed information on topography, vegetation and soils in digital terrain models (overlays) serve as the data base for watershed analysis, classification of snow in Landsat imagery and automatic generation of parameter decks for operating distributed simulation models of snowcover dynamics and streamflow generation. The computer programs that generate the parameter decks have built-in calibration options for all major processes, that permit fast model calibration from an interactive computer terminal, on watersheds with varying characteristics.

Snow processes are simulated within square (5.76 ha) grid-cell elements. The hydrograph resulting from spring snowmelt is simulated by a lateral flow model of streamflow generation driven by the simulated spatially distributed input (snowmelt and rain).

Options are available for simulating the effects of forest management alternatives (thinning, clearcutting) on selected forest stands.

Line printer generated map overlays showing simulated snowcover parameters (depth, temperature) as well as the moisture content of the rooting zone, can be produced for any date between April 1 and July 31.

Snow course measurements and Landsat imagery are used for simulation update. These options are especially important for the simulation of snow-cover in blowing snow environments (alpine, prairie) and in areas with limited data for driving simulated models.

Examples of ouput from subsystems are included to illustrate the capabilities of the information system.

TABLE OF CONTENTS

TABLE OF CONTENTS
(continued)

TABLE OF CONTENTS
(continued)

LIST OF FIGURES

LIST OF FIGURES
(Continued)

LIST OF FIGURES
(Continued)

LIST OF TABLES

LIST OF TABLES
(continued)

I. INTRODUCTION

The central Rocky Mountains form the headwaters of four major river basins of the western United States. Rising to elevations over 4,600 meters the mountains form natural barriers to weather circulation patterns, causing air masses to rise, cool and precipitate over the mountains. Winter precipitation over the mountains accumulates in deep snowpacks and only become available for use during the summer snowmelt season. In Colorado, well over half the states water originates from the snow zone. Although water supplies in Colorado are generally adequate at present, increasing demands from irrigators, municipalities and energy developments are expected to result in shortages in the near future. The efficient use and management of the water resources will, therefore, receive increasing emphasis in the years to come.

Perhaps the most important requirement for water resource management is timely accurate information on expected water supplies. In Colorado and the western states, resource decisions are based on stream flow forecasts for mountain snow zone watersheds.

Several approaches have been tried for making snowmelt runoff forecasts. The traditional approach, developing a statistical relationship between seasonal runoff volumes and index snow courses, does not give information on timing of flows and is subject to error if late season precipitation occurs. A more recent approach is to simulate snowpack dynamics using computer simulation models. The potential advantages of this approach include (1) simulation of the physical processes occurring in the snowpack permit snowpack status and melt to be calculated on a daily basis, and (2) the simulation or forecast can be updated or modified upon the recenipt of new information.

The simulation of snowmelt runoff from high mountain watersheds has traditionally suffered from a number of serious deficiencies. These include (1) a lack of basic data to drive the model and (2) a lack of information on the spatial variation of input data and resulting processes. These problems relate to the physical characteristics of mountain snow zone watersheds.

Similarly, the same watershed characteristics which cause such diversity in processes, also tends to limit data collection from mountain watersheds. Rugged topography and deep snowpacks limit access to mountain watersheds. In addition, broad areas within the mountains have been designed as National Parks and wilderness area, with access limited and permanent measurement installation prohibited. As a result, measurement of snowpack and climatic parameters wit-in the mountains are not sufficient to characterize spatial variations or even average conditions within a watershed.

This study was designed to investigate alternatives to traditional snowmelt forecasts. In particular, the study presents a watershed information system designed to present spatially variable watershed data, to simulate snowmelt and runoff processes on a spatial basis and to utilize remote sensing data; specifically Landsat, as a nontraditional means of providing current information to the simulation process.

Objectives

The primary objective of this study has been to investigate potential application of remote sensing methods in determining hydrologic operating parameters of remote mountain watersheds. The approach taken was (1) to review remote sensing systems and potential applications in hydrology and (2) to develop a watershed simulation model which utilized traditional data sources plus available remote sensing data as a means of improving simulation results.

Specific objectives are:

1. To review existing remote sensing sensors and systems with reference to potential applications in hydrology.

2. To develop a watershed simulation model which utilizes remote sensing data, in addition to traditional data sources, for simulating snowmelt runoff from remote mountain watersheds.

This Report

This report is presented in two parts. Part I presents a review of remote sensing applications in hydrology. Included are sections on the physics of remote sensing and capabilities of existing remote sensing systems and sensors.

Part II presents a Watershed Information System which utilizes a spatial data system, spatial simulation of snowmelt and runoff processes, and application of remote sensing data as a direct input into the simulation model. The model was developed and tested in the Williams Fork Watershed in central Colorado.

II. STUDY AREA

The Williams Fork Watershed

The Williams Fork Watershed was selected as a suitable study area (Fig. 2.1) since it was considered to be representative of high mountain watersheds in Colorado. Results obtained here should be applicable to similar watersheds within the region with few or no changes to the models. The Williams Fork River is a tributary to the Colorado River at Parshall, Colorado.

The Williams Fork Watershed, above Williams Fork Reservoir, covers 476 km^2 and ranges in elevation from 2,380 m at the reservoir to 4,131 m at the highest point on the Continental Divide (Pettinger Peak). Vegetation types range from irrigated meadows at the lower elevation to almost barren alpine areas along the Divide. Between these extremes is a cover-type transition with elevation through sagebrush, lodgepole pine and spruce-fir. Aspen is frequently present in small stands or mixed with other vegetation types except for the highest elevation.

Monthly mean temperatures at the lowest elevations range from -11°C in January to 17°C in July. At the highest elevations temperatures for the same months range from -12°C to 10°C.

Mean annual precipitation ranges from approximately 400 mm (at Parshall) to 800 mm in the alpine region.

Soils information used in this study was determined from a broad soils/vegetation map and, therefore, of extensive nature. Only soil water characteristics were of interest for this study. Soils are deepest (>200 cm) on the flood plains becoming shallow (50 cm) as slopes increase to very shallow on alpine rock outcrops.

Due to water diversions for industrial (AMAX Henderson Mine) and agricultural uses and lack of data on vegetation and soils for areas outside the Araphaho National Forest only the upper half (231 km^2) of the Williams Fork Watershed was considered for study.

The Data Base

In the following section watershed parameters and driving variables for watershed simulation and their sources will be discussed.

Figure 2.1. Map Segment Showing the Williams Fork Study Area.
Map Scale 1:250,000.

Continuous records of temperature and precipitation within the study area were not available. Therefore, the station[1] at Berthoud Pass was selected as the best base station for simulation.

Mean monthly temperatures from stations at Hot Sulphur Springs (7,800 ft)[2], Amax Camp (8,550 ft)[3] and Berthoud Pass (11,314 ft) for the years 1969 through 1976 were used to establish monthly lapse rates for the area. The calculated lapse rates are shown in Table 2.1.

Table 2.1. Monthly Temperature Lapse Rates (^{o}F/100 ft) Calculated for the Williams Fork Watershed and Vicinity.

Month	Elevation (Feet)						
	13,500	12,500	11,500	10,500	9,500	8,500	7,500
Jan.	0.1	0.2	0.3	0.4	0.6	1.0	1.8
Feb.	0.1	0.2	0.3	0.6	1.2	2.0	3.0
Mar.	0.3	0.4	0.5	0.9	1.9	3.2	4.8
Apr.	0.5	0.8	1.2	1.6	3.0	5.5	6.0
May	0.6	0.8	1.2	1.6	3.0	5.5	6.1
June	0.7	0.9	1.4	1.8	3.0	5.5	6.2
July	0.5	0.6	1.0	1.6	3.0	5.5	6.1
Aug.	0.5	0.6	0.8	1.5	3.0	5.5	6.1
Sept.	0.3	0.5	0.8	1.5	2.9	5.0	5.5
Oct.	0.3	0.5	0.8	1.4	2.6	5.0	5.3
Nov.	0.1	0.2	0.3	0.6	1.8	3.2	3.6
Dec.	0.1	0.2	0.3	0.4	0.6	1.0	1.8

An attempt was made to establish a similar relationship between precipitation and elevation, but calculated precipitation for higher elevations were obviously too high, and the relationship had to be found experimentally during model calibration.

[1]Q-12 Park, Forest Service Avalanche Station (Judson, 1977).

[2]English units used when data are to be used with non-metric simulation models.

[3]Data made available by the Amax Corporation.

Potential Evapotranspiration

Potential evapotranspiration (PET) was calculated using a revised version of the Jensen-Haise equation as suggested by Wymore (1974):

$$\text{PET (Summer)} = (.014T - \text{INTERCEPT1})\text{RAD}$$

$$\text{PET (Winter)} = (.006T + \text{INTERCEPT2})\text{RAD}$$

where:

PET = Daily potential evapotranspiration for month

INTERCEPT = Intercept value (Table 2.2)

RAD = Potential solar radiation converted to inches

of evaporation equivalent

T = Mean monthly temperature

Table 2.2. Summer and Winter Intercept Values for the Modified Jensen-Haise Equation.

Elevation (Feet)	Intercept 1 (Summer)	Intercept 2 (Winter)
13,500	0.41	0.09
12,500	0.40	0.08
11,500	0.39	0.07
10,500	0.38	0.06
9,500	0.37	0.05
8,500	0.36	0.04
7,500	0.35	0.03

Monthly mean temperatures used in potential ET calculations are shown in Table 2.3. Potential solar beam radiation was obtained from tables (Frank and Lee, 1966) and converted to inches of evaporation equivalent (1 Langley = 0.000673 inches). Table 2.4 shows the calculated monthly potential ET using the summer equation for months with mean temperatures exceeding $40^\circ F$. In Figure 2.2 calculated potential ET is compared to observed Class A pan evaporation for stations at Climax and Grand Lake.

Table 2.3. Monthly Mean Temperatures[1] Used in Potential Evapotranspiration Calculations

Month	Elevation (Feet)						
	13,500	12,500	11,500	10,500	9,500	8,500	7,500
Jan.	9.7	9.8	10.0	10.4	10.9	11.7	13.1
Feb.	10.6	10.8	11.0	11.5	12.4	14.0	16.5
Mar.	16.2	16.1	17.0	17.7	19.1	21.7	25.7
Apr.	22.4	23.0	24.0	25.4	27.7	32.0	37.7
May	32.4	33.0	34.0	35.4	37.7	43.0	47.8
June	41.1	41.9	43.0	44.6	47.0	51.3	57.1
July	49.7	50.2	51.0	52.3	54.6	58.9	64.7
Aug.	47.8	48.3	49.0	50.2	52.4	56.7	62.5
Sept.	40.0	40.4	41.0	42.2	44.4	48.3	53.6
Oct.	31.0	31.4	32.0	33.1	35.1	38.9	44.1
Nov.	19.6	19.8	20.0	20.5	21.7	24.2	27.6
Dec.	11.6	11.8	12.0	12.4	12.9	13.8	15.5

[1]Calculated using lapse rates presented in Table 2.1 and monthly mean temperatures for Berthoud Pass.

Table 2.4. Calculated Monthly Potential Evapotranspiration in Inches[1]

Month	Elevation (Feet)						
	13,500	12,500	11,500	10,500	9,500	8,500	7,500
Jan.	0.00	0.00	0.00	0.02	0.12	0.23	0.38
Fbe.	0.00	0.00	0.00	0.09	0.23	0.42	0.66
Mar.	0.10	0.27	0.45	0.64	0.90	1.82	1.73
Apr.	0.76	0.99	1.27	1.58	1.99	2.60	3.87
May	2.09	2.38	2.70	3.07	3.55	4.59	6.43
June	3.37	3.81	4.32	5.15	5.88	7.31	9.17
July	5.94	6.29	6.73	7.32	8.19	9.65	11.54
Aug.	5.14	5.48	5.87	6.40	7.21	8.61	10.42
Sept.	2.25	2.48	2.76	3.16	3.77	4.74	6.01
Oct.	1.16	1.31	1.47	1.68	1.94	2.34	3.23
Nov.	0.23	0.33	0.42	0.53	0.67	0.88	1.14
Dec.	0.00	0.00	0.01	0.10	0.20	0.30	0.45
Total	21.0	23.3	26.0	29.7	34.7	43.5	55.0

[1]These seemingly high potential ET values are calculated assuming potential incoming solar radiation(clear skies). In the simulation model (Leaf and Brink, 1973) the values shown here are adjusted for available radiation before being used in evapotranspiration calculations.

Vegetation and Soils

Information on vegetation and soils was obtained from the Routt National Forest, Steamboat Springs, Colorado. Soil types were related to broad vegetation types. The data obtained were in the form of a vegetation/soils map with an interpretation key. Only texture information was available for the seven soil types present in the study area and soil-moisture data were estimated from this information (Table 2.5).

Table 2.5. Soil Moisture Data for Rooting Zone Estimated from Soil Texture Information.

Soil Type ID Number	Name	Field Capacity (Inches)	Wilting Point (Inches)
21	Rubel Land	3.9	1,3
24	Histic Crysquolls	4.2	1.4
38	Leighcan Gravelly Sandy Loam	5.3	1.7
39	Cebone Loam	3.0	1.0
43	Leighcan Bouldery Sandy Loam	4.6	1.5
53	Cryorthents-to-rock Outcrop Complex	4.6	1,5

Streamflow

Streamflow measurements were available for a number of stream gages within the study area (Fig. 2.1). Discharge data from the gage on the Williams Fork near Leal (USGS Gage No. 0903600) was used most frequently when the total area was simulated. This station, however, is influenced by upstream diversion through the August P. Gumlick Tunnel and the gaged discharge had to be adjusted for the amount of diverted water.

Two smaller individually gaged watersheds, without upstream diversion, were used in model validation; the South Fork of the Williams Fork Watershed (USGS Gage No. 09035900) and Darling Creek (USGS Gage No. 09035800).

Snow Courses

Measurements were available for two low elevation snow courses within the study area (Fig. 2.1); Glen Mar Ranch and Middle Fork Campground. In addition, measurements from two higher elevation snow courses (Jones Pass and Berthoud Pass Summit) outside the area were used in simulation update (USDA, SCS Snow Survey, 1970-1976).

Pan Evaporation (Inches)
(May-October)
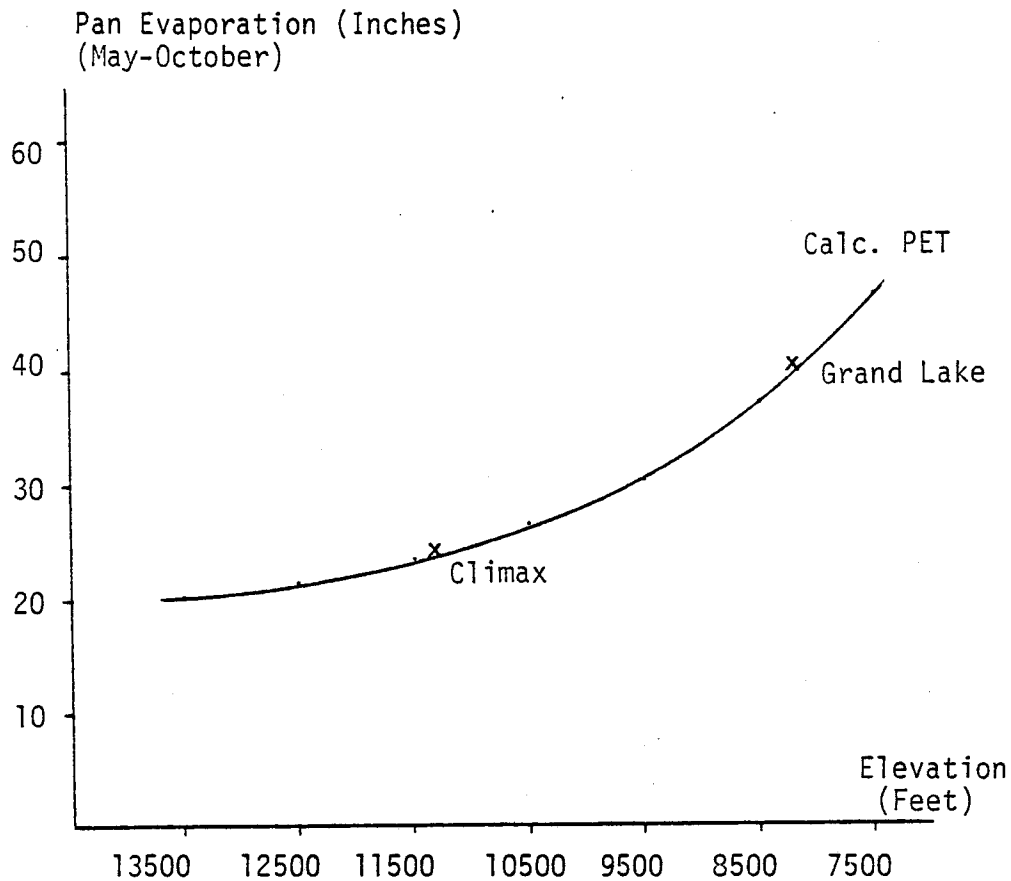
Figure 2.2. Calculated Potential Evapotranspiration and Observed Class A Pan Evaporation for Stations at Climax and Grand Lake. Period: May - October

III. DIGITAL TERRAIN MODELS

Digital Terrain Models

A spatial or grid approach to the simulation of watershed parameters has several advantages. Foyster (1973) states that a grid approach facilitates data storage, retrieval and processing because each square is defined by a pair of Cartesian coordinates. Other important advantages are the possibility of using remotely sensed digital data as input to the simulation and developing computer programs for data analysis and automatic generation of parameter decks for model operation.

Spatial watershed simulation requires an extensive data base with digitized watershed parameters. Several techniques for converting map data to digital form are available (Amidon, 1978). Manual methods are less costly than automated systems if the amount of data is limited. If large areas are to be digitized automated systems are often competitive.

This chapter describes an all-manual system for the digitization of map data. A manual approach was selected because the amount of data was limited and several persons were involved in the process. The system developed required no prior experience with digitization.

Digitization Watershed Information

In this study, a square grid technique was selected as the most efficient for registering and coding spatial data. A 5.76 ha square grid cell (pixel) was selected as a convenient size. This corresponds to a 1 x 1 cm square on a 1:24,000 USGS 7.5 minute series topographic map. The 5.76 ha pixel also represents a compromise between digitization and computing time, and map resolution. Increasing the cell size decreases the time required for digitization and computation but also decreases the spatial resolution. Although a 5.76 ha pixel was used in this study, any convenient size could be used.

The procedure for digitizing the maps was first to draw a grid of "macrocells" on the base maps. Macrocells consist of grid squares containing 10 x 10 or 100 microcells (Figure 3.1). In this study it was found somewhat more convenient to photographically adjust map scales to a standard 1:24,000 corresponding to the USGS 7.5 minute quadrangles. It should also be possible to adjust macrocell and pixel sizes to correspond to a different scale. The important point is that macrocells on one map should cover the identical terrain on other maps.
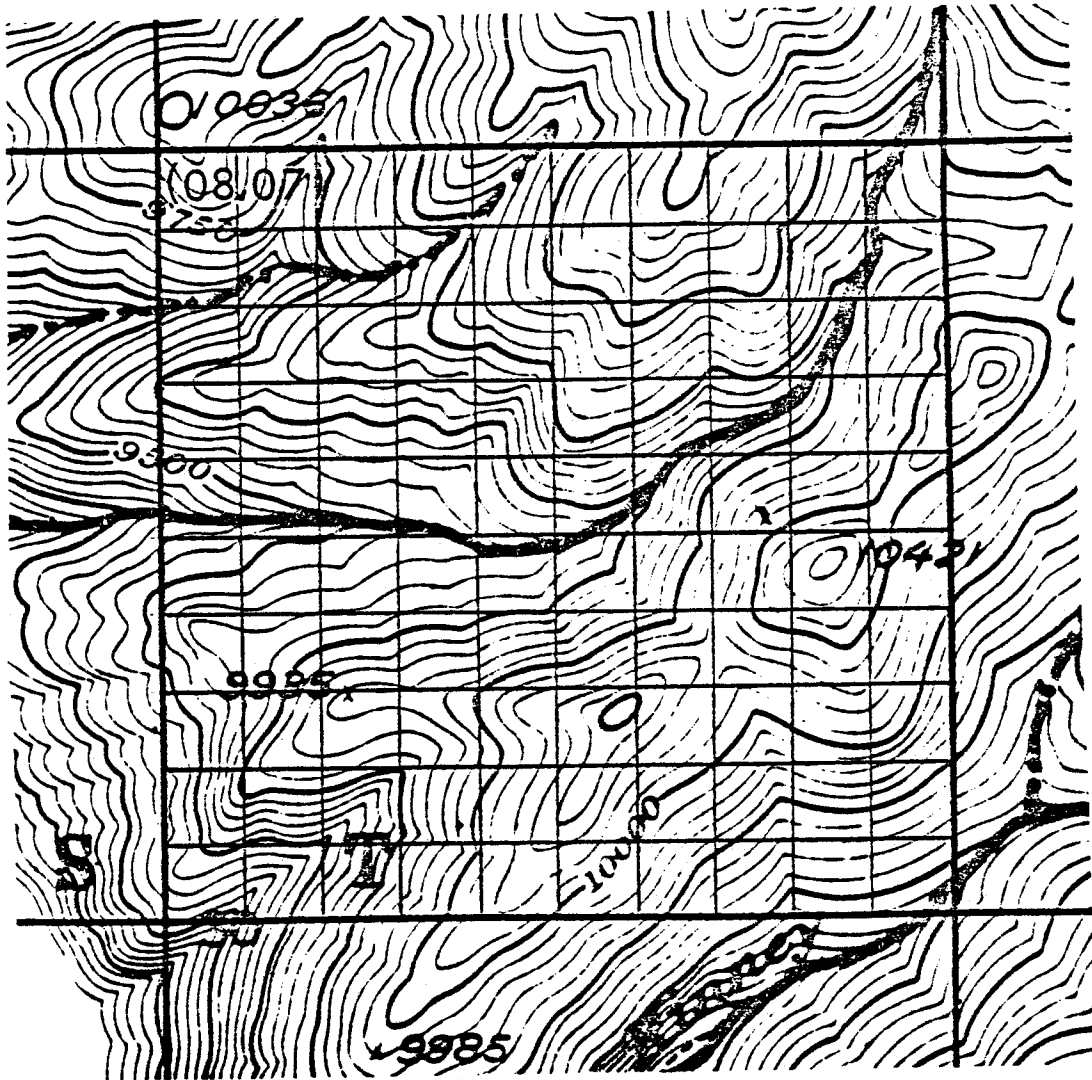
Figure 3.1. Macrocell with 100 5.76 ha Microcells.
Each Microcell is 1 x 1 cm square
Map Scale 1:24,000.

Once the macrocells are drawn on the maps, a mylar transparency with the 100 microcells is overlain on the macrocell and the watershed data is read from each microcell. Data can be recorded as either a point value such as elevation, read from the center of the pixel, or a mean value, such as aspect, representing the average aspect of the pixel. Watershed information was first recorded on coding forms and then punched onto computer cards.

Creation of Watershed Overlays

A computer program (INGRID) was developed to create digital terrain models or overlays from the digitized watershed information. The macrocell data were arranged spatially according to their coordinate number (line, column) and can be read into the computer in any order. Program INGRID prints the coded data as they are read in (Table 3.1) for convenient data editing. After editing overlays are stored as permanent computer files.

In most instances, the overlays created are digital representations of the data input. For example, elevation, aspect, vegetation type, etc. However, it is also possible to generate additional overlays. For example, program SOILDAT uses the previously created soil type overlay and known soil-water data (Table 2.5) to create digital overlays of field capacity, wilting point, and soil moisture levels. Another program (IDNUMBR) creates the watershed ID overlay.

Table 3.2 summarizes the spatial watershed information and the resulting overlays created and used in this study.

Display of Overlays

Digital watershed overlays can be accessed for analysis and display in either tabular, histogram or map-life form. Examples of tabulated and histogrammed output will be given in later chapters and only a program for gray-mapping watershed overlays will be discussed here.

Gray Maps of Watershed Overlays

Computer program GRTONES was developed for the display of watershed overlays as gray maps on a standard line printer. Overlays are displayed with a maximum eight gray levels, as specified by the user. The generated maps are scaled to overlay a watershed base map with an approximately scale of 1:75,000. Figures 3.2 to 3.5 show examples of watershed overlays in gray-mapped form.

Table 3.1. Output from Program INGRID

PRINTOUT OF ORIGINAL DATA AND PREPROCESSED DATA FOR CHECKING

14

Table 3.2, Creation of Watershed Overlays with Grid Cell Data

Input	Program	Output
Grid Cell Data on Punched Cards		11 Overlays with Grid Cell Data
1. Watershed ID's[1]	INGRID	IDNUMBR
2. Elevation		ELEVAT
3. Aspect		ASPECT
4. Slope		SLOPE
5. Vegetation Type		VEGTYPE
6. Vegetation Density		VEGDENS
7. Soil Type		SOILTYP
8. Dist. to Stream[2]		DSTREAM
9. Field Capacity[3]		FIELDC
10. Wilting Point[3]		WILTPT
11. Soil Moisture[3]		SOILML

[1] Overlay IDNUMBR created by program IDBUMBR.

[2] Overlay DSTREAM used by lateral flow model LATFLOW.

[3] Overlays with soil moisture information created by program SOILDAT.
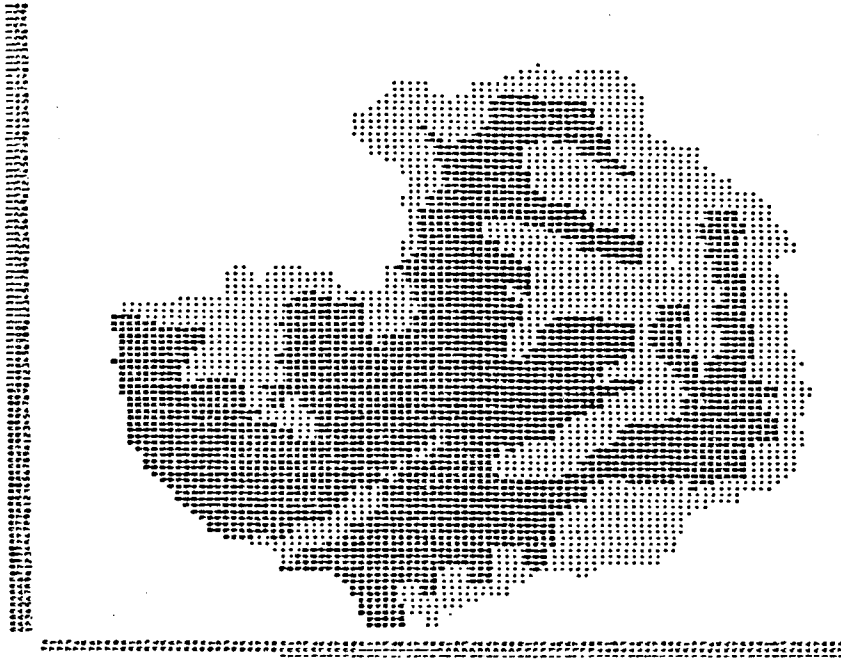
Figure 3.3. Vegetation types in the Williams Fork Watershed (Five classes)
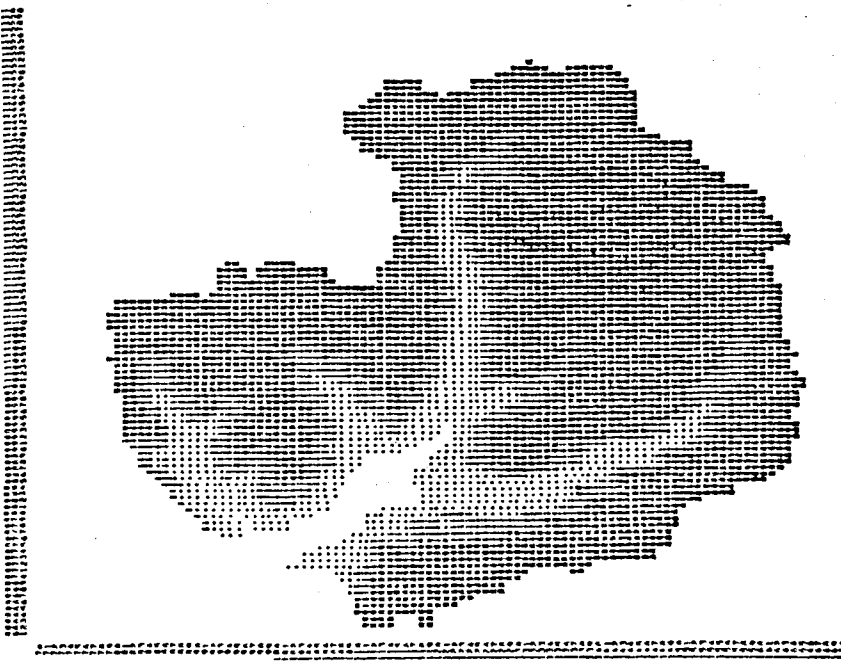
Figure 3.2. Gray Map Showing the Distribution of Elevations within the Williams Fork Watershed (eight classes from 8500 to 12,500 feet).
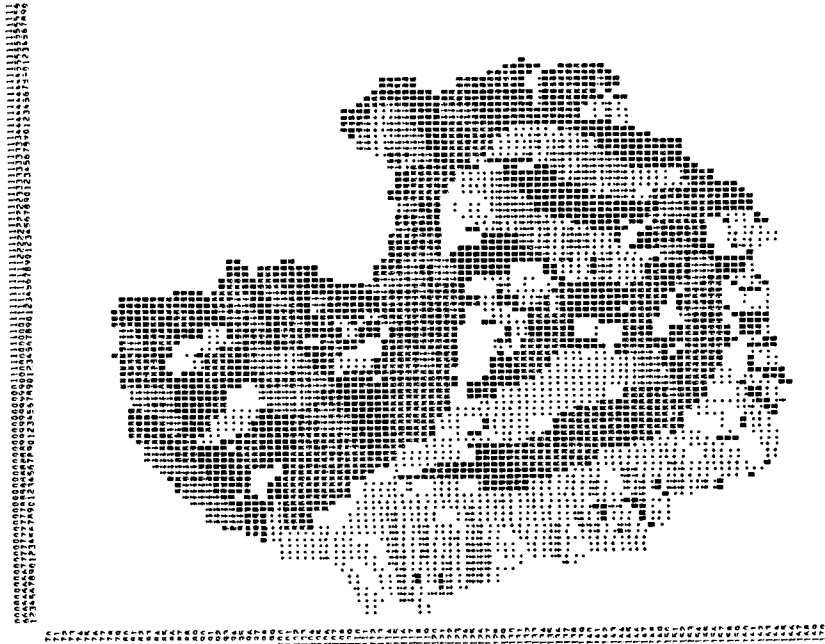
Figure 3.5. Gray Map of Aspect.
Compass Octants.
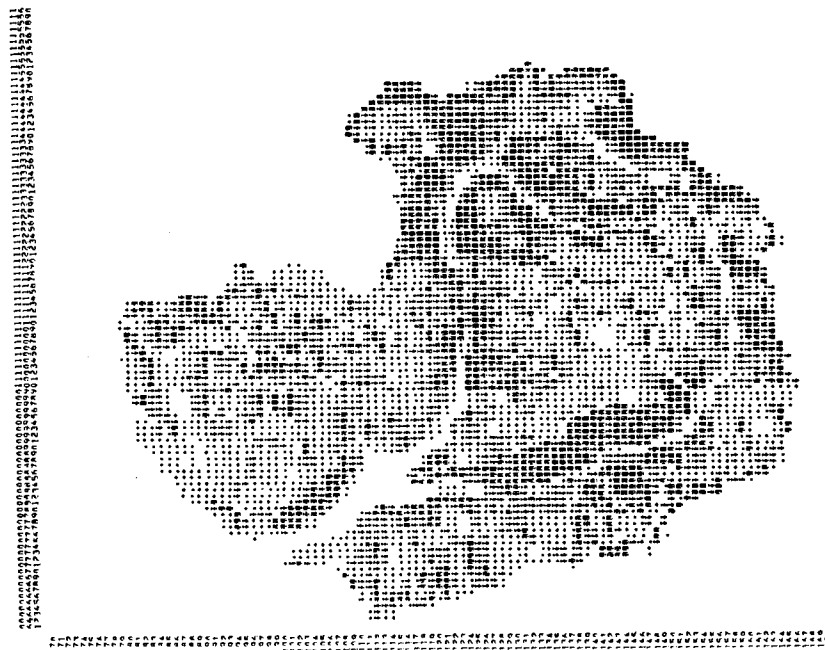
Figure 3.4. Gray Map of Slope.
Eight Classes from 0 to >70 percent.

IV. AUTOMATIC GENERATION OF PARAMETER DECKS

Major snow process models of Colorado conditions developed in the 1970's (Leaf and Brink, 1973; Leavesley, 1973) were developed for semi-distributed simulation of mountain watersheds. Watersheds were subdivided into typically less than 25 hydrologic response units (HRU's). HRU's are defined as areas that are reasonably uniform with respect to exposure, vegetation and soils. Parameter decks for operating the models were created manually from data tabulated for each unit. Parameter optimization was accomplished by changing the estimated parameters one at a time either manually or automatically for self-calibrating models until a good fit between simulated and observed processes was obtained. The first approach can be tedious and time consuming and the second approach expensive in computer time.

This chapter introduces procedures for the automatic generation of large parameter decks and parameter optimization in either batch - or preferably - interactive computing mode. Two computer programs for the generation of parameter decks were developed for this study. Program EXTRACT generates parameter decks for a distributed water yield model and FLOPARM generates parameter decks for a lateral flow model of streamflow generation. Only EXTRACT will be discussed here. FLOPARM is discussed in Chapter VI.

Program EXTRACT

Program EXTRACT was developed for the automatic generation of parameter decks for operating the modified simulation model WATBAL.[1] Eight overlays with watershed information are used by EXTRACT in defining hydrologic response units (HRU's) and calculating their parameters:

1. Watershed ID Numbers
2. Elevation
3. Aspect
4. Slope
5. Vegetation Type
6. Vegetation Density
7. Field Capacity
8. Wilting Point

Hydrologic response units consist of grid cells (5.76 ha) similar with respect to aspect, slope and vegetation type. For each HRU, elevation and other parameters are calculated as the mean of individual grid-cell values.

---

[1]The modified WATBAL is discussed in Chapter V.

A grouping scheme had to be devised in order to fit the simulation problem on even a large computer (CYBER 171 or 172) and reduce computing costs. In the computer, watershed parameters are represented as three dimensional[1] variables of the following form:

$$ELEVAT \ (IASP, \ ISLP, \ IVEG)$$

where

ELEVAT = Mean elevation of HRU
IASP = Aspect of HRU (Max. 8 classes)
ISLP = Slope of HRU (Max. 5 classes)
IVEG = Vegetation Type of HRU (Max. 5 classes)

If very detailed simulation is desired the watershed can be divided into separate elevation bands with parameter decks being created for each band. This option can improve the simulation especially if the same vegetation type occurs over a larger elevation range.

The grouping scheme adopted for this study is flexible and can be modified. For application to other watersheds, it might be advantageous to use elevation or vegetation density as grouping subscripts.

Besides watershed overlays, card decks with potential evapotranspiration data and slope/aspect correction factors are used in generating a parameter deck (Table 4.1).

Ninety-three HRU's were defined within the entire Williams Fork study area (23,075 ha). A total of 104 HRU's were present, but subunits with fractional areas less than 0.001 were excluded to reduce computing costs. Table 4.2 shows the 85 subunits defined within the South Fork of the Williams Fork Watershed.

The information given in Table 4.2 is used by a number of subroutines within Program EXTRACT in generating the parameter deck. In the following sections parameters are discussed in the order they are calculated.

1. Vegetation Transmissivity

Vegetation transmissivity is defined as the percentage of solar radiation available for snowmelt below the forest canopy. Forest canopy transmissivity is considered a function of canopy density; the "high" and the "low" curves in Figure 4.1 are obtained from Leavesley (1973). Three more curves were drawn in as calibration options for different tree species and varying conditions. Transmissivity values for 5% increments in cover density were read from the curves (Table 4.3) and made available to subroutine TRCOEFF in data statements.

[1]The CSU computer systems only allow 3 subscripts.

Table 4.1. Creation of Parameter Decks for Operating a Water
Balance Simulation Model[1] on Specified Watersheds.

	Input	Program	Output
1.	9 Overlays with Grid Cell Data		Parameter Deck for Operating Water Balance Model
	A. IDNUMBR	EXTRACT	Card Images Written to File WBMDECK
	B. ELEVAT		
	C. ASPECT		
	D. SLOPE		
	E. VEGTYP		
	F. VEGDENS		
	G. FIELDC		
	H. WILTPT		
	I. SOILML		
2.	Card Deck with Potential ET Data		
3.	Card Deck with Slope/Aspect Correction Factors		

[1]Modified version of "Hydrologic Simulation Model of Colorado
Subalpine Forest", by Charles F. Leaf and Glen E. Brink, USDA
Forest Service. Research Paper RM-107, May 1973, 23 pp.

Table 4.2. Hydrologic Subunits with Calculated Parameters for the South Fork of the Williams Fork Watershed.

WATERSHED PARAMETERS FOR WATERSHED(S) * 300

SUMMARY FOR ELEVATION ZONE * 7500-13500 FEET

SUBCLASS	ASPECT	SLOPE	VEG. TYPE	VEG. DENS.	FIELDCAP.	SOIL MOIST. LEV.	WILT. POINT	FRAC. AREA	MEAN ELEVAT.

TOTAL NUMBER OF CELLS= 1219

NUMBER OF HYDROLOGIC SUBUNITS= 85

SUM OF FRACTIONAL AREAS= 1.000
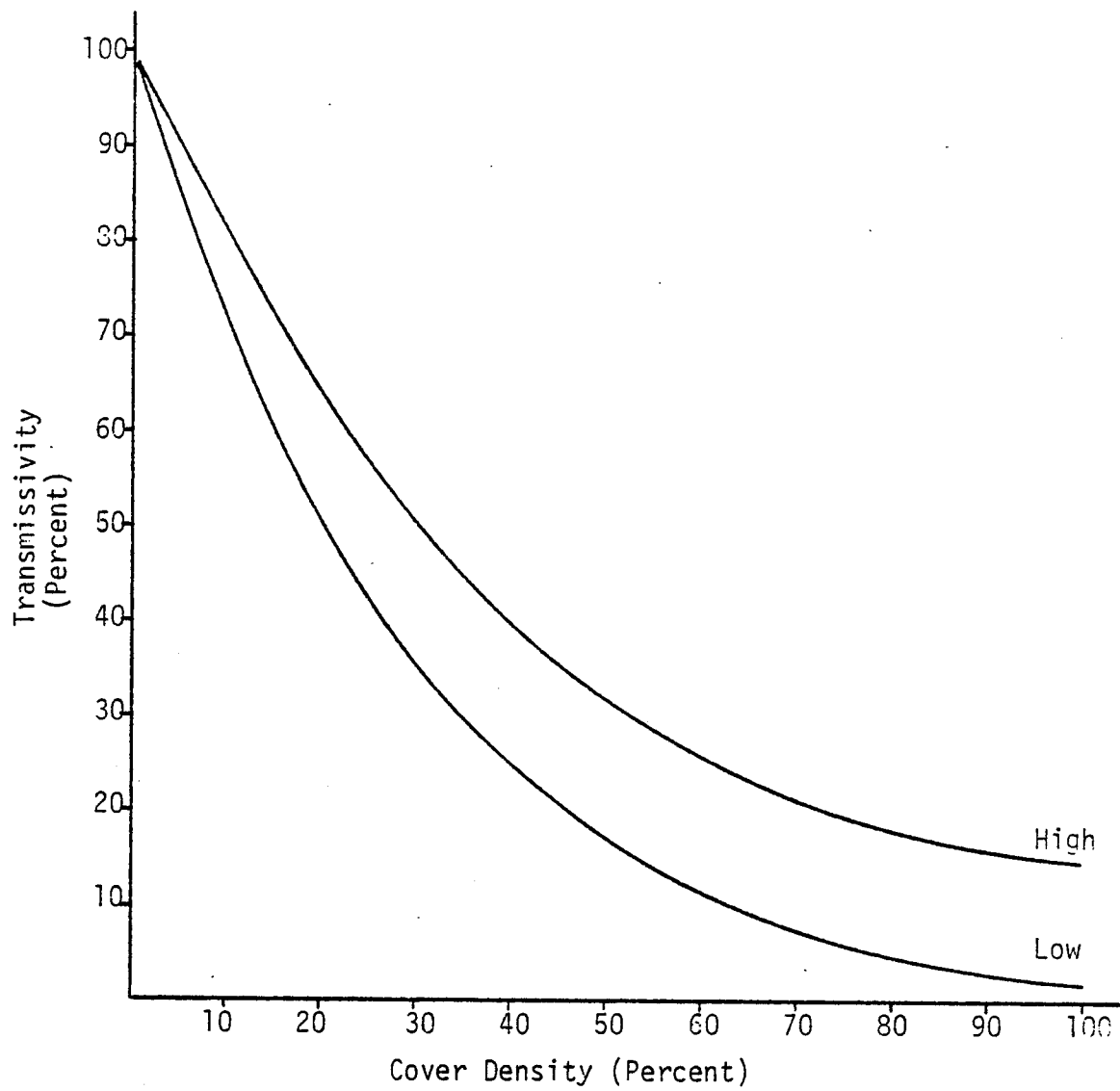
Figure 4.1. "High" and "Low" Transmissivity Curves for
            Vegetation Types in the Williams Fork
            Watershed. (After Leavesley, 1973).

22

Table 4.3. Transmissivity Values Used in Generating the Parameter Deck for Operating the Water Balance Simulation Model.

Cover Density (Percent)	Index	Transmissivity (Percent)				
		5	4	3	2	1
0		100	100	100	100	100
5	1	86	87	88	89	90
10	2	72	74	76	78	80
15	3	61	64	67	69	72
20	4	51	54	58	61	64
25	5	43	47	50	54	57
30	6	36	40	44	47	51
35	7	31	35	38	42	45
40	8	26	30	33	37	40
45	9	21	25	29	32	36
50	10	18	22	25	39	32
55	11	15	19	22	26	29
60	12	12	16	19	23	26
65	13	10	14	17	21	24
70	14	8	12	15	19	22
75	15	6	10	12	17	20
80	16	5	8	12	15	18
85	17	4	7	11	14	17
90	18	3	6	10	13	16
95	19	2	5	9	12	15
100	20	2	5	9	12	15

Subroutine TRCOEFF reduces the cover density for aspen (deciduous) to a specified fraction (0.60) before assigning transmissivity values.

2. Reflectivity Threshold Temperatures

During initial snow accumulation, no snowmelt is allowed if the daily mean temperature is below the reflectivity threshold temperature.

Leaf and Brink (1975) give examples of reflectivity threshold temperatures for some elevations and aspects. The base temperatures given in Table 4.4 are estimated from these values.

Table 4.4. Reflectivity Threshold Temperatures for Elevation Zones and Aspects. Temperatures in Degrees Fahrenheit.

Elevation (Feet)	Index	Aspects							
		N	NE	E	SE	S	SW	W	NW
7,500	1	45	43	40	60	70	58	45	45
8,500	2	45	43	40	60	70	58	45	45
9,500	3	42	41	38	58	68	57	45	43
10,500	4	38	37	35	55	65	55	45	41
11,500	5	32	32	32	46	60	53	45	37
12,500	6	32	32	32	46	60	53	45	37
13,500	7	32	43	32	46	60	53	45	37

Reflectivity threshold temperatures are assigned in subroutine TRSHOLD.

3. Initial Soil Moisture Levels

If initial soil moisture levels are not known, subroutine INITIAL will assign probable initial soil moisture values to each vegetation type on the starting date (usually October 1) of simulation.

4. Evapotranspiration

Potential evapotranspiration rates were calculated as discussed in Chapter II. The PET rates shown in Table 2.4 were expanded for combinations of slopes and aspects by adjusting temperatures for aspect (Figure 4.2) and potential solar beam radiation for the effect of terrain.

Calculated PET rates were transferred to punched cards, that are read by subroutine POTETIN and assigned to subunits by subroutine GETPET.

Subroutine GETPET has calibration options (adjustment factors) for potential evapotranspiration calculated for elevation zones.

5. Temperatures

Based on temperature lapse rates presented in Table 2.1 and temperature variations with aspect (Figure 4.2) two sets of temperature correction values were calculated. One set for winter (Nov. - Mar.) conditions and one set for summer (Apr. - Oct.) conditions. The data sets given in Table 4.5 and Table 4.6 will adjust the daily temperatures recorded at Berthoud Pass to a subunit with a given elevation and aspect.
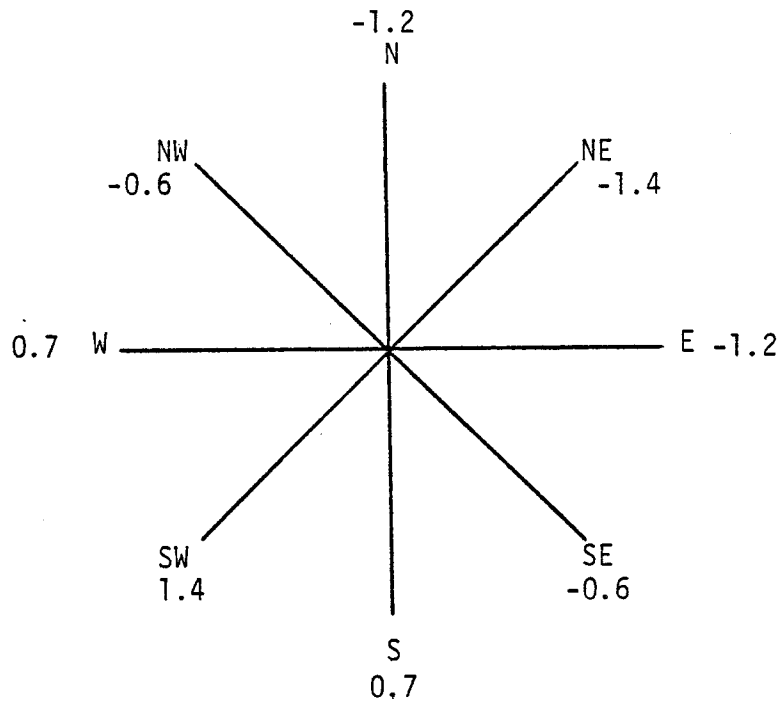
Figure 4.2. Temperature Variation Due to Aspect.
Adjustments Relative to a Horizontal Surface.
Temperatures in Degrees Fahrenheit.
(After Wymore, 1974).

Table 4.5. Winter (Nov.-Mar.) Temperature Adjustment Values for Subunits. Corrections
Relative to Temperatures Recorded at Berthoud Pass. Temperatures in
Degree Fahrenheit

Elevation (Feet)	Index	N	NE	E	SE	S	SW	W	NW
6,500	1	6.4	6.2	6.4	7.0	8.3	9.0	8.3	7.0
7,500	2	3.7	3.5	3.7	4.3	5.6	6.3	5.6	4.3
8,500	3	1.5	1.3	1.5	2.1	3.4	4.1	3.4	2.1
9,500	4	0.0	-0.2	0.0	0.6	1.9	2.6	1.9	0.6
10,500	5	-0.8	-1.0	-0.8	-0.2	1.1	1.8	1.1	0.2
11,500	6	-1.2	-1.4	-1.2	-0.6	0.7	1.4	0.7	-0.6
12,500	7	-1.5	-1.7	-1.5	-0.9	0.4	1.1	0.4	-0.9
13,500	8	-1.6	-1.8	-1.6	-1.0	0.3	1.0	0.3	-1.0
14,500	9	-1.7	-1.9	-1.7	-1.1	0.2	0.9	0.2	-1.1

Table 4.6. Summer (Apr. - Oct.) Temperature Adjustment Values for Subunits. Corrections
Relative to Temperatures Recorded at Berthoud Pass. Temperatures in Degrees
Fahrenheit

Elevation (Feet)	Index	Aspect							
		N	NE	E	SE	S	SW	W	SW
6,500	1	17.6	17.4	17.6	18.2	19.5	20.2	19.5	18.2
7,500	2	11.7	11.5	11.7	12.3	13.6	14.3	13.6	12.3
8,500	3	6.3	6.1	6.3	6.9	8.2	8.9	8.2	6.9
9,500	4	2.3	2.1	2.3	2.9	4.2	4.9	4.2	2.9
10,500	5	0.1	-0.1	0.1	0.7	2.0	2.7	2.0	0.7
11,500	6	-1.2	-1.4	-1.2	-0.6	0.7	1.4	0.7	-0.6
12,500	7	-2.0	-2.2	-2.0	-1.4	-0.1	0.6	-0.1	-1.4
13,500	8	-2.5	-2.7	-2.5	-1.9	-9.6	0.1	-0.6	-1.9
14,500	9	-3.0	-3.2	-3.0	-2.4	-1.1	-0.4	-1.1	-2.4

Temperature adjustment values estimated for 6,500 and 14,500 feet elevation zones were added to the data sets to allow for temperature calibration by "sliding" an elevation zone up or down when assigning adjustment values. Temperature correction values are assigned in subroutine TMPCOEF.

6. Precipitation

A relationship between elevation and total annual precipitation was established partly from precipitation data for a number of stations around the study area and partly through model calibration. The precipitation curves in Figure 4.3 show the developed relationships.

Precipitation factors relative to Berthoud Pass Summit (Table 4.7) are assigned in subroutine PCPCOR.

Table 4.7. Precipitation Adjustment Factors Relative to Precipitation Recorded at Berthoud Pass. (See Precipitation Curves in Figure 4.3).

Elevation (Feet)	Index	Adjustment Factor		
		1	2	3
7,500	1	.42	.42	.42
8,500	2	.46	.46	.46
9,500	3	.58	.57	.56
10,500	4	.70	.68	.66
11,500	5	.85	.79	.74
12,500	6	.96	.86	.77
13,500	7	1.00	.89	.78

7. Slope and Aspect Correction

Factors for adjusting solar beam irradiation received on a horizontal surface for the effect of slope and aspect were calculated using tables published by Frank and Lee (1966).

Correction factors are read from cards and assigned to subunits by subroutine SLPASP.

8. Isothermal Dates

Isothermal dates are the dates on which the snow reaches $0^{\circ}C$ and melt can take place. Isothermal dates can be determined in the snowpack temperature simulation or can be specified to the simulation models as an option. The dates given in Table 4.8
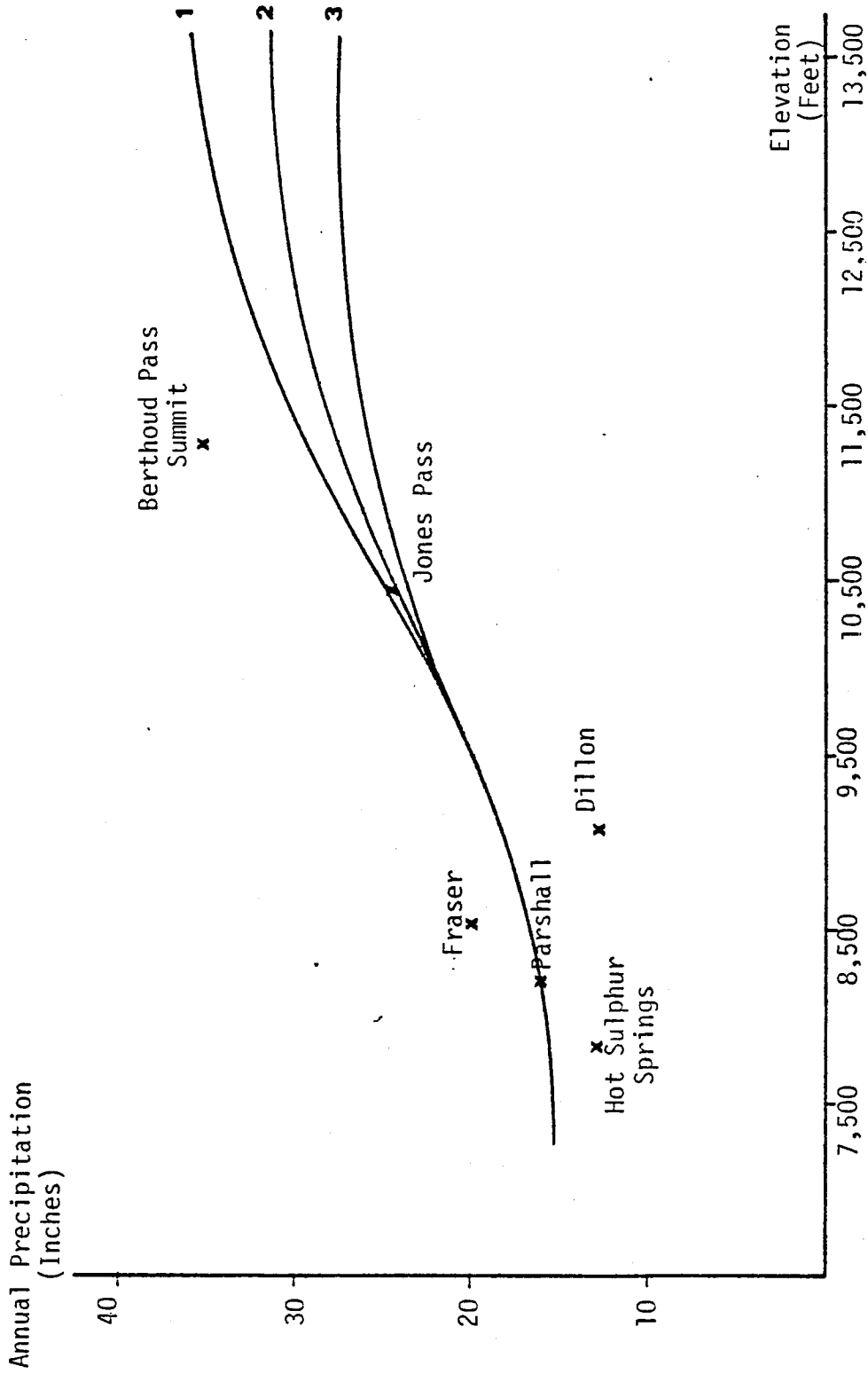
Figure 4.3. Precipitation Curves for the Williams Fork Watershed Shown with Annual Precipitation for Six Stations Near the Study Area.

Table 4.8. Mandatory Isothermal Dates for Elevation Zones and Aspects.
Data Format: Month-Day-Year

Elevation (Feet)	Index	N	NE	E	SE	S	SW	W	NW
6,500	1	41570	42570	40570	32470	31570	22570	31570	32570
7,500	2	42570	50570	41570	40570	32570	30570	32570	40570
8,500	3	50570	51570	42570	41570	40570	31570	40570	41570
9,500	4	51570	52570	50570	42570	41570	32570	41570	42570
10,500	5	52570	60570	51570	50570	42570	40570	42570	50570
11,500	6	60570	61570	52570	51570	50570	41570	50570	51570
12,500	7	61070	62070	60170	52070	51070	42070	51070	52070
13,500	8	61570	62670	60570	52570	51570	42570	51570	52570
14,500	9	62070	70170	61070	60170	52070	50170	52070	60170

are all estimated mean values. Program EXTRACT will change the
year according to input data.

The isothermal date can be calibrated by "sliding" an elevation
zone up or down. Isothermal dates with correction for year are
assigned in subroutine ISOTHRM.

V. SPATIAL SIMULATION OF SNOW PROCESSES

Simulation of snowmelt from high mountain watersheds has traditionally suffered from a number of serious deficiencies. These include a lack of basic data required to drive the model including precipitation (snow) inputs, and solar radiation or air temperatures to drive the snowmelt subroutines; and a lack of information on the spatial variation of the input data and the resulting processes. It is well known that both precipitation and air temperature vary with elevation, and many simulation models use elevation lapse rates to estimate the input data. It is also well known that snowmelt rates vary not only with elevation, but also with slope, aspect and the forest cover.

Spatial Watershed Simulation

As discussed in Chapter IV existing models will only simulate snow processes in a "semi-distributed" fashion by considering a relatively small number of hydrologic units within a watershed. Spatial watershed models simulate individual grid cell - or groups of similar cells - and processes are, therefore, accounted for in much more detail.

Spatial simulation has a number of distinct advantages and disadvantages over traditional approaches. Some of these are listed below:

Advantages

1. Simulation close to "real" events in time and space.
2. Automatic generation of parameter decks.
3. Fast-model calibration (because of 1 and 2).
4. Display of simulated parameters in map-like form (gray-maps).
5. Simulation update with remotely sensed spatial snow data on a pixel basis.
6. Input to drive distributed models of streamflow generation.
7. Detailed simulation of forest management options.

Disadvantages

1. Requires extensive spatial data base (overlays).
2. Computer programs more complex.
3. Requires large computers.

Selection of a Simulation Model

Two "state-of-the-art" watershed simulation models were considered for adaption to spatial simulation of snow processes in mountain terrain. Both models were developed for the simulation of Colorado subalpine conditions but also have been successfully tested on a variety of watersheds in other states.

The first model considered was "A Mountain Watershed Simulation Model" developed at Colorado State University by George Leavesley (1973) and first tested on the Little Beaver Creek Watershed within the Roosevelt National Forest. The second model considered was a "Hydrologic Simulation Model of Colorado Subalpine Forest" developed by the U.S. Forest Service (Leaf and Brink, 1973) and initially tested on watersheds within the Fraser Experimental Forest.

Both models were considered equally suitable, but the latter selected because the model by Leavesley was being re-written at the time of review, and the model by Leaf and Brink had already been partly modified during a previous study for the spatial simulation of snow cover.

Modification of the Selected Model

The selected snow process model (WATBAL) was intially validated on watersheds within the Fraser Experimental Forest, which borders on the study area in the Williams Fork Basin.

A number of modifications were made to the simulation model in order to facilitate spatial simulation of snow processes. Most of the modifications were only concerned with the peripheral routines, and no significant changes that would have required model revalidation were made to the core water balance routines. The most important modifications are listed below:

1. Maximum number of "hydrologic subunits" increased from 25 to 200.

2. Field capacity of subunits made a variable instead of fixed at 5.3 inches.

3. Vegetation types alpine, aspen and meadow added to lodgepole and spruce-fir as allowable types.

4. Temperature regression for subunits changed, so winter and summer temperatures are adjusted differently.

5. Precipitation correction factor can be specified for each subunit.

6. Isothermal date, peak water content of snowpack and its
date do not have to be specified.

7. A variable format card for input data is added to the
parameter deck.

8. Simulated snow cover and soil moisture information for
each subunit for dates between April 1 and July 31 is
written to a permanent file.

Data Requirements for Simulation

Required driving variables for WATBAL are the daily minimum
and maximum temperatures and precipitation. If daily observed
radiation is not available, incoming radiation is calculated in
the model from the temperature data using a degree day approach.
Temperatures are also used for the separation of precipitation
into rain, snow or mixed events.

Calculated (or observed) radiation is mainly used in calcu-
lating the radiation balance (temperature) of the snowpack and
actual evapotranspiration.

Model Calibration

The water balance simulation model, WATBAL, was initially
calibrated on wateryear 1970. The model was calibrated by sel-
ecting a precipitation curve in program EXTRACT, so that observed
and simulated total annual runoffs were equal. After model cal-
ibration the entire study area was simulated with data for
wateryear 1971, and lineprinter gray-maps displaying simulated
snow cover and soil moisture parameters were generated.
Gray-maps were generated by computer programs SIMRES and
GRTONES. Program SIMRES creates overlays (digital models)
with simulated parameters, that are then displayed by program
GRTONES.

The simulated water equivalent of snowpack can be seen
in gray-mapped form in Figures 5.1 through 5.4. There is a
slight increase in snow-water between April 1 and May 1.
After May 1, snowmelt progresses faster than new snow is
accumulating, resulting in a general reduction in snow-water
equivalent. Figure 5.3 shows how spring snowmelt is controlled
by terrain. Snow on "warm slopes" with aspects between south
and west is melting faster than snow on "cold slopes" with
aspects between north and east. Also forest cover is a major
controlling factor reducing the amount of solar radiation
available for snowmelt. On July 1 (Fig. 5.4) only slopes with
north-facing aspects and heavy forest cover have retained any
significant snow cover.

Figure 5.2.   Simulated Water Equivalent of Snowpack (May 1, 1971). Eight classes from <2.0 to >14.0 inches.

Figure 5.1.   Simulated Water Equivalent of Snowpack (April 1, 1971) Eight classes from <2.0 to >14.0 inches.
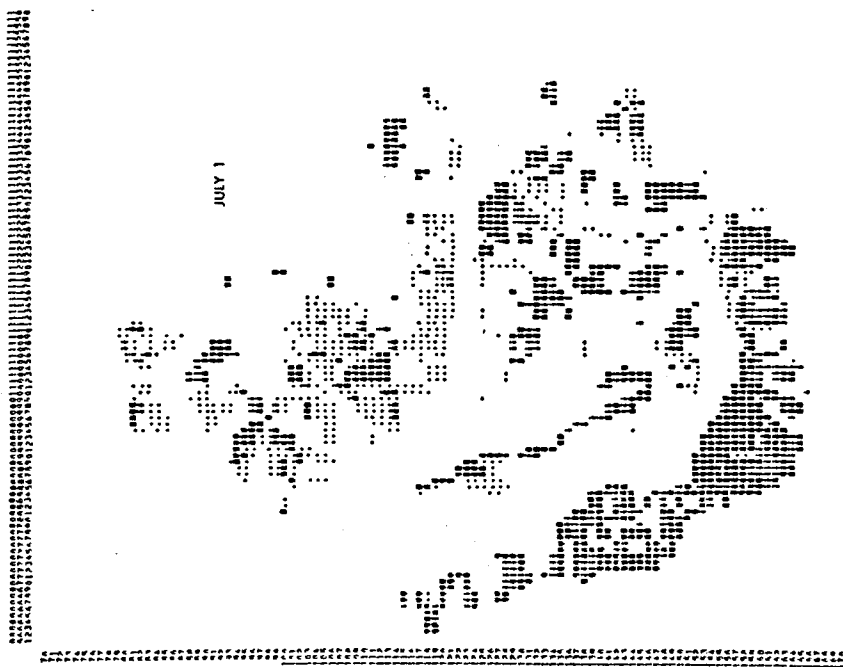
Figure 5.4. Simulated Snow Water Equivalent, July 1, 1971. (Eight classes from < 0.1 to > 21.0 inches).
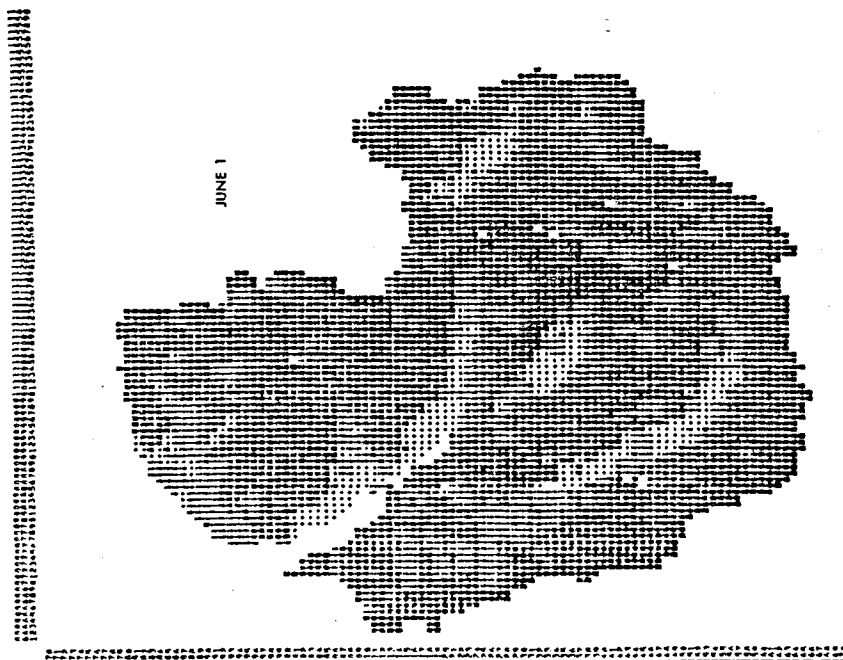
Figure 5.3. Snow Water Equivalent, June 1, 1971. (Eight classes from < 0.1 to > 21.0 inches)

Water from the melting snowpack will recharge the soil mantle
and reduce the recharge requirement of the rooting zone. Figure
5.5 shows that considerable melt has already taken place on exposed
slopes as early as April 1.

The mean snow temperature on April 1, is displayed in Figure 16.
The few cells colder than $-2.0^{o}C$ are caused by non-representative
isothermal dates.

After the specified isothermal date is reached, radiation
balance is computed by subroutine RADBAL in simulation model
WATBAL instead of being controlled by a temperature diffusion
model in subroutine DIFMOD, causing apparent instabilities in
temperature calculations. This problem could have been avoided
by not specifying isothermal dates. However, it was found that
mandatory isothermal dates improved simulation slightly for some
years.

Model Validation

WATBAL does not simulate stream hydrographs. No routing
is performed, and soil water in excess of field capacity is
assumed to run off instantly. In order to compare a simulated
hydrograph with the observed streamflow, a lateral flow model
was developed to route water from simulated snowmelt and input
in the form of rain through soil and groundwater storages to the
nearest stream channel. The lateral flow model is discussed in
detail in Chapter VI.

Model validation is attempted here by operating the calibrat-
ed model with climatic data for additional years and comparing
the resulting hydrographs with the gaged streamflow. To test
the spatial validity of the model, hydrographs for subwatersheds
were calculated from the simulation of the entire area. As a
final check parameter decks were generated specifically for
subwatersheds and simulated hydrographs again compared to observed
streamflow. Figures 5.7 and 5.8 show simulated hydrographs for
the entire study area (230.6 km^2) for the spring of 1970. Water-
year 1970 was used for calibrating the simulated total runoff as
mentioned previously. Simulated snowmelt obviously starts and
peaks too late. Calibration of temperature adjustments could
have eliminated this problem for 1970, but would have adversly
affected other years with good timing. Simulated snowmelt for
the same area in 1971 is slightly underestimated, but displays
good timing. Figure 5.9 shows the 1971 hydrographs for the South
Fork of the Williams Fork watershed only. Input data for
hydrograph simulation is calculated from the same simulation
of the entire area. A comparison shows, that the two simulated
hydrographs are similar, but the total runoff for the South Fork
is slightly overestimated instead of being underestimated.

Figure 5.6. Simulated Mean Snowpack Temperature. Eight Classes From <1.1 to >8.0°C.

Figure 5.5. Simulated Recharge Requirement (April 1, 1970). Eight Classes From <1.0 to >7.0 Inches.
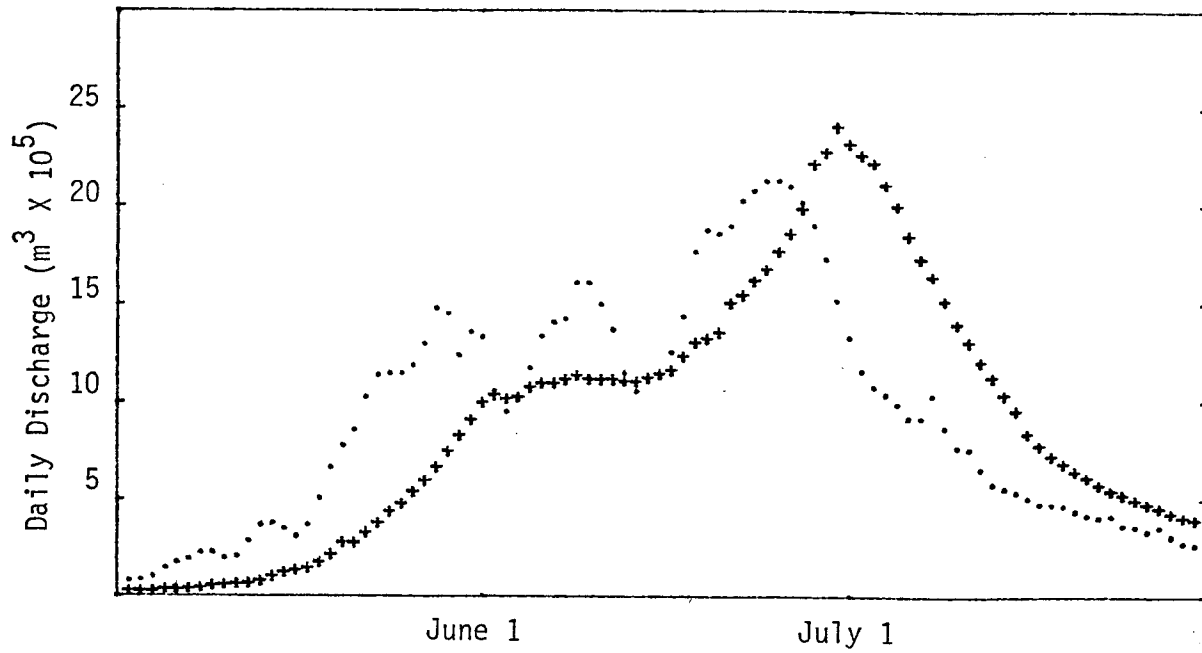
Figure 5.7. Observed (·) and Simulated (+) Snowmelt Hydrographs for the Williams Fork Watershed (WY 1970).
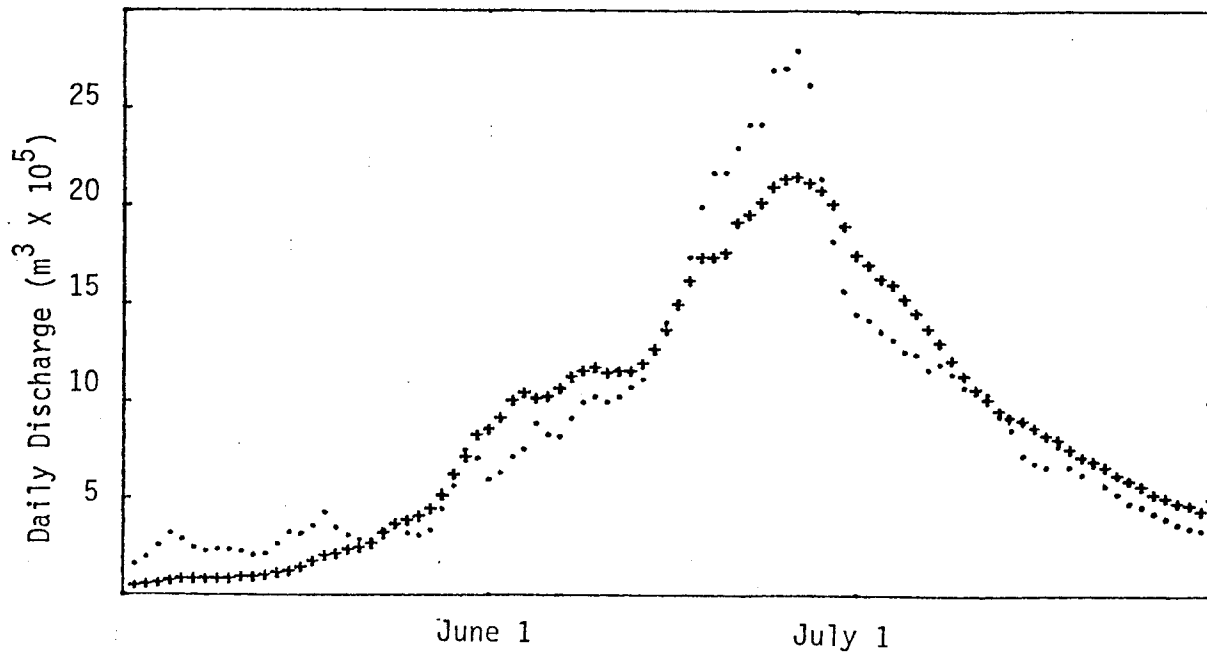
Figure 5.8. Observed (·) and Simulated (+) Hydrographs for the Williams Fork Watershed (WY 1971).
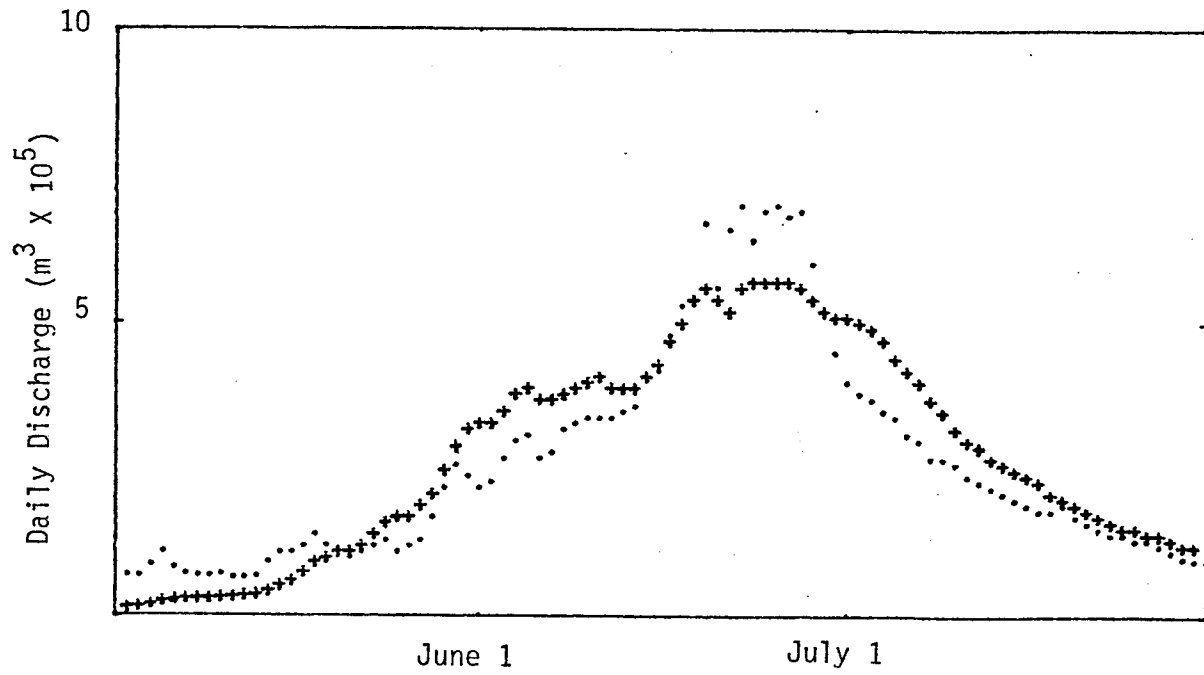
Figure 5.9. Observed (·) and Simulated (+) Snowmelt Hydrographs
            for the South Fork of Williams Fork Watershed
            (WY 1971).
            Date Extracted from Simulation of Entire Area.

Without changing the calibration, parameter decks were extracted for the simulation of the same two years on the Darling Creek (21.2 km^2) and the South Fork (70.4 km^2) watersheds. Both these watersheds are individually gaged with no upstream diversion. Hydrographs for the Darling Creek (Figs. 5.10 and 5.11) indicate the same timing problem for 1970. Snowcover for 1971 is strongly underestimated causing the hydrograph to start rising too early and not produce enough total runoff. Hydrographs for the South Fork (Figs. 5.12 and 5.13) are similar to the hydrographs for the entire area. Individual simulation of the South Fork watershed for 1971 did not change the simulated hydrograph significantly from the simulation shown in Figure 5.9.

Simulation of Forest Management Options

The computer program, EXTRACT, that generates the parameter deck for operating the water balance simulation model, WATBAL, has options for simulating watershed response to thinning or (clear-cutting) of all or selected timber stands.

Two WATBAL parameter decks were generated to demonstrate this capability. First, a run was made to simulate non-disturbed conditions on the South Fork of the Williams Fork watershed for wateryear 1972. Next, the effect of removing 75% of the crown cover in a uniform thinning of all timber stands was simulated. Before and after treatment data are given in Table 5.1. Predicted changes are very small. Thinning reduced total evapotranspiration and reduced the soil moisture deficit at the end of the wateryear. Runoff was not significantly increased.

Wateryear 1972 was a below average year with respect to precipitation. A higher predicted increase in runoff would be expected following treatment for average or above average precipitation years and for watersheds with denser forest cover.

Table 5.1. Predicted Effects of Reducing Forest Cover on the South Fork of the Williams Fork Watershed by 75%. Data for Wateryear 1972.

Simulated Parameter	Before Treatment (Inches)	After 75% Thinning (Inches)
Precipitation	25.83	25.83
Evapotranspiration	8.06	7.80
Snowpack (9-30-72)	0.13	0.12
Change in Soil Moisture	+0.63	+0.83
Runoff	17.01	17.08
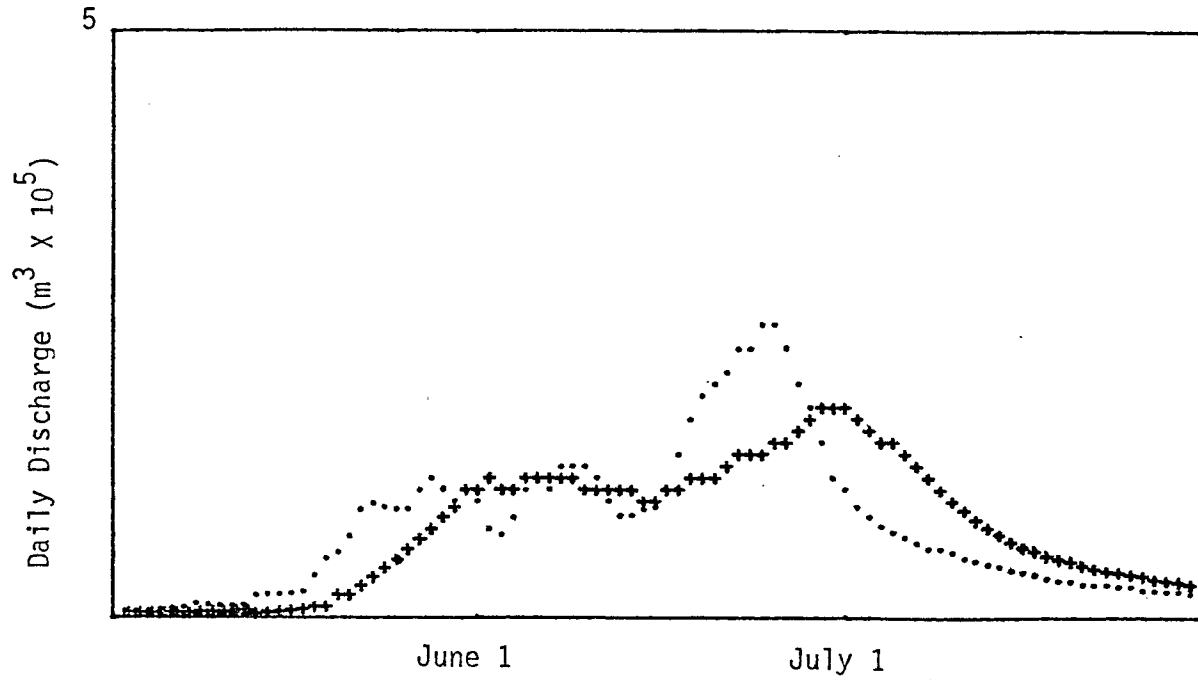
Figure 5.10.   Observed (·) and Simulated (+) Snowmelt Hydrographs
for the Darling Creek of Williams Fork Watershed.
(WY 1970).
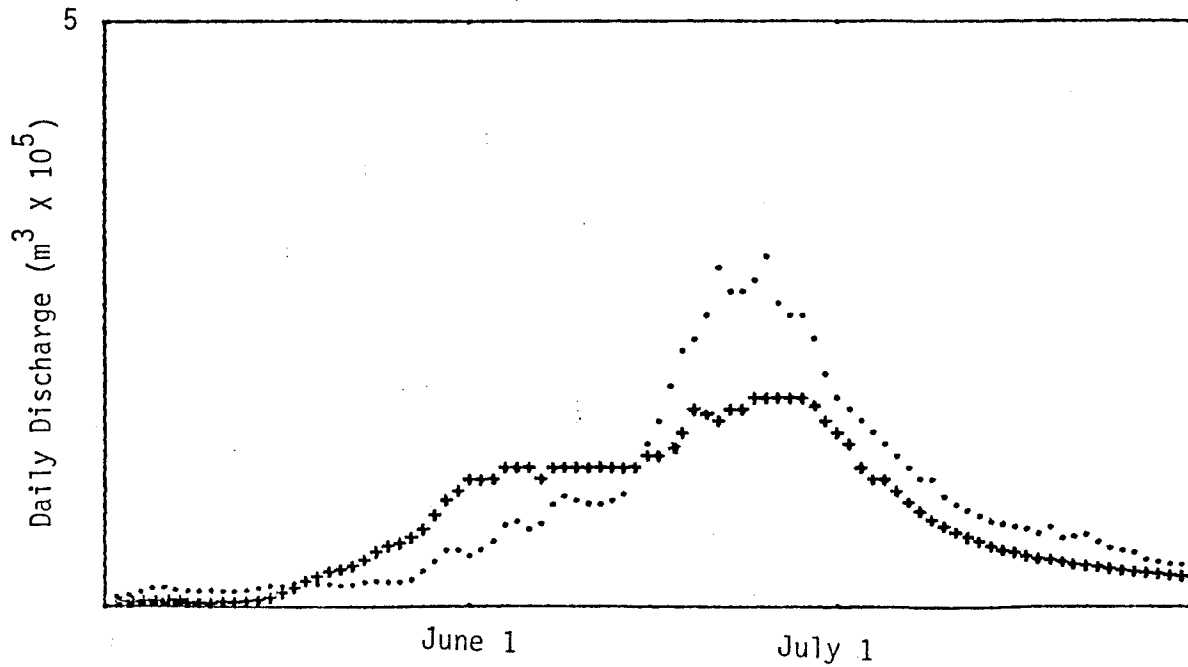
Figure 5.11.   Observed (·) and Simulated (+) Snowmelt Hydrographs
for the Darling Creek of Williams Fork Watershed
(WY 1971).
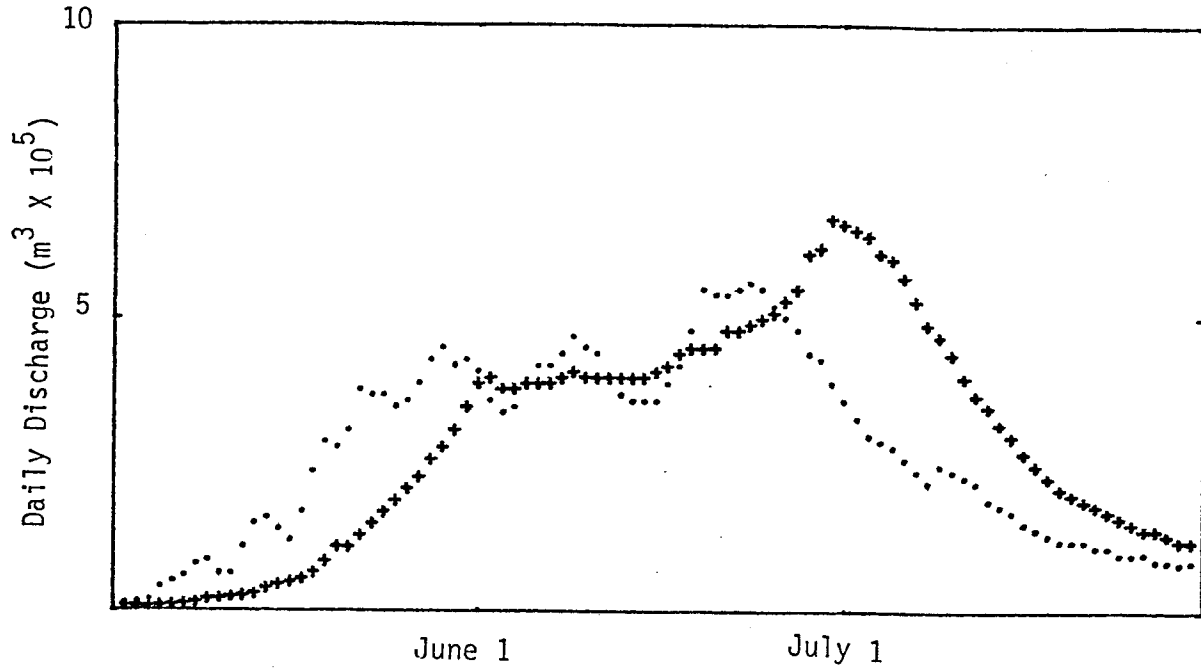
Figure 5.12.   Observed (·) and Simulated (+) Snowmelt Hydrographs
for the South Fork of Williams Fork Watershed
(WY 1970).
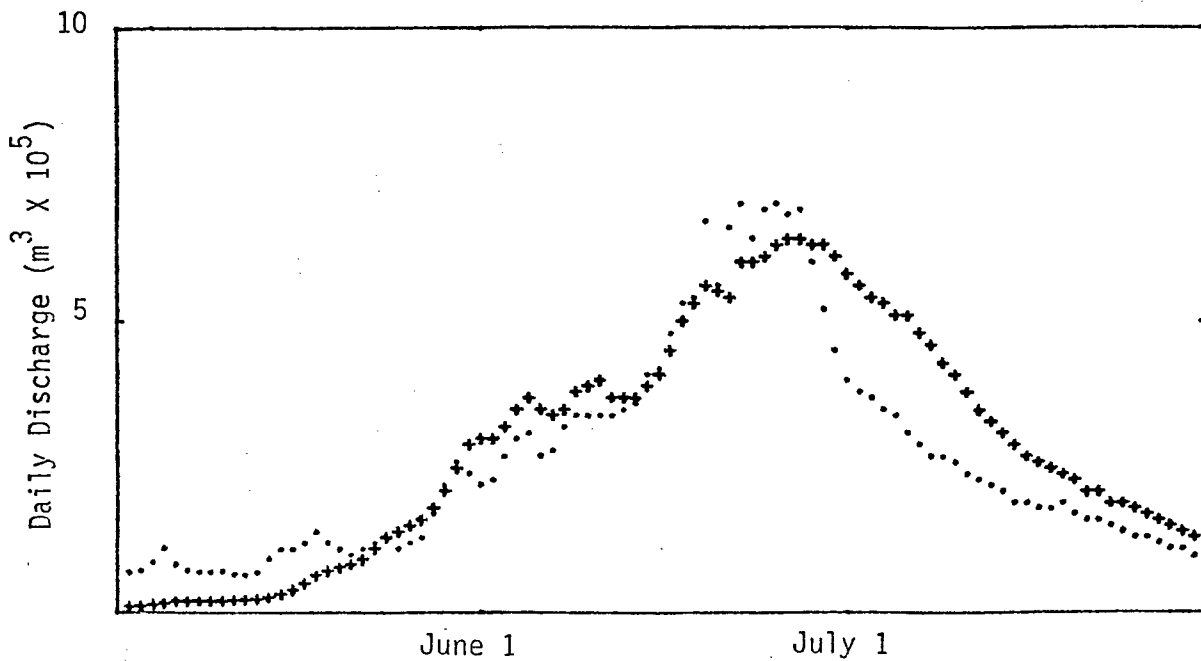
Figure 5.13   Observed (·) and Simulated (+) Snowmelt Hydrographs
for the South Fork of Williams Fork Watershed
(WY 1971).

More noticeable effects of the 75% thinning are illustrated in Figures 5,14 and 5,15, Thinning causes the hydrograph to rise faster due to increased melt rates in the forest covered areas,

Discussion

The developed procedures and computer programs for the spatial simulation of snow processes in mountain terrain are considered potentially useful for the watershed manager in the evaluation of watershed management options and in spring runoff forecasting on large watersheds, where manual generation of parameter decks and model calibration is not feasible. The approach offers possibilities of direct simulation update on a pixel basis, if periodical remotely sensed (or other forms of) snowpack information is available in overlay form.

Spring runoff forecasting capabilities could be improved by the development of procedures for generation of stochastic driving variables (temperatures and precipitation) for operating the simulation model between the last date with observed data and the end of the snowmelt season. Another possible extension is the incorporation of snow transport models for improved simulation of alpine and prairie conditions.
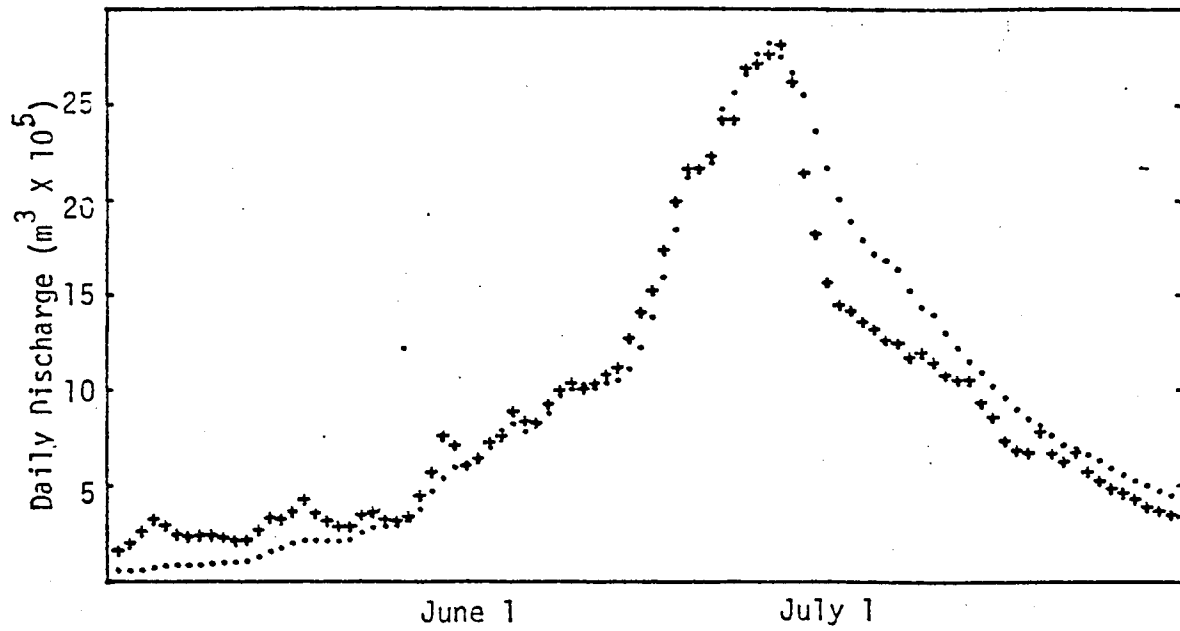
Figure 5.14. Observed (+) and simulated (·) hydrographs, Williams Fork Watershed, 1971.
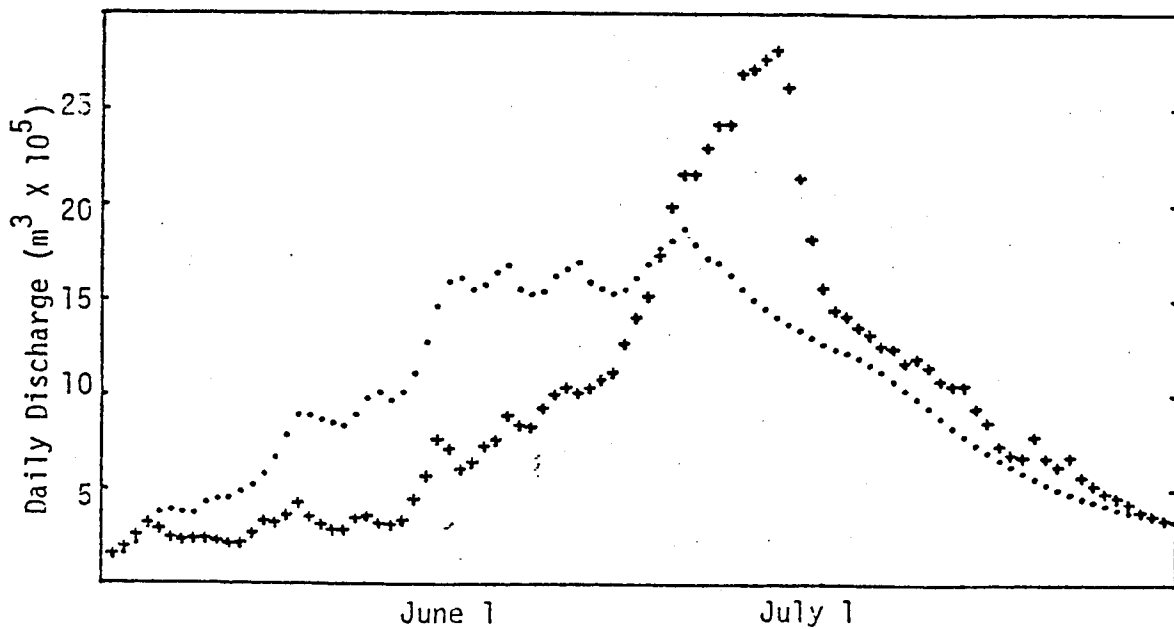
Figure 5.15. Observed (+) and Predicted (·) hydrographs showing effect of simulated 75% thinning. Williams Fork Watershed, 1971.

VI. HYDROGRAPH SIMULATION WITH
SPATIALLY DISTRIBUTED INPUT

The lateral flow model described here was developed in accordance with recent theories of streamflow generation in forested watersheds. Kirkby (1978) gives a review of the current concepts of runoff processes on hillslopes. In this model, lateral flow is simulated within slope compartments following the concept of "dynamic contributing area".

Experiments with simple lateral flow models of the gravitational movement of water released from melting snowpack suggested that spring hydrographs could be successfully simulated. The early models assumed a uniform input for all slope segments with flow taking place on top of the assumed impervious bedrock only.

The promising results obtained with the experimental models led to the development of a more complete model of runoff generation, simulating overland flow and baseflow contributions to the snowmelt hydrograph as well as the dominant lateral flow component.

The model developed does not consider Hortonian-type infiltration excess-overland flow since infiltration rates within the study area are generally much higher than any likely input (snowmelt and rain) event. Simulated overland flow can only take place when the entire soil horizon is saturated (saturation-overland flow).

The lateral flow model simulates lateral flow and deep seepage within variable length slope segments (compartments). A Darcy-type equation and the continuity equation are used for the calculation of lateral flow. Deep seepage and baseflow, from groundwater storage are treated vey empirically at this point.

Development of a Lateral Flow Model

A compartment model was adopted for the simulation of lateral flow downslope towards the nearest stream channel. Each compartment has two soil horizons. The top horizon is defined as the mean rooting depth of the dominant vegetation types, and the bottom horizon is defined as the remaining depth to bedrock or confining layer.

A fraction of the lateral flow in the bottom horizon is routed to the groundwater storage compartment. The daily streamflow is the sum of overland flow and lateral flow from the compartment adjacent to the stream channel and baseflow from groundwater storage.

The infiltration capacities of soil types encountered in the Williams Fork watershed are generally high (steady-state infiltration rates are approximately 10 cm/hr) and all input (snowmelt and rain) is assumed to infiltrate without producing any overland flow if the topsoil is saturated. Table 6.1 gives a summary of the soil-water information available for the study area. The daily input is assumed to reach the bottom horizon within the same day. If the bottom horizon reaches saturation the excess input is added to the water content of the top horizon. If this horizon also reaches saturation, excess input will flow to the next compartment as overland flow, and will be added to the input for this compartment.

Lateral flows between compartments are calculated on a daily basis using a Darcy-type equation and the continuity equation (Hillel, 1972). The hydraulic conductivity is calculated as a function of the relative saturation of the soil horizon. It is assumed that no flow occurs if the soil wetness is below field capacity. Besides being a function of soil wetness, lateral flow is also a function of the mean slope of the compartment. Like the daily input and overland flow, lateral flow from both horizons is added to the bottom compartment of the adjacent downslope compartment.

Groundwater recharge is calculated as a specified fraction of the lateral flow entering the stream channel. Baseflow from groundwater storage increases exponentially with the amount of groundwater in storage. The initial volume of groundwater in storage on the first date to be simulated must be estimated and specified to the lateral flow model.

A flow chart of a three-compartment lateral flow model and the various flow equations being used are shown in Figure 6.1.

Lateral flow compartments are defined by the distance in the direction of flow from the center of each grid cell to the nearest live stream channel. If the width of the lateral flow compartments is specified at 100 m, the compartment nearest to the stream is comprised of cells with distances to stream between 0 and 100 m. The next compartment contains cells with distances between 100 and 200 m and so on.

Figure 6.2 shows the distance to stream overlay for the Williams Fork in gray-mapped form. For the simulation runs included here, compartment width was specified at 100 m.

Table 6.1. Summary of Soils Information Used in Lateral
Flow Simulation

Soil Type[1]	Horizon	Depth[1] cm	HYDCON cm/hour	SATWC cm	FILDC mm	WILTPT[2] mm
21	1	20	3	9	49	16
	2	152	1	71	297	99
34	1	20	3	9	53	18
	2	76	1	35	126	42
38	1	64	10	27	67	22
	2	152	33	37	67	22
39	1	5	3	2	15	5
	2	152	3	64	354	118
43	1	64	10	27	63	21
	2	152	33	36	53	18
45	1	64	10	27	63	21
	2	152	33	36	53	18
53	1	56	10	24	60	20
	2	152	20	38	58	19

[1]Data (unpublished) obtained from the U.S. Forest Service,
Routt National Forest, Steamboat Springs, Colorado. Remaining
soil-water data estimated from texture information. Names of
soil types are given in Table 2.5.

[2]Wilting point not used for the simulation runs included here.

STREAM   COMPART 1   COMPART 2   COMPART 3

Input

Horiz. 1

Horiz.2

Lateral Flow in
Two Horizons (QL_{ij})
Ground Water
Recharge (QR_i)

GROUND WATER STORAGE (GWS)

Baseflow (QB)
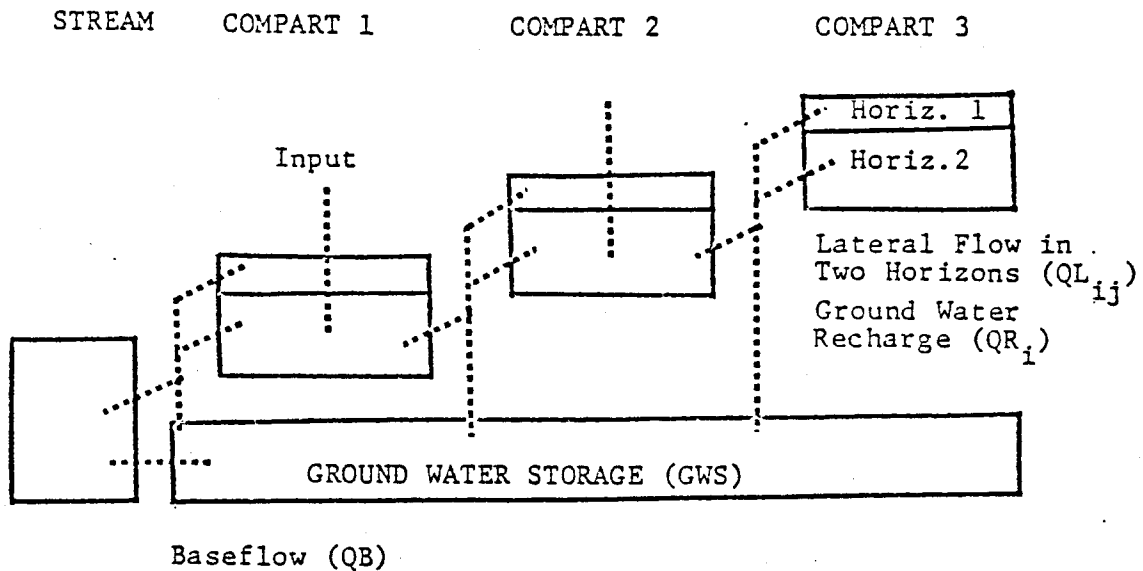
Equations:

$$KW_{ij} = KS_{ij}((WI_{ij}-WF_{ij})/(WS_{ij}-WF_{ij}))^a$$

$$QL_{ij} = b * 24 * KW_{ij} * A_{ij} * H_i$$

$$QB = c * GWS^d$$

$$QR_i = FRACT * QL_{i2} * \sum_{j=1}^{2} QL_{ij} / \sum_{i=1}^{n} \sum_{j=1}^{2} QL_{ij}$$

$$QS = \sum_{j=1}^{2} Q_{1j} + QO_1 + QB$$

Figure 6.1. Flow Chart of a Three-Compartment Lateral Flow Model.
(Overland Flow Not Included)

Figure 6.1 continued

Where:

a,b,c,d = Constants

i, j = Compartment and horizon subscripts

n = Number of compartments

FRACT = Fractional deep seepage

GWS   = Groundwater storage

A_{ij} = Cross-section area

H_i = Fractional slope

KS_{ij} = Saturated hydraulic conductivity

KW_{ij} = Adjusted hydraulic conductivity

WF_{ij} = Water content at field capacity

WS_{ij} = Saturated water content

WI_{ij} = Initial water content

QB   = Baseflow

QL_{ij} = Lateral flow

QO_i = Overland flow

QR_i = Groundwater recharge

QS   = Stream flow

Figure 6.2. Gray Map of Distance to Stream for the Williams Fork Watershed. Eight Classes From <200 to >1400 meters

Automatic Generation of Parameter Decks

Program FLOPARM extracts the information for creating the parameter deck for operating the lateral flow model using watershed information in digital terrain models and tabular soil-water information. Deep seepage rates can be specified for each flow compartment or left to default to probable values. Initial water contents of soil horizons within compartments will likewise default to probable values if not specified.

The recharge requirement of the top horizon is simulated by the watershed simulation model and initial water contents can be calculated from the simulated data. Initial water contents of the bottom layers was estimated during model calibration.

Table 6.2 shows the parameter deck for operating the lateral flow model on the South Fork of the Williams Fork watershed. Parameters are calculated as average values of data for individual grid cells within each compartment. Soil moisture information units are in meters to yield calculated flow volumes in cubic meters per day. Areas (ha) and volumes are corrected for the effect of slope.

Calculation of Input to Lateral Flow Model Compartments

The watershed simulation model simulates the daily input (snowmelt and rain) to the soil horizon below the mean rooting depth of the dominant vegetation types. The information is written to a permanent file for use by other programs for display or further processing.

Program INPFLOW calculates the mean daily input to each flow compartment from the simulated input for single grid cell elements within compartments. Program INPFLOW also takes daily streamflow information and creates a permanent file with date, input to flow compartment and streamflow information as data input to the lateral flow model.

Table 6.3 shows lateral flow model input data for the South Fork of the Williams Fork watershed, for snowmelt season 1970 (input in inches and streamflow in cfs/sec). The input summary line shows that higher elevations (further away from stream) receive higher total input than lower elevations.

Lateral Flow Simulation (Model Application)

A computer program LATFLOW was developed to simulate lateral flow as outlined previously. Operating equations are shown in Figure 6.1.

Table 6.2. Parameter Deck for Operating the Lateral Flow Model on the South Fork.

LATERAL FLOW MODEL PARAMETERS FOR WATERSHED(S) = 300

SUMMARY FOR ELEVATION ZONE = 7500-13500 FEET

COMPART	D-TO-STR	NO-CELLS	AREA	SLOPE	SEEP-AR	VOLUME	H-COND	SATWC	FIELDC	WILTPT	SEEP-AT	INT-MOIST
1	100	219	1296.4	23.7	76769.3	7849561.	.10	.26	.06	.02	0.02	.06
2	200	199	1211.2	34.1	191739.9	11704960.	.08	.37	.06	.02	0.02	.06
3	300	136	836.6	37.5	60935.7	7204362.	.07	.27	.06	.02	0.02	.06
4	400	137	840.5	39.5	174228.5	14410544.	.10	.25	.06	.02	0.02	.06
5	500	148	913.3	38.4	466955.5	5014854.	.06	.37	.06	.02	0.02	.06
6	600	84	515.4	36.7	119070.7	12716754.	.08	.25	.06	.02	0.02	.06
7	700	79	485.8	37.4	147324.2	25084418.	.06	.25	.06	.02	0.02	.06
8	800	58	354.2	35.3	149946.2	2096935.	.10	.37	.06	.02	0.02	.06
9	900	42	257.7	36.7	150227.8	5381134.	.25	.25	.06	.02	0.02	.06
10	1000	33	202.6	36.8	129557.8	3082338.	.10	.37	.06	.02	0.02	.06
11	1100	25	157.1	34.0	126661.0	3053360.	.10	.25	.06	.02	0.02	.06
12	1200	10	62.3	41.0	73543.6	7034668.	.25	.37	.06	.02	0.02	.06
13	1300	15	92.2	37.3	26864.4	2866250.	.10	.25	.06	.02	0.02	.06
14	1400	12	72.1	29.6	69166.9	7046634.	.25	.26	.06	.02	0.02	.06
15	1500	7	42.5	33.6	19537.4	2071680.	.04	.25	.06	.02	0.02	.06
16	1600	9	54.6	33.3	144469.0	6344146.	.06	.38	.06	.02	0.02	.06
17	1700	1	6.0	30.0	109621.7	5414465.	.26	.27	.06	.02	0.02	.06
18	1800	0	0.0	0.0	36771.1	3917405.	.03	.27	.05	.02	0.02	.05
19	1900	5	30.4	38.0	208922.2	11080676.	.10	.29	.06	.02	0.02	.06
					84718.4	30788222.	.03	.37	.06	.02	0.02	.06
					21848.4	8955839.	.25	.25	.06	.02	0.02	.06
					33603.0	23118554.	.04	.24	.06	.02	0.02	.06
					47556.6	2363559.	.05	.24	.06	.02	0.02	.06
					49930.8	9432250.	.02	.38	.06	.02	0.02	.06
					13136.8	5262296.	.02	.25	.06	.02	0.02	.06
					14006.0	14018077.	.07	.38	.06	.02	0.02	.06
					10506.6	1095634.	.23	.24	.06	.02	0.02	.06
					22557.4	2380176.	.10	.24	.05	.02	0.02	.06
					30074.4	6464478.	.10	.27	.06	.02	0.02	.06
					7872.7	325436.	.26	.37	.06	.02	0.02	.06
					368.5	2304591.	.33	.06	.05	.02	0.02	.05
					0.3	38447.	.03	.00	.00	.00	0.00	.00
					1612.8	112532.	.10	.24	.06	.02	0.02	.06
					4377.6	46030.	.20	.38	.06	.02	0.02	.06

TOTAL NUMBER OF CELLS= 1219

Table 6.3. Simulated Input Data for the Lateral Flow Model. South Fork, 1970.

LATERAL FLOW MODEL INPUT DATA FOR WATERSHED(S) = 300

SUMMARY FOR ELEVATION ZONE = 7500-13500 FEET

DATE	1	2	3	4	5	6	7	8	9	10	11	12	13	14	15	16	17	18	19	20	21	22	23	24	25	FLOW

TOTALS 515. 516. 516. 516. 317. 516. 516. 917. 616. 418. 517. 717. 016. 618. 319. 816. 916. 4 0.021.1 0.0 0.0 0.0 0.0 0.0

Flows are calculated by three subroutines within LATFLOW. Subroutine INPUT adds input as calculated by program INPFLOW to each compartment. The input is added directly to the bottom soil layer. If saturation occurs, the excess input is added to the top horizon. If this horizon also reaches saturation, overland flow can take place. Lateral flow is calculated as the next step in subroutine FLOCALC. This subroutine also calculates deep seepage and baseflow from groundwater storage. Finally, state variables are updated in subroutine STATE after flows have been calculated.

Table 6.4 shows the simulated soil water contents during the 1970 snowmelt season. The water contents (in percent of saturation) at the beginning of the period are all at field capacity. Since no lateral flow is assumed below field capacity, the simulated streamflow is initially all baseflow from ground-water storage. Throughout the period all flows are taking place in the bottom soil layers and the top layers stay at field capacity.

The summary of flows in Table 6.4 show that in 1970, no overland flow was simulated, the total simulated flow agrees well with the total recorded flow and groundwater storage at the end of the simulated period is 3,971,263 m^3. (Groundwater storage at the beginning of the periods was specified at 2,500,000 m^3.)

Figures 6.3 through 6.9 show simulated and observed hydro-graphs for two subwatersheds within the Williams Fork watershed; South Fork and Darling Creek. For all simulation runs the initial calibration of WATBAL with 1970 data was maintained.

The general agreement between simulated and observed hydro-graphs is good except for the 1971 snowmelt season. The hydro-graphs indicate two problems related to the nature of the climatic data used in the snowmelt simulation. In most years the simulated snowmelt starts either too soon or too late due to the temperature data. Also, the predicted amount of snow accumulated up to the onset of the snowmelt season deviates from the true amount resulting in problems with matching the time and amount of peak runoff.

The simulated hydrograph for Darling Creek in 1971 (Fig. 6.7) displays the poorest fit of the hydrographs. Figure 6.9 shows the same hydrograph from a recalibrated simulation run. The fit is now much better due to a better simulation of the amount of snow accumulated at the beginning of the snowmelt season.

Table 6.1. Simulated Water Contents for Lateral Flow Model Compartments and Resulting Flows. South Fork, 1970.

LATERAL FLOW MODEL OUTPUT DATA FOR WATERSHED(S) = 300

SUMMARY FOR ELEVATION ZONE = 7500-13500 FEET

DATE	1	2	3	4	5	6	7	8	9	10	11	12	13	14	15	16	17	18	19	20	21	22	23	24	25	BASEFL	SIMLFL	STRMFL
4 170																										12629.	12629.	13701.
4 270																												
5 270																										19302.	423394.	435495.
5 870																										20898.	458847.	450174.
5 970																										22719.	491669.	415922.
5 070																										24772.	519020.	425708.
5 170																										27042.	530412.	408502.
6 170																										29494.	527462.	357204.
6 270																										31940.	488394.	337631.
6 370																										34170.	469242.	352310.
6 470																										36288.	463987.	391456.
6 570																										62144.	485087.	545592.
6 270																										64034.	498438.	562718.
6 470																										66007.	504614.	550485.
6 570																										67988.	509270.	518679.
6 670																										69956.	510316.	496660.
6 770																										71870.	512600.	479534.
6 870																										73742.	525799.	440388.
6 970																										75691.	503705.	425708.
6 070																										77313.	486241.	389009.
7 170																											452705.	252650.
7 070																										46701.	85437.	83184.
7 170																										45567.	82244.	85631.

TOTAL OVERLAND FLOW   =   0.
TOTAL BASEFLOW   =   4346383.
TOTAL SIMULATED FLOW   =   26387640.
TOTAL RECORDED FLOW   =   26052662.
GROUND WATER STORAGE   =   3971261.

55
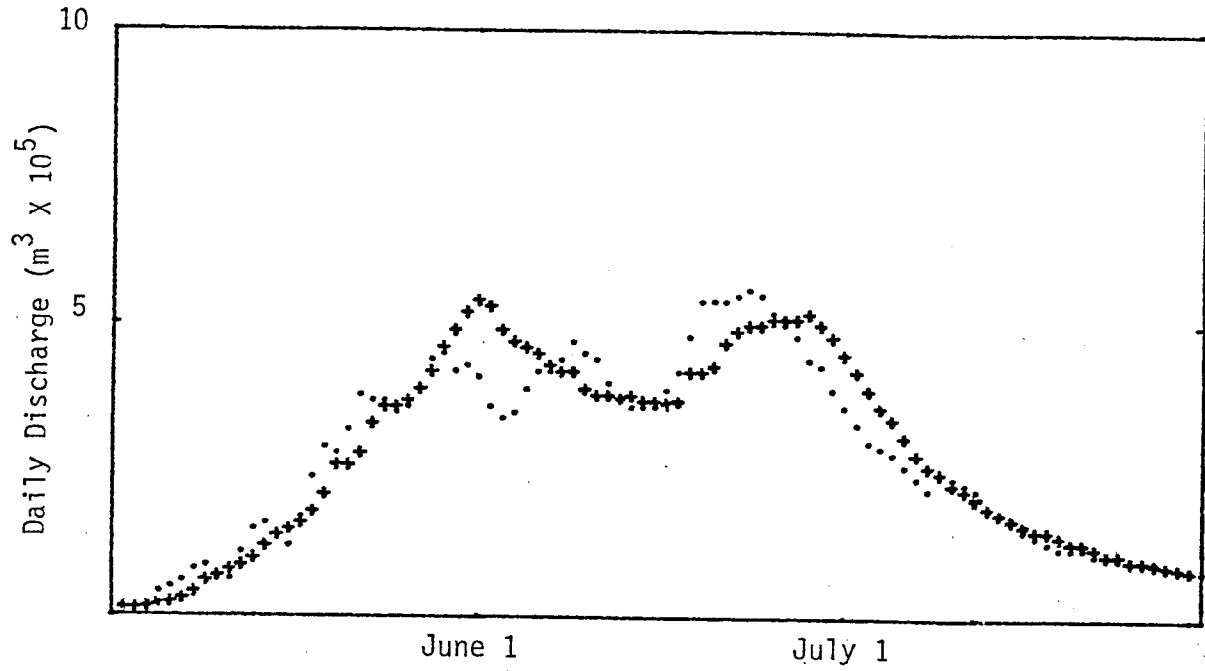
Figure 6.3. Observed (·) and Simulated (+) Hydrographs for the South Fork (WY 1970).
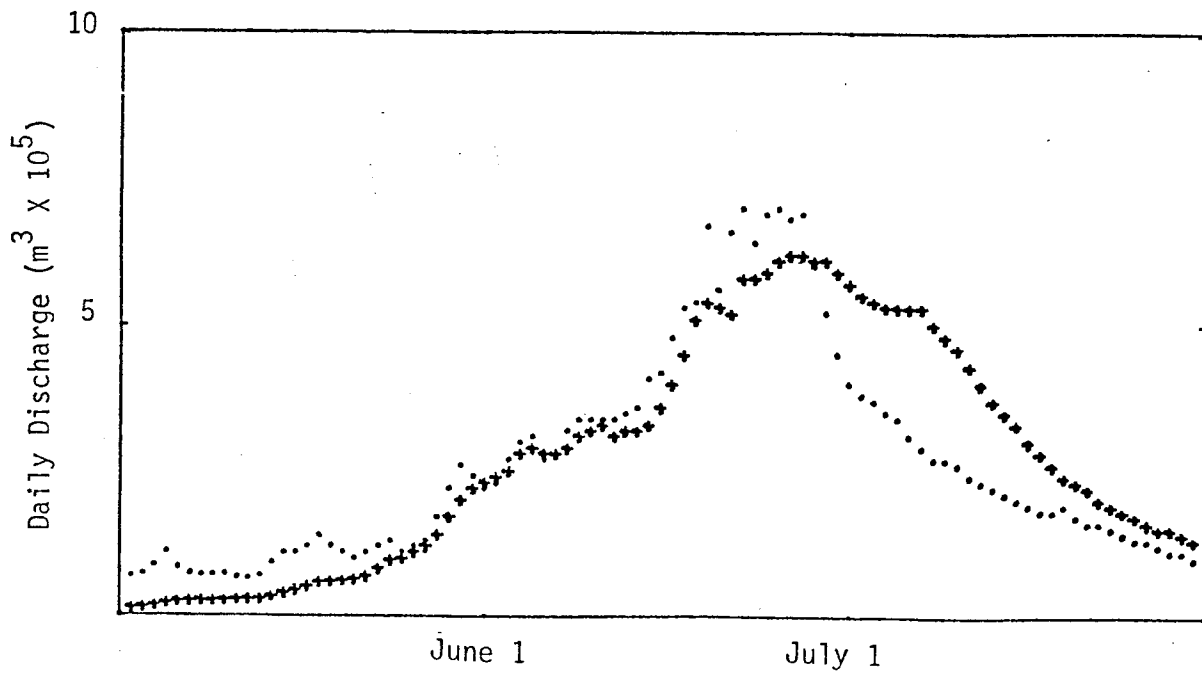
Figure 6.4. Observed (·) and Simulated (+) Hydrographs for the South Fork (WY 1971).
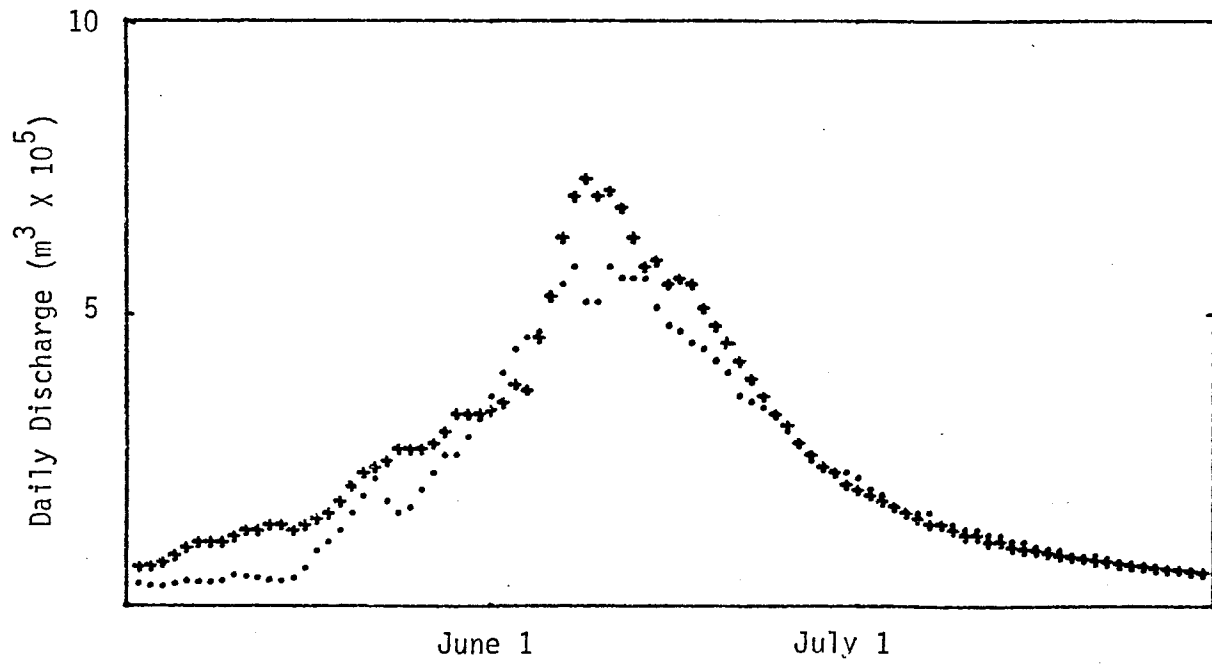
Figure 6.5. Observed (·) and Simulated (+) Hydrographs for the South Fork (WY 1972).
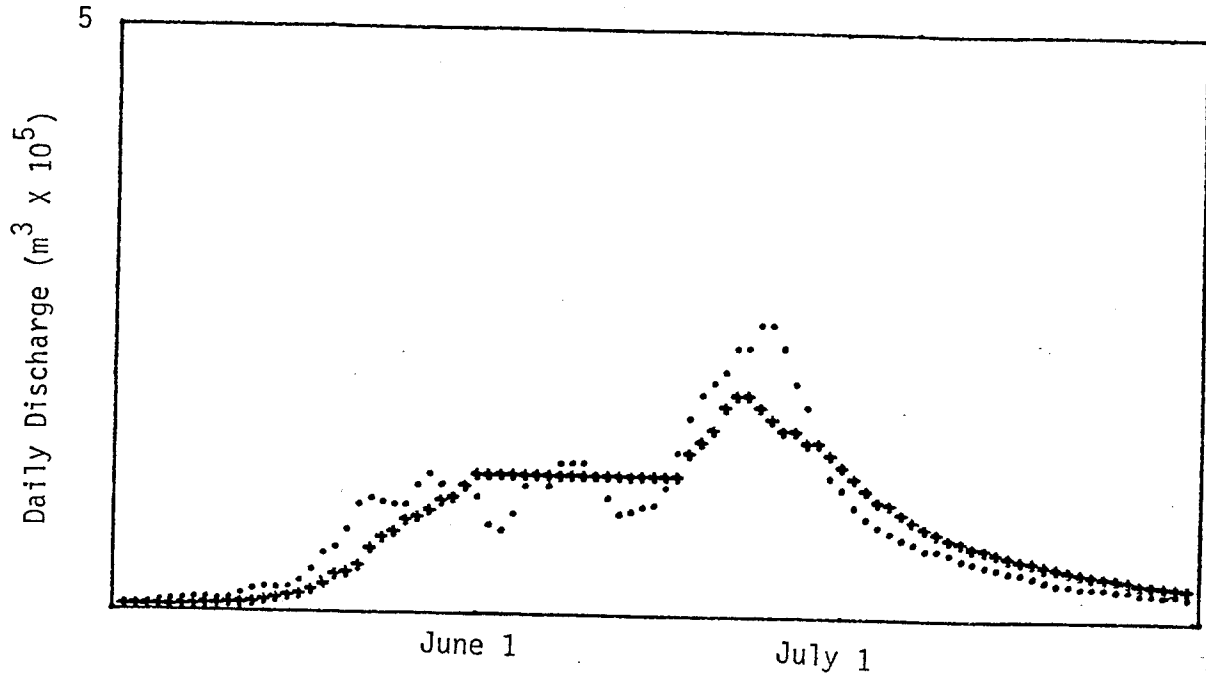
Figure 6.6. Observed (·) and Simulated (+) Hydrographs for Darling Creek (WY 1970).
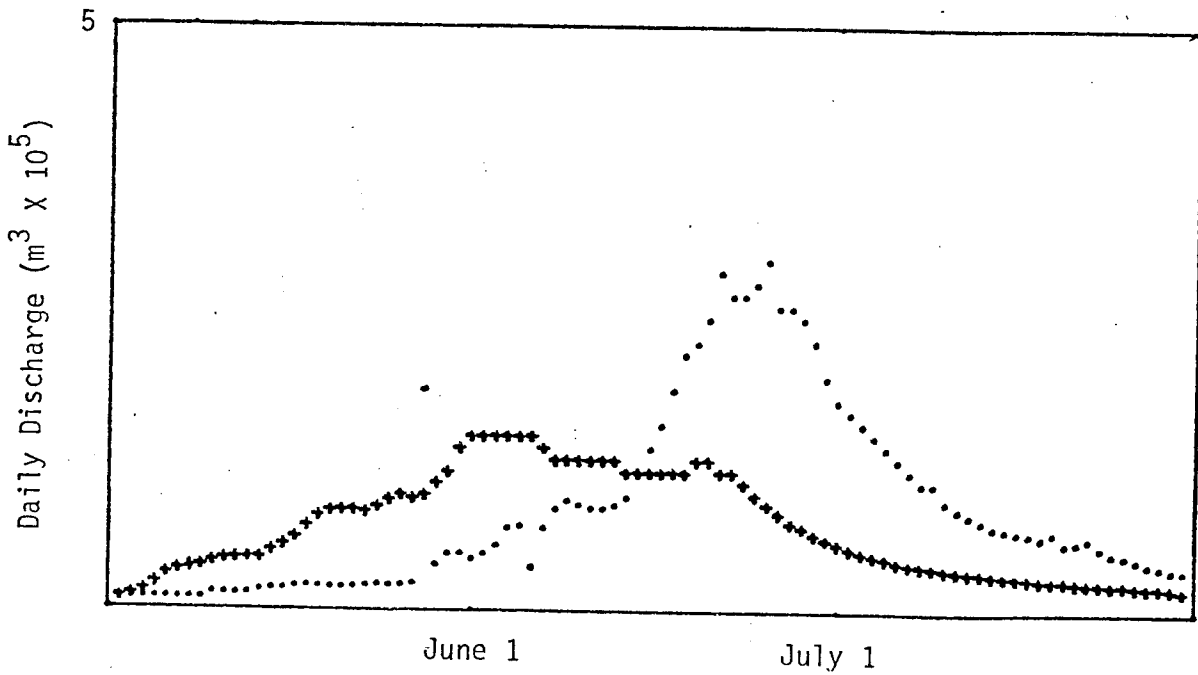
Figure 6.7. Observed (·) and Simulated (+) Hydrographs for Darling Creek (WY 1971).
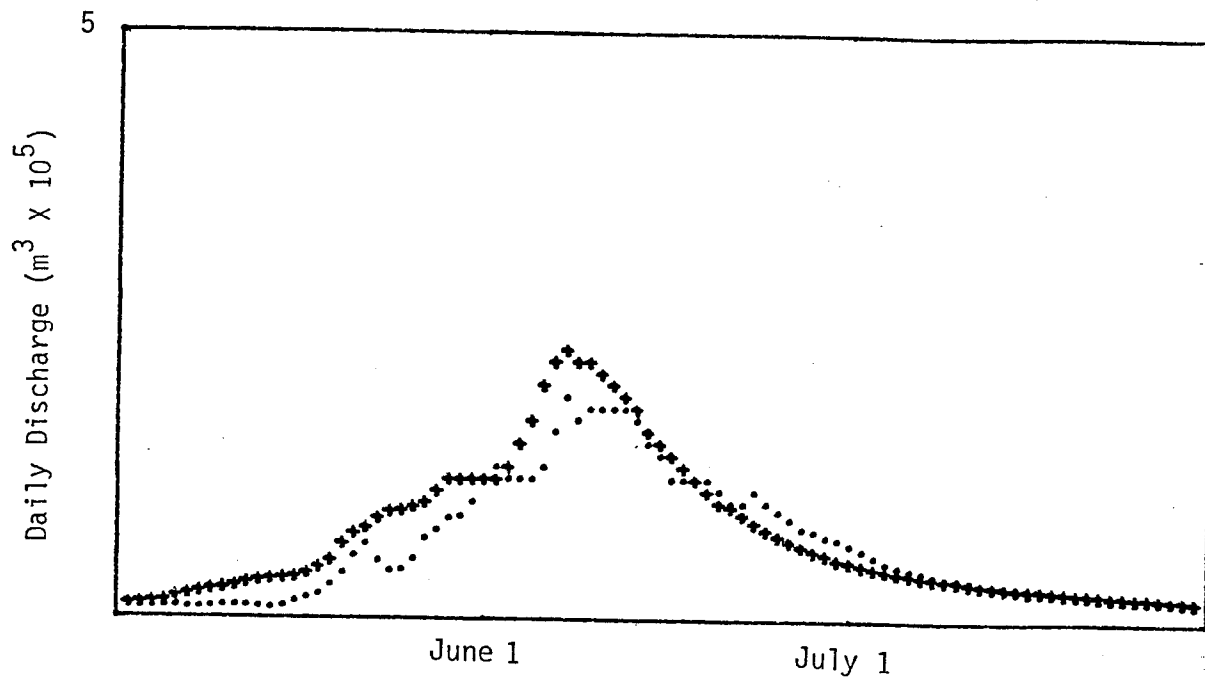
Figure 6.8. Observed (·) and Simulated (+) Hydrographs for Darling Creek (WY 1972).
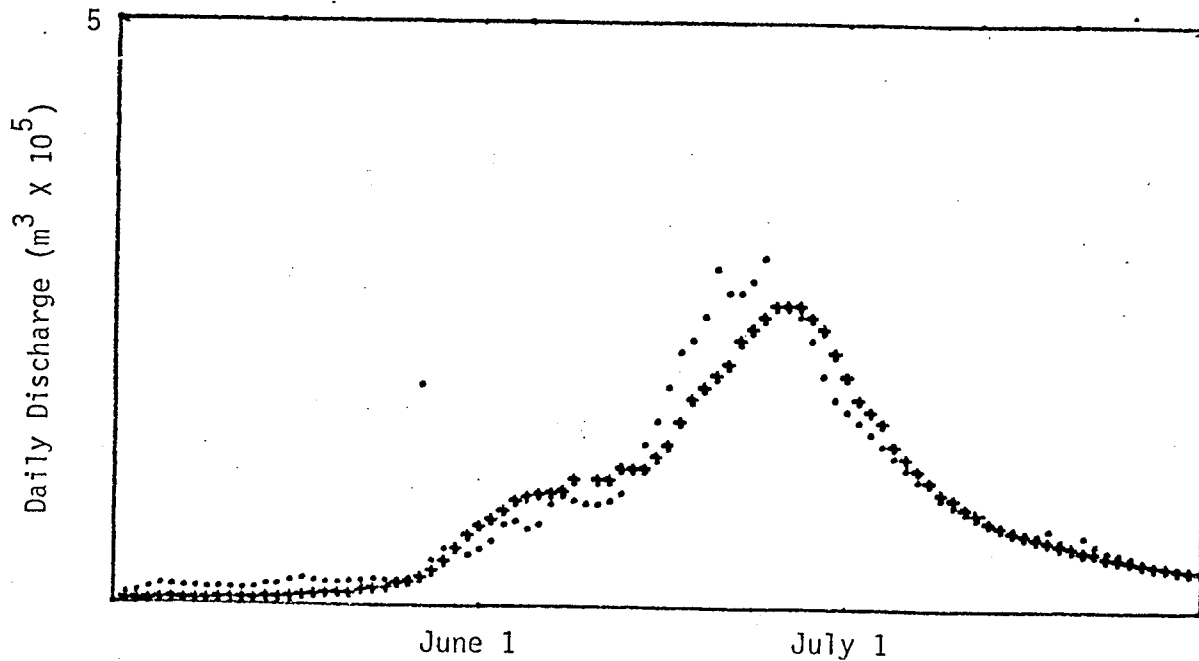
Figure 6.9. Observed (·) and Simulated (+) Hydrographs for Darling Creek After Recalibration. (WY 1971).

The dashed line in Figure 6.9 indicates the total input to all compartments. It is obvious, that the daily input without routing through soil and groundwater storages is not a good predictor of the actual streamflow.

Model Calibration and Sensitivity Analysis

The lateral flow model was initially calibrated with simulated input and observed streamflow data for 1970. Optimized values for parameters and state variables are shown in Table 6.5.

Table 6.5. Optimized Values for Parameters and State Variables in Lateral Flow Model (Equations given in Figure 6.1).

Parameter or State Variable	South Fork	Darling Creek
Watershed Area	70.4 km^2	21.2 km^2
a	1.75	1.75
b	8.00	8.00
c	5×10^{-4}	13×10^{-14}
d	2.72	2.72
Fract	0.20	0.20
GWS(initial)	$2,500,000$ m	$800,000$ m^3

Model response was found to be rather insensitive to up to 30% changes in the values of parameters a and b and the initial values were maintained.

The model was found more sensitive to the quality of the input data than the parameter values. It is believed that the model will simulate the stream hydrograph well if given input that is representative of real events in time and space (Figs. 6.7 and 6.9).

Discussion

The lateral flow model and associated computer programs for the generation of parameter decks for model operation and calculation of input to model compartments is believed to be a valuable extension to the general simulation in snowcover dynamics. The simulated hydrograph indicates how well the simulated snowmelt agrees with real events in time and also spatially within the watershed.

For other applications, such as water quality modeling, the lateral flow model could easily be applied to the simulation of lateral flow contribution to streamflow within specified sections of the stream channel.

Another possible extension would be a self-calibration option for some of the parameters in the model. This would be especially useful if the model was to be applied to several watersheds with highly variable soil moisture characteristics.

VII. SNOW MAPPING USING DIGITAL LANDSAT IMAGERY

Three satellite systems are at present of primary interest for operational snowcover mapping. These are the NOAA VHRR[1] (Very High Resolution Radiometer), GOES (Geostationary Operational Environmental Satellite), VISSR (Visible and Infrared Spin Scan Radiometer) and Landsat.

The NOAA/NESS program for operational snowcover mapping utilizes both VHRR and VISSR imagery for areal snowcover measurements for thirty basins in the United States and Canada (Schneider, 1979). Snow maps are produced from enlarged and rectified visible VHRR and VISSR imagery with about 1 km spatial resolution, using a Bausch and Lomb Zoom Transfer Scope for transferring the snow line on the image to a hydrologic basin map.

The Norwegian Water Resources and Electricity Board and IBM of Norway has developed a method for computerized snow mapping using visible NOAA VHRR or TIROS AVHRR (advanced VHRR) digital imagery (Odegaard, 1979). VHRR data received in Norway (or France) is geometrically corrected and registered to each basin of interest. Snow in each pixel (ground resolution element) is then classified into classes according to percent snowcover assuming a linear relationship between sensor response and areal snowcover.

High resolution (80 m) multispectral Landsat data has received considerable attention from hydrologist for snowcover mapping, especially on smaller watersheds. Both manual and digital mapping procedures have been described in the literature (Barnes and Bowley, 1979). Only a digital snow classifier for use with Landsat digital imagery and ancillary terrain data developed for this study will be discussed here.

Whereas data from the environmental satellites are available on a daily basis at near real time (within 20 hours in Norway), Landsat data can only be used in a quasi-operational mode until the delivery time for imagery is reduced from approximately 30 days from overflight to significantly less than a week.

---

[1]Effective early 1979, the NOAA satellite series has been replaced by the TIROS-N satellite series.

Landsat digital imagery was used for this study, but the developed programs and procedures should work equally well with lower resolution digital data from the environmental satellites. Five computer programs were developed for the processing and display of digital Landsat imagery.

1. HISTOGR - Histograms data in overlay for selected classes.

2. SYNTRAD - Calculates a synthetic band 5 image for a specified date.

3. REGISTR - Registers a Band 5 Landsat image on a synthetic image calculated for the same date automatically.

4. OVERLAY - Overlays a Landsat image on selected watersheds.

5. SNOWPCT - Classifies a Landsat scene into snowcover classes according to the areal extent of snowcover within pixels.

Ancillary data in the form of six digital terrain models with digitized map data are used in scene modeling (synthetic image) and snow classification.

1. Watershed identification numbers

2. Elevation

3. Aspect

4. Slope

5. Vegetation type

6. Vegetation density

Image Registration

Accurate image registration is important for a number of image analysis tasks. Good alignment is especially critical if multidate imagery is used for automatic detection of scene changes and for image classification using ancillary data.

Manual registration usually relies on aligning linear features that appear on both imagery and base map. Lakes, stream patterns and strong geological or cultural features are especially useful for manual registration.

Automatic techniques of high accuracy can be developed through the use of digital terrain models (Horne and Bachman, 1978). These techniques are based on matching a real image with a synthetic image created from models of surface topography, vegetation cover and solar position. Automatic techniques are area-based and, therefore, potentially more accurate than feature-based manual methods.

A method for registering Landsat data with a digital terrain model is described in the following sections.

Preprocessing for Square Pixels

A number of programs available on the Colorado State University computer systems were used for preprocessing of Landsat digital tapes. The preprocessing performed included three steps:

1. Conversion - Satellite data in the Landsat tape format is converted to a format compatible with the image processing system.

2. Filtering - This optional step smoothes Landsat data by calculating a new value for each point in the grid system by taking a weighted average of the eight surrounding points.

3. Rotation - This step is performed in order to overlay Landsat data on North-oriented maps or terrain models, eliminate image distortion due to earth rotation and data sampling rate, and convert data to square pixels (240 x 240 m). During rotation the dynamic range for the selected spectral bands were modified to an 8 bit range.

Creation of Synthetic Image

The surface reflectance model adopted for the creation of synthetic images of Landsat spectral Band 5 (0.6 - 0.7 m) has only three factors, i.e., surface "albedo", a solar irradiance and a scaling factor. Calculated radiance values are expressed in 8 bit Landsat brightness values.

$$BV = (ALB * IRR) * SCALE$$

where BV = Landsat brightness value
ALB = surface albedo as a function of surface cover type and density or elevation band.

IRR = Instantaneous direct solar radiation as a function of
surface slope inclination, elevation angle of the sun
and the different between the sun's azimuth and the
slope's aspect.

SCALE = Scaling factor (=256) that adjusts the calculated
brightness values to an 8-bit range (1-256).

Figure 3.3 shows the vegetation type overlay in gray-mapped
form. Each of the five vegetation types were divided into
three classes according to vegetation density or elevation band.
Table 7.1 shows the selected cover type classes and their associated
albedo values.

Table 7.1. Albedo Values for Selected Cover Classes

Vegetation Type	Vegetation Density (%)	Elevation Range (Feet)	Albedo (Fraction)
1. Alpine		<11,500 11,500 - 12,000 >12,000	.20 .26 .30
2. Meadow			.16
3. Aspen	0-30 31-60 61-90+		(.16)[1] (.15) (.14)
4. Lodgepole	0-30 31-60 61-90+		(.14) .13 .12
5. Spruce Fir	0-30 31-60 61-90+		(.12) .11 .10

[1]Albedo values in parenthesis are estimated.

In order to improve the visible appearance of the synthetic
image for dates with snowcover, three snow albedo values for
snowcover in 500 feet elevation bands above an estimated snowline
were included:

Band 1 = .75
Band 2 = .90
Band 3 = 1.00

Figure 7.1 shows how albedo values for cover types were estimated from a Landsat Band 5 image. A summer scene (2528-16552, July 3, 1976) with minimal snowcover was registered with the digital terrain models and brightness values for near horizontal surfaces (slopes < 16.7°) were histogrammed for the various classes. Landsat brightness values were converted into "albedo" values by dividing by the brightness value at sensor saturation (256).

Tables 7.2 through 7.5 show the instantaneous direct solar radiation calculated for the middle of the months of April through July. Radiation values for the various slopes and aspects are all calculated as fractions of the instantaneous irradiation on a horizontal surface on July 15 at the approximate time of satellite overpass (9:30 a.m.). The radiance values are calculated relative to the July date in order to be compatible with the albedo values (extracted from a July Landsat scene).

The direct incident radiation relative to a horizontal surface was calculated using the following theoretical model (Robinson, 1966).

$$\cos Z = \cos E * \sin Y + \sin E * \cos t\, Y * \cos A$$

where:

Z = Zenith angle
E = Slope inclination
Y = Elevation angle of the sun
A = Difference between the sun's azimuth and the slope's aspect.

All cos Z values shown in Tables 7.2 and 7.5 are calculated for latitude 40 N. Solar elevation and solar azimuth angles were obtained from the Smithsonian Meteorological Tables (List, 1966).

Table 7.2. Relative Direct Incident Radiation on April 15 for 40° N Latitude.
Where Solar Elevation = 44° and Solar Azimuth = 121°

Slope Class (%)	Class Midpoint (°)	N	NE	E	SE	S	SW	W	NW
0-19	5.7	.82	.88	.94	.95	.91	.84	.79	.78
20-39	16.7	.70	.90	1.06	1.09	.97	.77	.62	.59
40-59	26.6	.57	.87	1.12	1.17	.98	.68	.73	.38
60-79	30.0	.45	.84	1.15	1.21	.98	.59	.27	.21
80-99+	42.0	.34	.80	1.17	1.23	.96	.50	.13	.07

HISTOGRAM OF DATA FOR WATERSHED(S)   = 100 110 200 300

SUMMARY FOR ELEVATION ZONE = 7500-13500 FEET

RADIANCE, BAND 5

NO OF CELLS

TOTAL NUMBER OF CELLS =   413
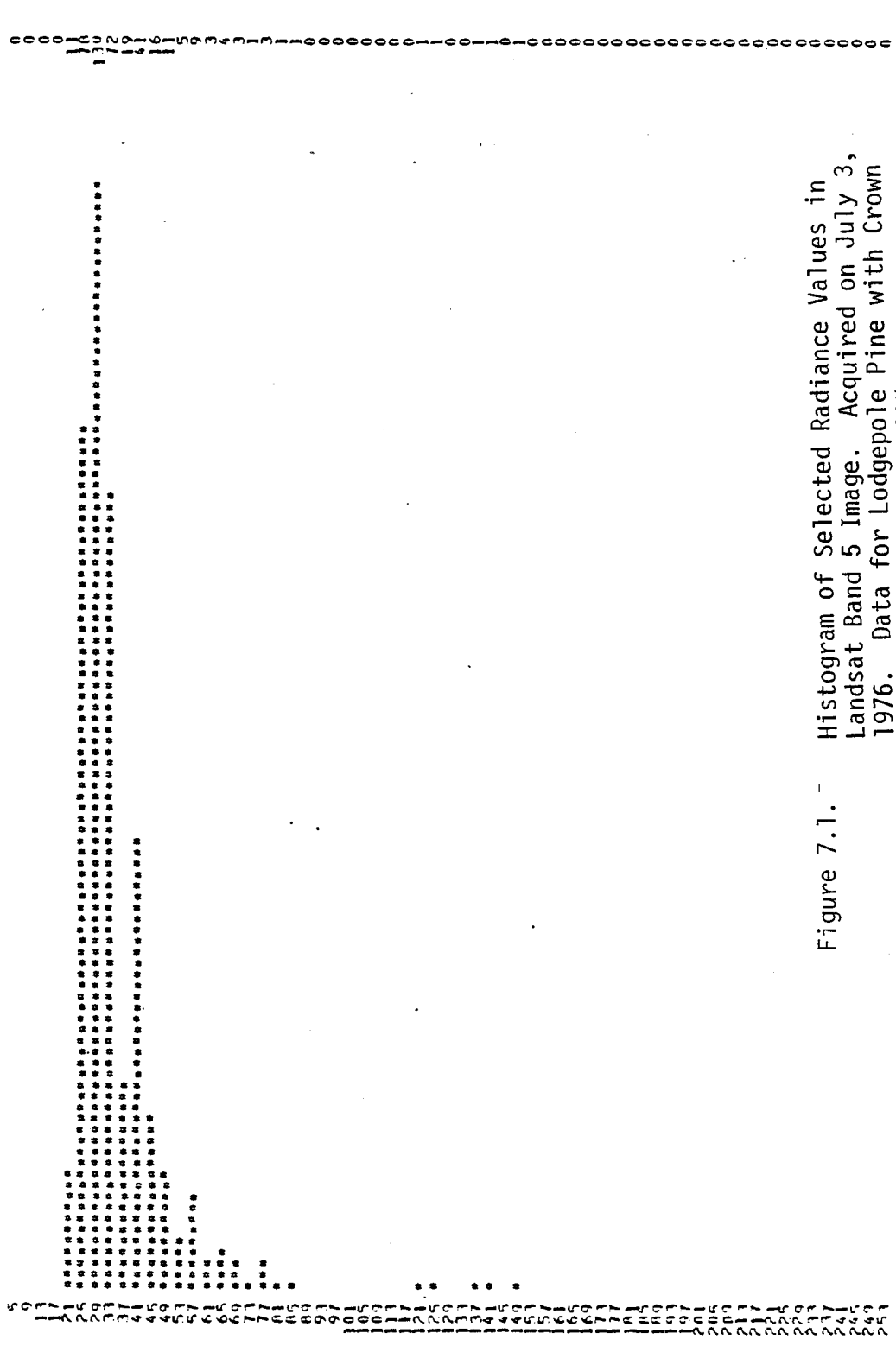
Figure 7.1. — Histogram of Selected Radiance Values in Landsat Band 5 Image. Acquired on July 3, 1976. Data for Lodgepole Pine with Crown Cover Density from 31-60%. Calculated "Albedo" = 13.

Table 7.3. Relative Direct Incident Radiation on May 15 for 40°N
Latitude,
Where Solar Elevation = 51° and Solar Azimuth = 111°,

Slope Class (%)	Class Midpoint (°)	Aspect							
		N	NE	E	SE	S	SW	W	NW
0-19	5.7	.94	.99	1.04	1.03	.98	.93	.89	.89
20-39	16.7	.85	1.02	1.14	1.13	1.01	.83	.71	.72
40-59	26.6	.74	1.01	1.19	1.18	.99	.72	.53	.54
60-79	35.0	.63	.98	1.22	1.21	.96	.62	.38	.39
80-99+	42.0	.53	.94	1.22	1.21	.91	.51	.23	.24

Table 7.4. Relative Direct Incident Radiation on June 15 for 40°N
Latitude.
Where Solar Elevation = 53° and Solar Azimuth = 108°

Slope Class (%)	Class Midpoint (°)	Aspect							
		N	NE	E	SE	S	SW	W	NW
0-19	5.7	.96	1.03	1.06	1.05	1.01	.95	.92	.92
20-39	16.7	.88	1.05	1.16	1.14	1.02	.85	.74	.76
40-59	26.6	.78	1.04	1.21	1.19	.99	.73	.57	.59
60-79	35.0	.68	1.01	1.22	1.20	.95	.62	.40	.43
80-99+	42.0	.58	.97	1.22	1.19	.89	.51	.26	.29

Table 7.5. Relative Direct Incident Radiation on July 15 for
40° N Latitude
Where Solar Elevation = 53° and Solar Azimuth = 105°

Slope Class (%)	Class Midpoint (°)	Aspect							
		N	NE	E	SE	S	SW	W	NW
0-19	5.7	.97	1.02	1.06	1.05	1.01	.95	.92	.92
20-39	16.7	.89	1.06	1.16	1.14	1.01	.84	.74	.76
40-59	26.6	.80	1.06	1.21	1.18	.97	.72	.56	.60
60-79	35.0	.70	1.03	1.23	1.19	.92	.60	.40	.44
80-99+	42.0	.61	.99	1.22	1.17	.87	.49	.25	.25

Figure 7.2 shows the synthetic image calculated for July 15 and Figure 7.3 shows the corresponding Landsat Band 5 image obtained on July 3, 1976. Both images are gray-mapped by Program GRTONES. The synthetic image appears slightly darker than the real image. This was expected for steeper slopes since only direct solar radiation is included in brightness calculations. Otherwise, the general agreement is satisfactory. The real image shows a gradual transition between forest cover and alpine areas. Because of the low quality (resolution) of the vegetation type and density data this transition is not present in the synthetic image.

Figures 7.4 and 7.5 show histograms of radiance values in the same two images for the South Fork of the Williams Fork watershed only. Grid-cells above an estimated snowline (11,750 feet) are excluded in the histograms. The histograms also show that the synthetic image is slightly darker than the real image and that a number of grid-cells in the real image are at least partially snow covered below the estimated snowline.

Registration of a Real Image with a Synthetic Image

Program REGISTR inputs a preprocessed Landsat image and a synthetic image calculated for the middle of the month of the Landsat overpass. Starting at a coordinate point specified relative to the upper left-hand corner of the synthetic image, the real image is superimposed on the synthetic image and an objective function of best registration is computed.

The objective function is simply the squared difference between overlaying grid points summed up for the entire area. Program REGISTR will calculate the objective function for coordinate starting points within a specified square area on the real image. Table 7.6 shows the results of registering the July 3 Landsat image on the corresponding synthetic image.

Manual registration of the same image was within one pixel of automatic registration both for the entire area and for the South Fork only.

Given the starting coordinate point obtained from manual or automatic registration, program OVERLAY will create a registered overlay with Landsat Band 5 radiance values for a specified area. Figure 7.3 shows the overlay for July 3, 1976 in gray-mapped form.

Figure 7.3.   Landsat Band 5   Image Acquired On
               July 3, 1976.   Eight classes from
               <40 to > 280.

Figure 7.2.   Landsat Band 5 Synthetic Image
               Calculated for July 15, 1976.
               Specified Snowline: 11,750 feet.
               Eight classes from <40 to > 280

Table 7.6. Registration Information for the Williams Fork Watershed Line 5 and Column 5 Selected as Best Relative Starting Point for Registering Landsat Image on Terrain Models.

REGISTRATION INFORMATION FOR WATERSHED(S) * 100 110 200 300

SUMMARY FOR ELEVATION ZONE * 7500-11700 FEET

LINE	COLUMN	OBJECTIVE FUNCTION
3	4	329778
3	5	294594
3	6	302054
3	7	416004
4	4	274464
4	5	193626
4	6	202707
4	7	333847
5	4	266535
5	5	179879
5	6	180711
5	7	304788
6	4	327513
6	5	243082
6	6	245759
6	7	371594
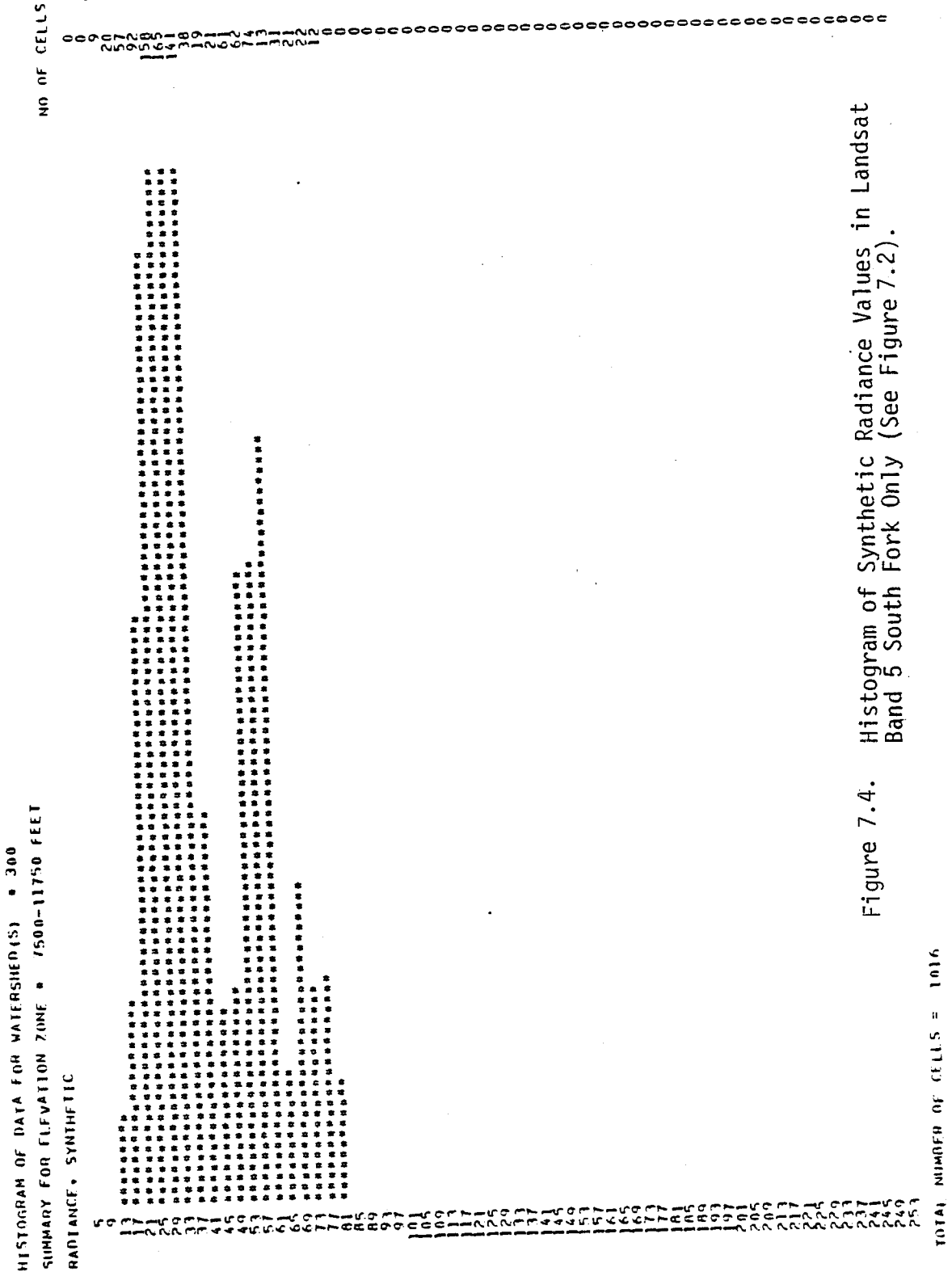
Figure 7.4. Histogram of Synthetic Radiance Values in Landsat Band 5 South Fork Only (See Figure 7.2).
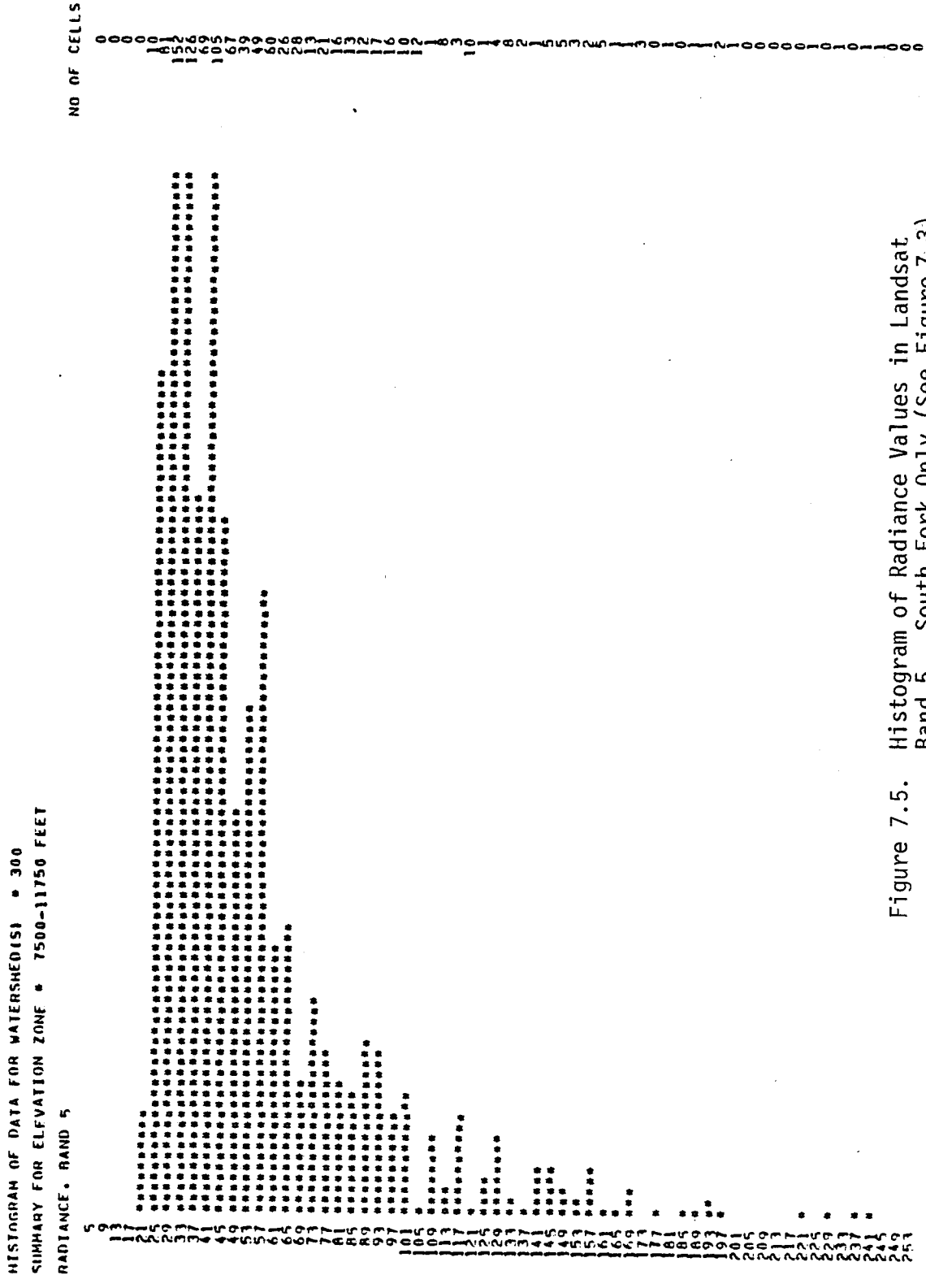
Figure 7.5. Histogram of Radiance Values in Landsat.
Band 5. South Fork Only (See Figure 7.3).

Automatic Classification of Snowcover

A snow classifier, SNOWPCT, was developed for classifying the fraction snow covered area within pixels. The classifier relies on change detection between a synthetic image calculated as being snow-free and a real Landsat image in Band 5. The synthetic image is created as discussed previously.

Figure 7.6 shows the assumed simple relationship between radiance difference and fractional snowcover. Table 7.7 shows the selected snow classes and their associated radiance difference ranges.
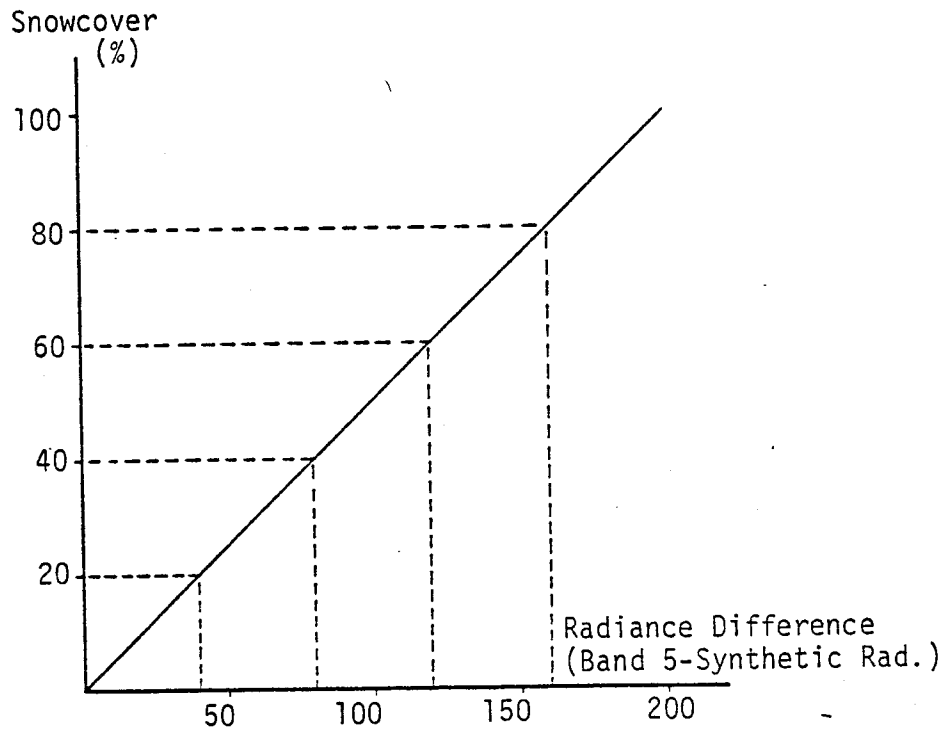
Figure 7.6. Assumed Relationship Between Radiance
Difference (Band 5-Synthetic Radiance)
and Percent Snowcover.

Table 7.7. Selected Snowcover Classes and Their Associated
Radiance Difference Ranges

Snowcover (%)	Radiance Diff, Range Rad, Counts
Less than 20	<40
20 - 39	40 - 79
40 - 59	80 - 119
60 - 79	120 - 159
Above 79	>159

Since the synthetic image is created from models of topography
and vegetation the radiance difference is assumed due to snowcover
only. Before classification, the radiance difference is normalized
for the effects of topography and image date by multiplying
the reciprocal of the relative irradiance values given in Tables
7.2 through 7.5. Program SNOPCT will adjust the radiance difference
for pixels with moderate canopy densities (<30%). Table 7.8 shows
the correction factors used.

Table 7.8. Assumed Factors for Correcting Radiance Difference
for Moderate Canopy Densities

Canopy Density (%)	Correction Factor
1 - 9	1.14
10 - 19	1.49
Above 20	2.00

Pixels with apparent snowcover will be reclassified into
clouds if their elevation is below a specified snowline, or the
crown cover density is above a specified threshold value.

Figure 7.7 and 7.8 show two examples of classified images.
One from a May Landsat overpass with almost the entire watershed
snow covered and another from a July overpass with little snow
present in the image. The images were not filtered before class-
ification. Table 7.9 and 7.10 show classification statistics for
the same two dates.

Figure 7.8. Map of Snowcover on July 3, 1976. Areas with Crown Cover Densities Above 50% Not Classified. Five Classes from <20 to >79 Percent.
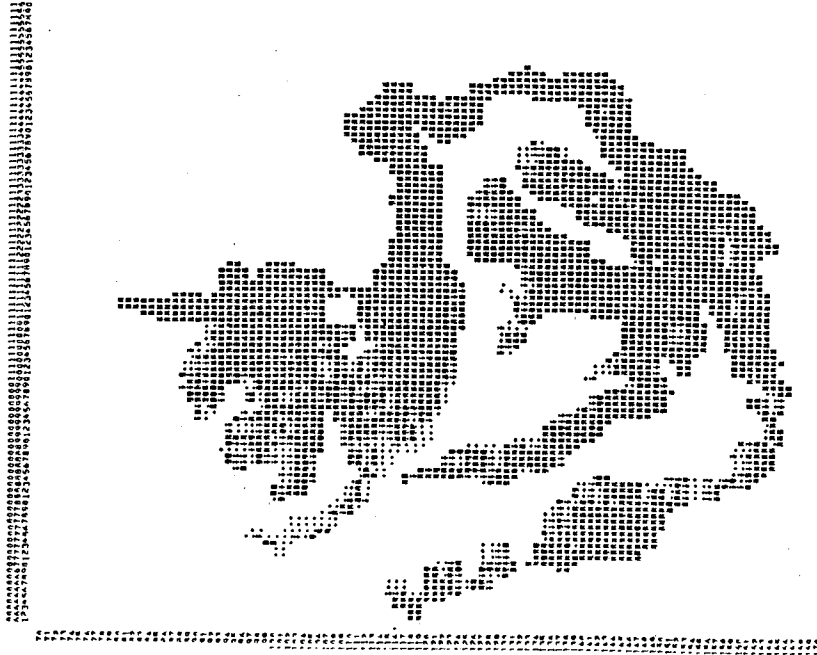
Figure 7.7. Map of Snowcover on May 1, 1976. Areas with Crown Cover Densities Above 50% Not Classified. Five Classes from <20 to >79 Percent.

Table 7.9. Classification Statistics for Landsat Band 5 Image
            Acquired on May 1, 1976. (See Figure 7,7)

CLASSIFICATION STATISTCS FOR WATERSHED(S) • 100 110 200 300

SUMMARY FOR ELEVATION ZONE • 7500-13500 FEET

CLASS		NO OF CELLS	PERCENT AREA
0 =	NOT CLASSIFIED OR CLOUD	0	0.0
1 =	LESS THAN 20 PCT SNOW	104	4.2
2 =	20-39 PCT SNOW	187	7.6
3 =	40-59 PCT SNOW	190	7.7
4 =	60-79 PCT SNOW	216	8.8
5 =	MORE THAN 79 PCT SNOW	1756	71.6

Table 7.10. Classification Statistics for Landsat Band 5 Image
             Acquired on July 3, 1976. (See Figure 7.8)

CLASSIFICATION STATISTCS FOR WATERSHED(S) • 100 110 200 300

SUMMARY FOR ELEVATION ZONE • 7500-13500 FEET

CLASS		NO OF CELLS	PERCENT AREA
0 =	NOT CLASSIFIED OR CLOUD	0	0.0
1 =	LESS THAN 20 PCT SNOW	1617	65.9
2 =	20-39 PCT SNOW	371	15.1
3 =	40-59 PCT SNOW	198	8.1
4 =	60-79 PCT SNOW	103	4.2
5 =	MORE THAN 79 PCT SNOW	164	6.7

Discussion

The system described for digital processing of Landsat imagery for snowcover mapping is considered operational (although it is not yet validated through comparison with larger scale imagery and other ground-truth). A trained operator should be able to do the processing of a large watershed within one working day after receiving the Landsat digital tape. The most time consuming task (using Colorado State University image processing software) is the preprocessing of the raw imagery. This uses about three-fourth of the total processing time.

The described snow classifier will detect clouds if certain conditions are satisfied (i.e., forest cover above a specified density). For processing of Landsat Data D data, when it becomes available in 1981, a routine for spectral cloud classification can be included utilizing the 1.55 - 1.75 µm cloud detection channel together with a visible channel.

VIII. SIMULATION UPDATE WITH SNOW COURSE MEASUREMENTS
AND CLASSIFIED LANDSAT IMAGERY

Imagery from Landsat and lower resolution environmental satellites has been used by other investigators for updating snowcover simulation. Usually the snow-covered area within a watershed is first found from manual or machine-aided interpretation of satellite imagery. The areal snowcover is then directly input to the simulation model (Dillard, 1979) or used in estimating the water equivalent of snowpack (Shafer, 1979).

The update procedures described here differ in that simulated snowcover is directly updated on a pixel basis. Thus, more of the information content in the imagery is utilized.

Landsat imagery is only useful for simulation update when snowmelt is in progress and the watershed only partly snow covered. Procedures for updating the accumulating snowcover with snow course measurements are also described.

Update with Snow Course Measurements

Simulated relationships between elevation, aspect and snow-water content for a given date were used in relating snow course measurements to areal distribution of snow-water content. The water balance model, WATBAL, was operated with climatic data for wateryear 1971 and simulaed snow-water content on April 1 and May 1 were used in the analysis.

Computer program HISTO2 was developed to histogram snow-water content as a function of elevation for a given aspect. Figures 8.1 and 8.2 show examples of output from this program. Figure 8.1 gives the distribution of simulated snow-water equivalent for northeast facing aspects on June 1, 1971. Figure 8.2 gives the similar distribution for southwest facing aspects. It is seen that the coldest slopes (NE) have retained much more snow than the warmest slopes (SW) on this date. The effect of aspect on snow depth during the early snowmelt season is less pronounced, although still important, especially for SW facing slopes.

Curves showing the simulated snow-water equivalent on April 1 and May 1 (Figs. 8.3 and 8.4) were constructed from histograms generated by HISTO2. Only three aspect classes were defined. No systematic differences in snow-water content as a function of elevation were found within these classes.

Measurements from four snow courses within or near the study area were combined to form an index of observed snow-water content. The snow courses with elevations near the mean elevation of the

HISTOGRAM OF DATA FOR WATERSHED(S)   = 100 110 200 300

SUMMARY FOR ELEVATION ZONE = 7500-13500 FEET

SNOW DEPTH, IN

NO OF CELLS   MEAN VALUE
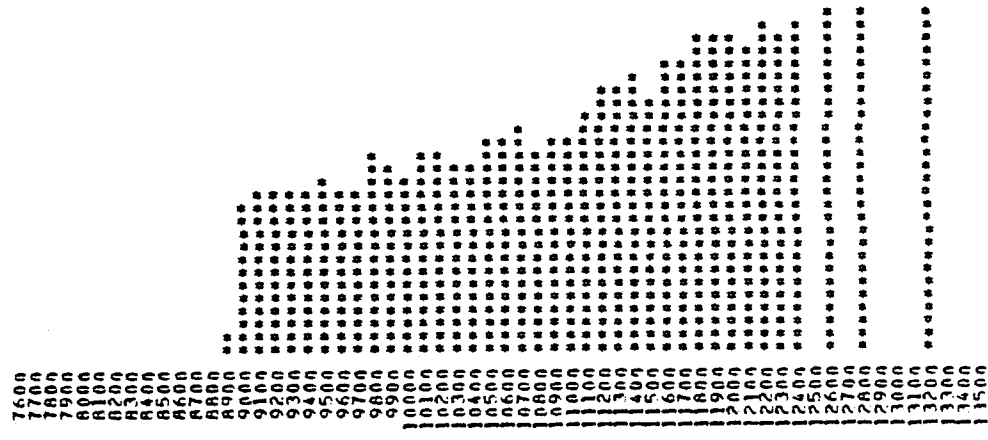
TOTAL NUMBER OF CELLS = 600

Figure 8.1.   Histogram of Simulated Snow-Water Content for NE Aspects on June 1, 1971.

HISTOGRAM OF DATA FOR WATERSHED(S)   = 100 110 200 300

SUMMARY FOR ELEVATION ZONE = 7500-13500 FEET

SNOW DEPTH, IN

NO OF CELLS   MEAN VALUE

TOTAL NUMBER OF CELLS = 613
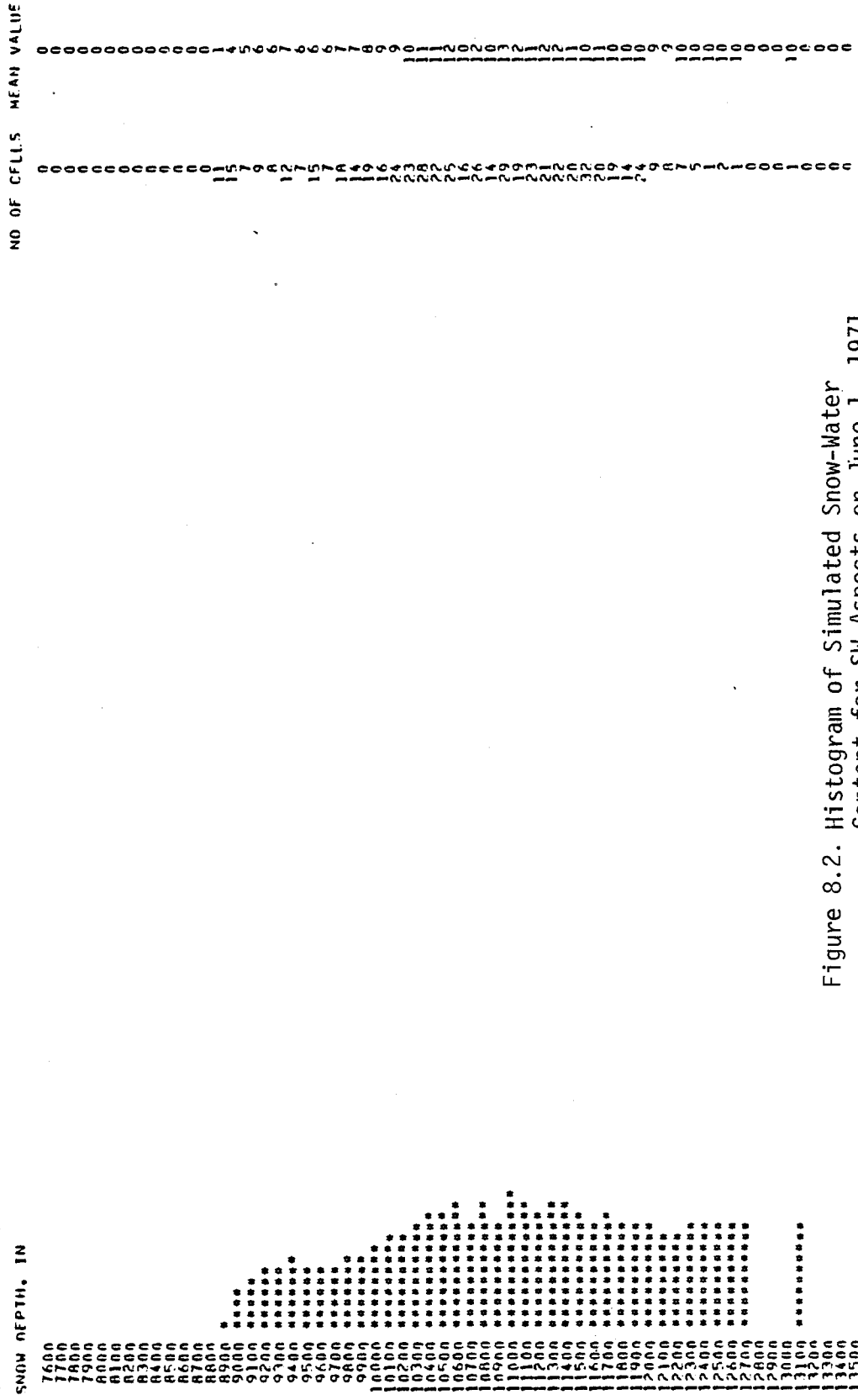
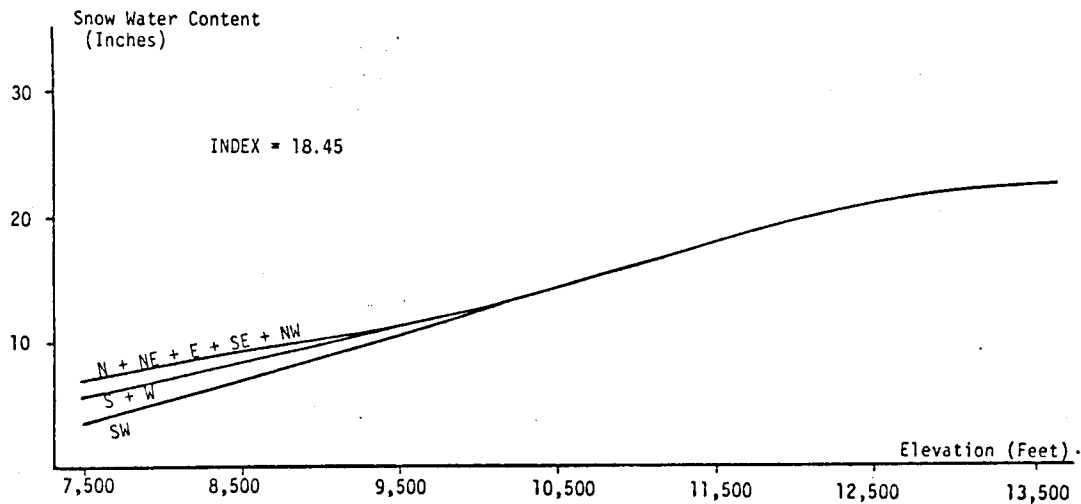Figure 8.2. Histogram of Simulated Snow-Water Content for SW Aspects on June 1, 1971.

Figure 8.3. Simulated Snow-Water Content for Aspects on
April 1, 1971. Snow-Cover Index = 18.45.
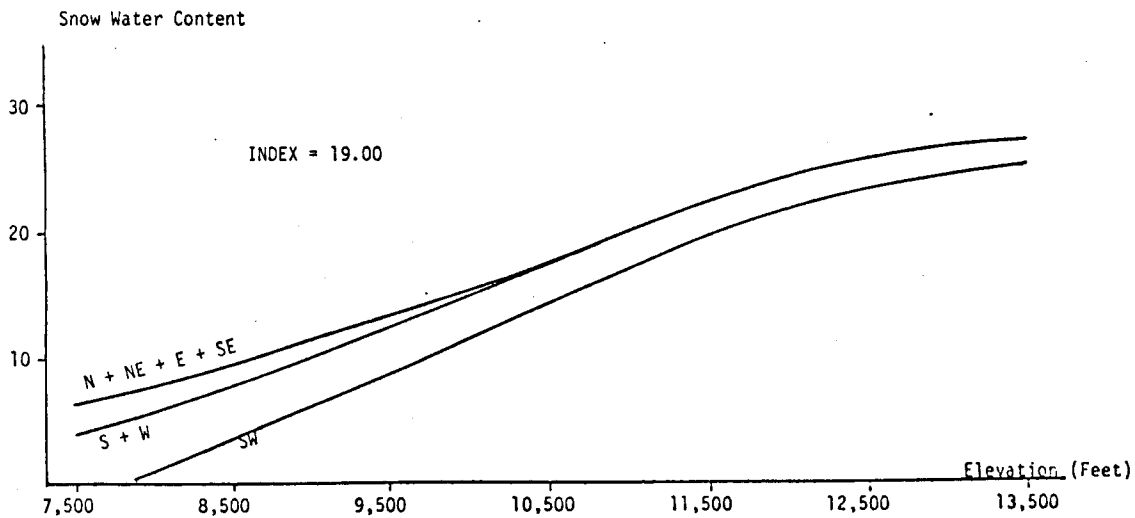
Figure 8.4. Simulated Snow-Water Content for Aspects on
May 1, 1971. Snow Cover Index = 19.00

watershed (No. 05K14S at Berthoud Summit (11,300 feet) and No. 05K21 at Jones Pass (10,400 feet)) were weighted by a factor of 2 and the snow courses with lower elevations (No. 05K04 at Middle Fork (9,000 feet) and No. 06K20 at Glen Mar (8,870 feet)) were weighted by a factor of 1 in calculating the index of snow depth.

Factors relating calculated snow indices and the curves of water content (Figs. 8.3 and 8.4) are given in Table 8.1 and 8.2. For a given year and date these factors are used for predicting water content at any point in the watershed from an index of snow course measurements.

Table 8.1. Factors for Converting a Snow-Water Index to Snow-Water Content on April 1.

Elevation (Feet)	Aspect							
	N	NE	E	SE	S	SW	W	NW
7,500	.40	.40	.40	.40	.32	.20	.32	.40
8,500	.51	.51	.51	.51	.47	.38	.47	.51
9,500	.62	.62	.62	.62	.60	.57	.60	.62
10,500	.78	.78	.78	.78	.78	.78	.78	.78
11,500	.98	.98	.98	.98	.98	.98	.98	.98
12,500	1.13	1.12	1.13	1.13	1.13	1.13	1.13	1.13
13,500	1.20	1.20	1.20	1.20	1.20	1.20	1.20	1.20

Table 8.2. Factors for Converting a Snow-Water Index to Snow-Water Content on May 1

Elevation (Feet)	Aspect							
	N	NE	E	SE	S	SW	W	NW
7,500	.34	.34	.34	.34	.21	.00	.21	.34
8,500	.51	.51	.51	.51	.43	.20	.43	.51
9,500	.69	.69	.69	.69	.65	.46	.65	.69
10,500	.92	.92	.92	.92	.91	.75	.91	.92
11,500	1.16	1.16	1.16	1.16	1.16	1.02	1.16	1.16
12,500	1.34	1.34	1.34	1.34	1.34	1.34	1.34	1.34
13,500	1.43	1.43	1.43	1.43	1.43	1.43	1.43	1.43

The updated snow-water content is calculated as the weighted mean of the simulated water content and water content calculated from the snow index. The weights can be specified by the user (equal weights were used for the runs included here) according to the level of confidence in the two-data sources. Simulated snow-temperatures are adjusted to probable minimum values specified by the user, if pixel temperatures are unrealistically low. Predicted soil moisture deficit can also be adjusted, by the user.

Figures 8.5 and 8.6 show the effect of updating the simulation used in the developing update procedures on May 1, 1971. Update on this date improved simulation slightly due to a reduction (intended) of snowcover at lower elevations by the idealized snowcover curves (Fig. 8.4). Update on April 1 did not change the simulation.

Overlays with updated parameter values (snow-water content, snow temperature and soil moisture deficit) were created after the update on May 1, 1971. The parameters are shown in gray-mapped form in Figures 8.7, 8.8 and 8.9.

Simulation runs with 1972 and 1973 climatic data were updated with snow course data on April 1. Update improved the simulation of 1972 (a low runoff year) slightly by reducing the amount of snow on the date of update (Figs. 8.10 and 8.11). The simulation of the hydrograph for 1973 (a high runoff year) was not improved by simulation update (Figs. 8.12 and 8.13).

Update with Classified Landsat Imagery

Snow in Landsat imagery was classified into percentage snow-cover classes as described in Chapter VII. Relationships between fractional snowcover and water content of snowpack had to be assumed (Fig. 8.14) because no Landsat images were available during the middle of the snowmelt season. The available images were either from early spring (fully snow covered) or late in the season (scattered snowcover). Furthermore, the functional relationship between snowcover and water content is likely to vary with location (topography) time of year and past history of snowpack.

For the update runs included here a particular snowcover/snow depth curve from the family of curves shown in Figure 8.14 was selected by comparing gray-maps of the classified Landsat image and the simulated water content. The selection can be further improved by considering the accumulated precipitation up to the date of update, storms during the late snowmelt season, etc.
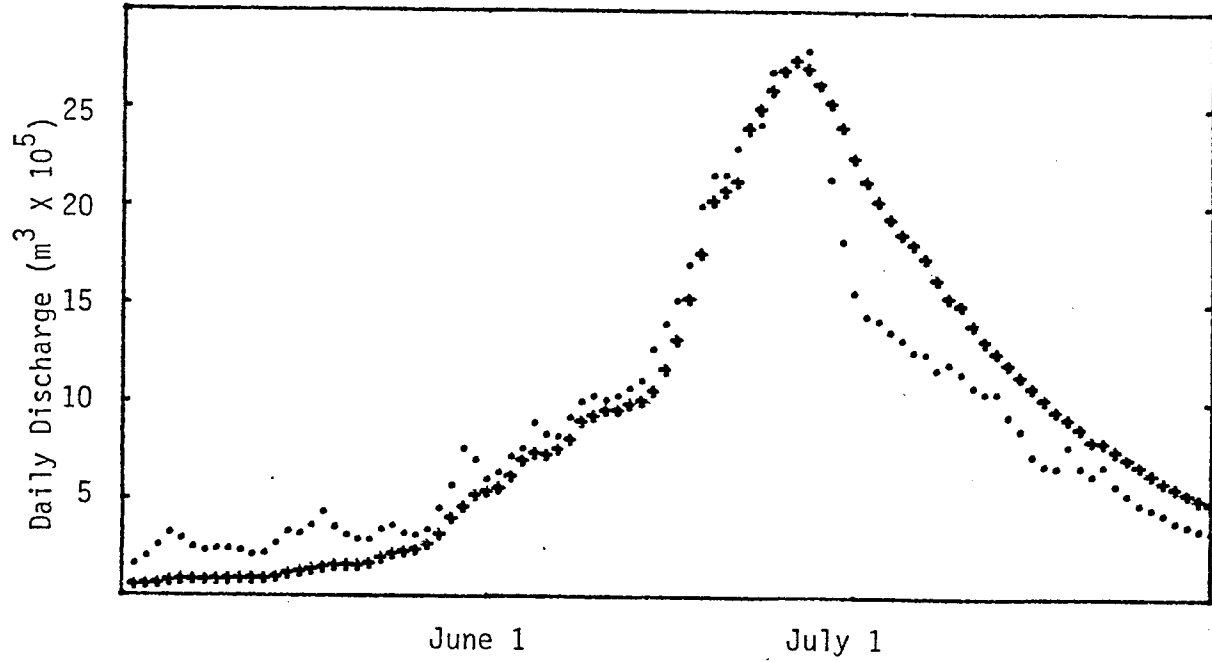
Figure 8.5.   Observed (·) and Simulated (+) Hydrographs for
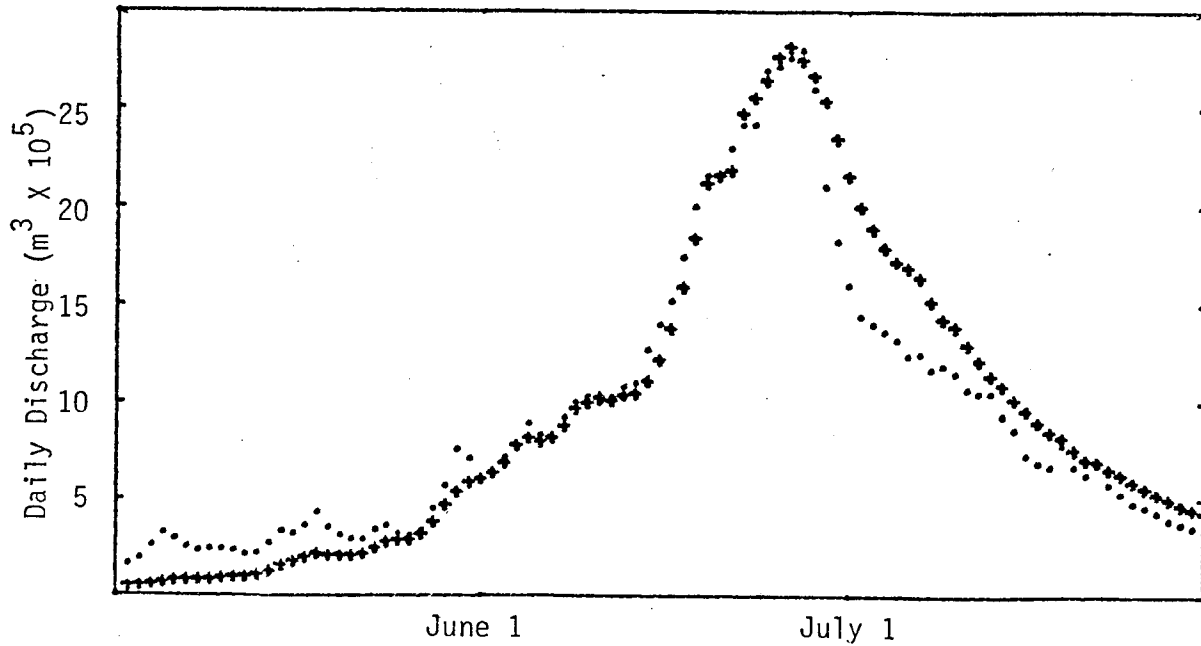   Williams Fork Watershed - Spring 1971.

Figure 8.6.   Observed (·) and Simulated (+) Hydrographs for
              Williams Fork Watershed. Simulation Updated
              on May 1, 1971.

Figure 8.8. Gray Map Simulated Mean Snow
Temperature After Update.
Simulation Updated on May 1, 1971.

Figure 8.7. Gray-Map of Simulated Snow-
Water Content After Update.
Simulation Updated on
May 1, 1972.

Figure 8.9. Gray-Map of Simulated Soil Recharge Requirement
After Update. Simulation Updated on May 1, 1971.
Eight Classes From <0.6 to >3.5 inches

Figure 8.10   Observed (·) and Simulated (+) Hydrographs for
Williams Fork Watershed - Spring 1972.

Figure 8.11   Observed (·) and Simulated (+) Hydrographs for
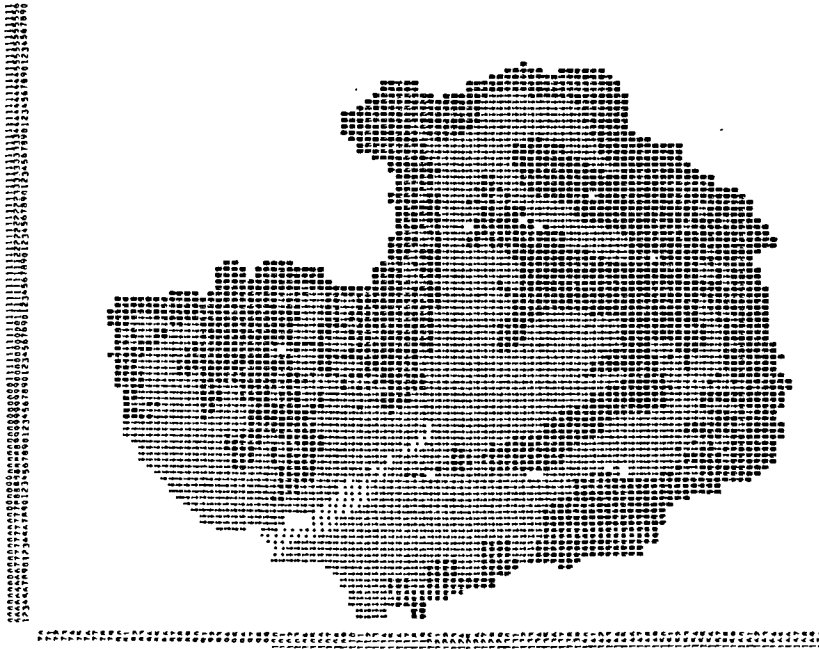Williams Fork Watershed.
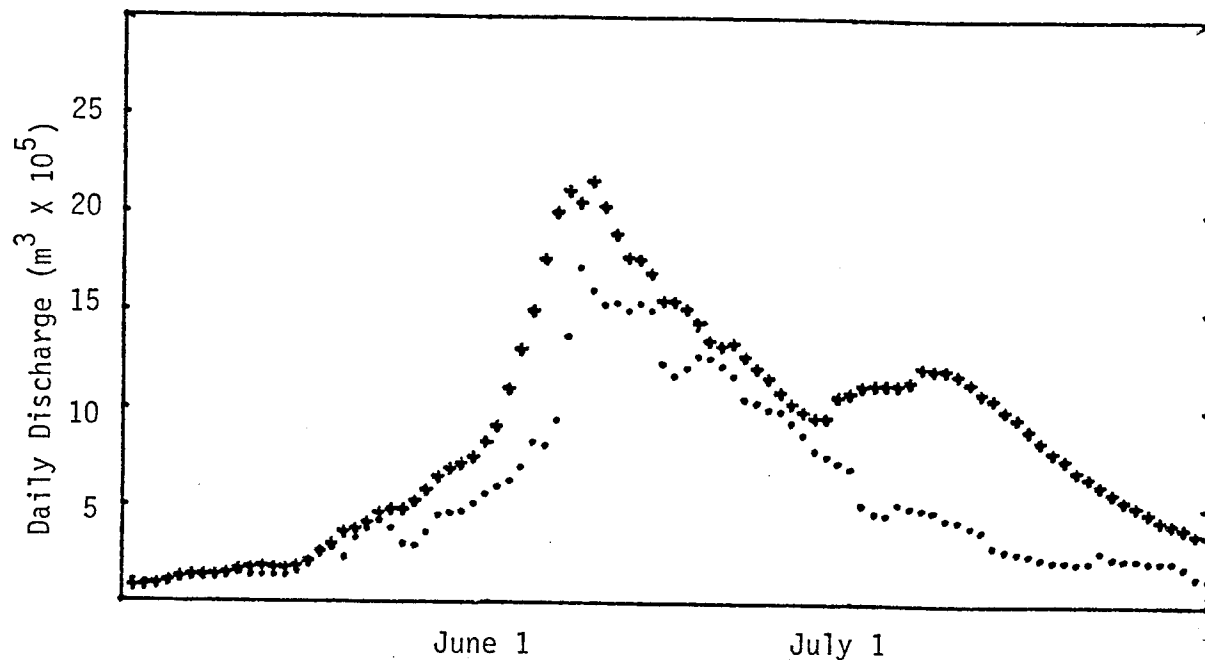Simulation Updated on April 1, 1972.

Figure 8.12. Observed (·) and Simulated (+) Hydrographs
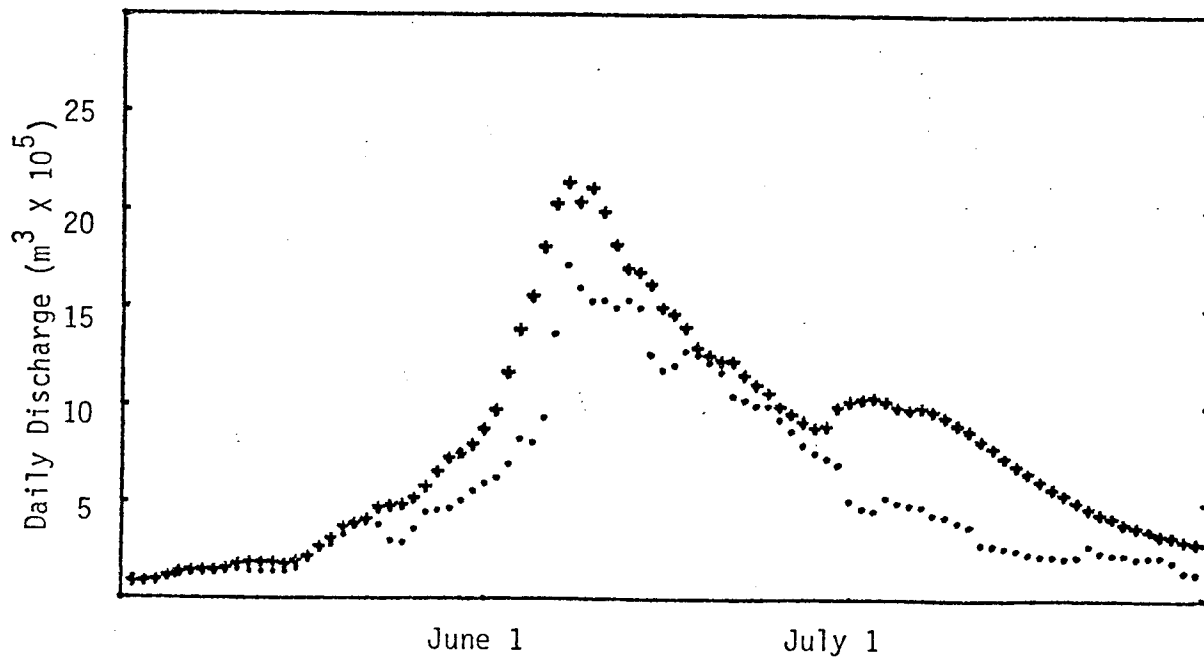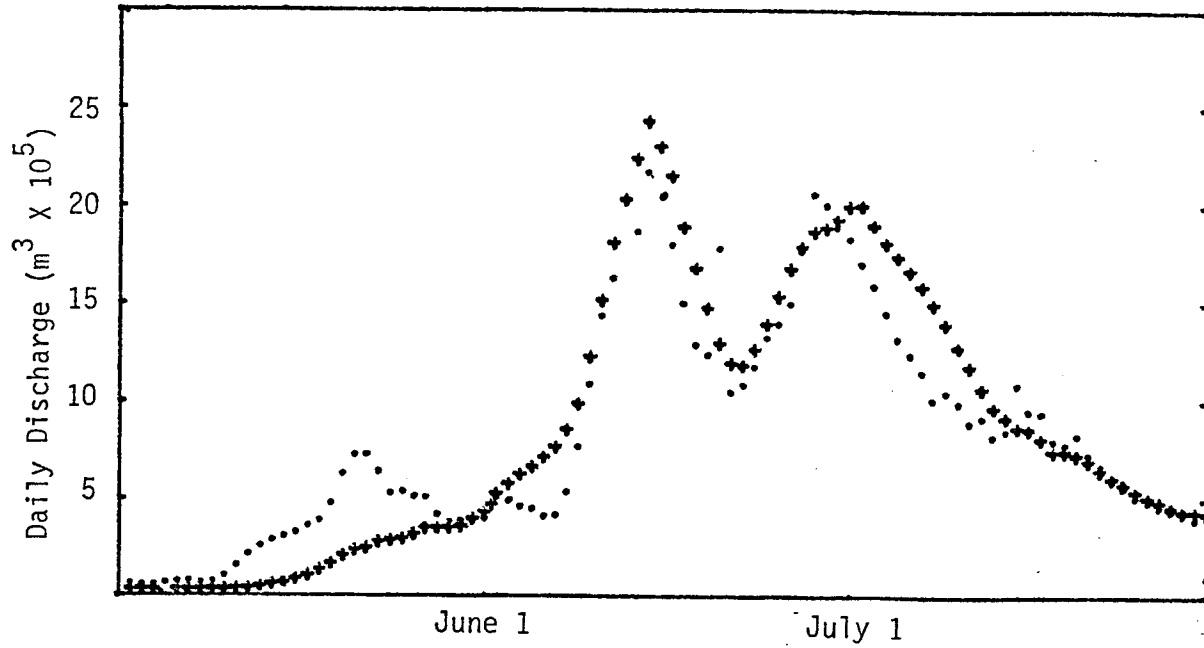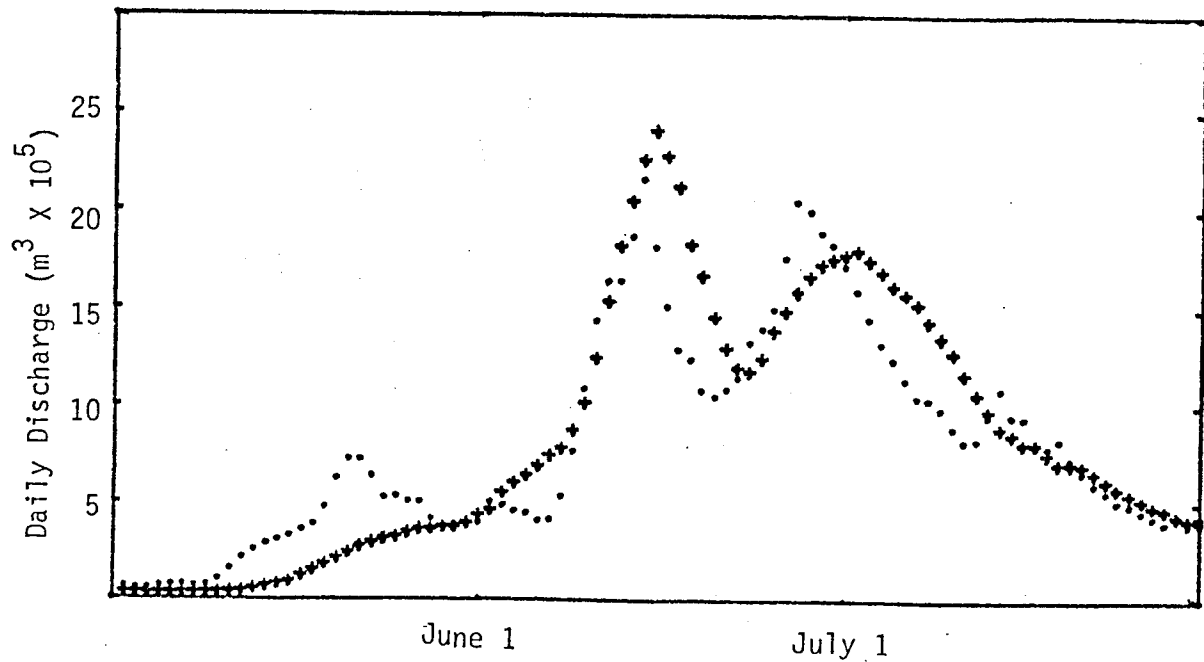for Williams Fork Watershed - Spring 1973.

Figure 8.13   Observed (·) and Simulated (+) Hydrographs for
Williams Fork Watershed.
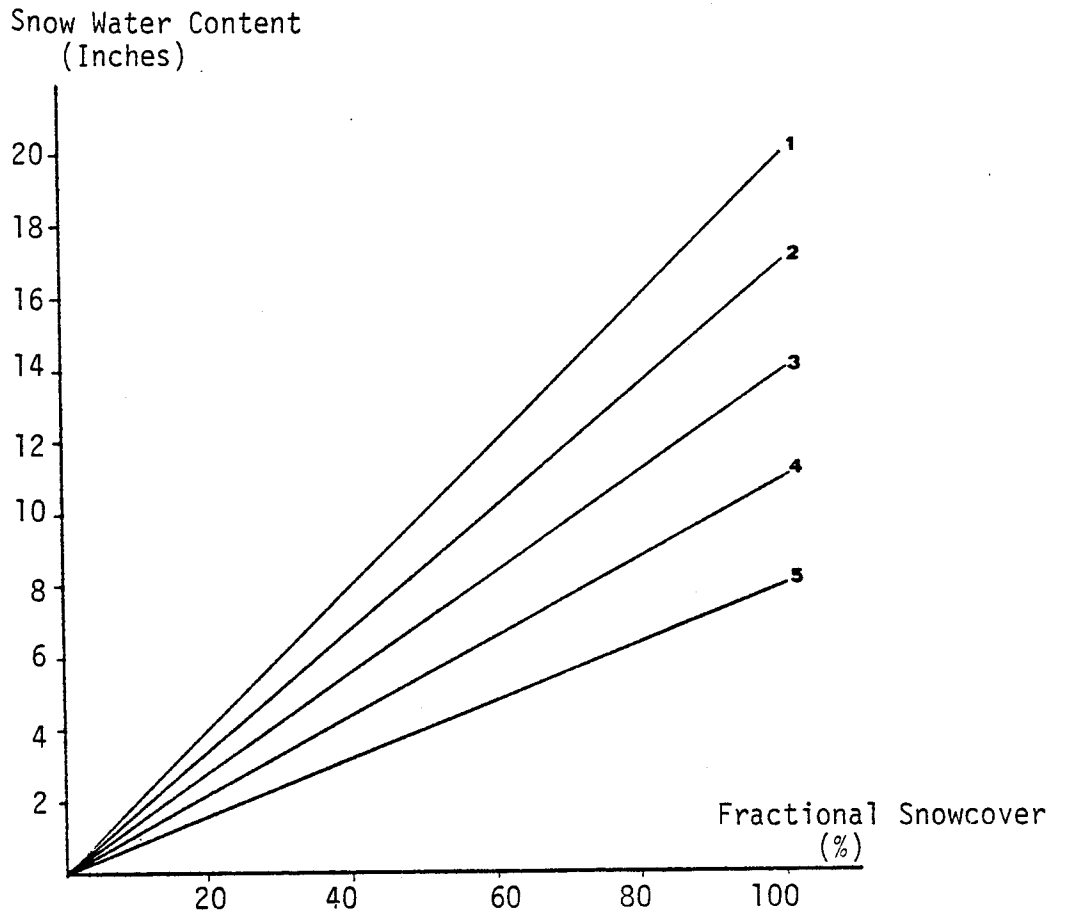Simulation Updated on April 1, 1973.

Figure 8.14. Assumed Relationships Between Fractional Snowcover Within Landsat Pixels and Snow-Water Content.

Update is performed by computer program UPDATE2, UPDATE2 is similar to UPDATE1 described previously. The only difference being the form of the snowcover data used in updating the simulation. Figure 8.15 shows a flow chart of a complete simulation run including the update option.

Suitable Landsat imagery with none to moderate cloud cover was available for 1976 only. The results from using both snow course measurements and Landsat imagery for simulation update are summarized in Table 8.3.

Table 8.3. Summarized Results from Using Snow Course Measurements and Landsat Imagery for Simulation Update on May 1, 1976.

Update Option	Simulated Runoff (Inches)
1. No Update or Recalibration	13.93
2. Update with Index of Snow Course Measurements	13.67
3. Update with Landsat Imagery Using Curve 2 in Figure 56.	13.15
4. Update with Landsat Imagery using Curve 3 in Figure 56.	12.79

Recorded runoff for wateryear 1976: 13.11 inches.

It is seen, that update using both snow course measurements and Landsat imagery improved the simulation of annual runoff for wateryear 1976.

Discussion

The spatially distributed approach to the simulation of snow processes offers possibilities of direct simulation update on a pixel basis, if periodical remotely sensed (or other form of) snowpack information is available in overlay form or as point measurements. The developed procedures and computer programs for simulation update were primarily intended to work with spatially distributed snowcover data (water equivalent, temperature). Since this data is not readily available, the update procedures were modified to accept point measurements of snow-water equivalent (snow course measurements) and fractional snowcover within pixels (classified Landsat imagery) as inputs.
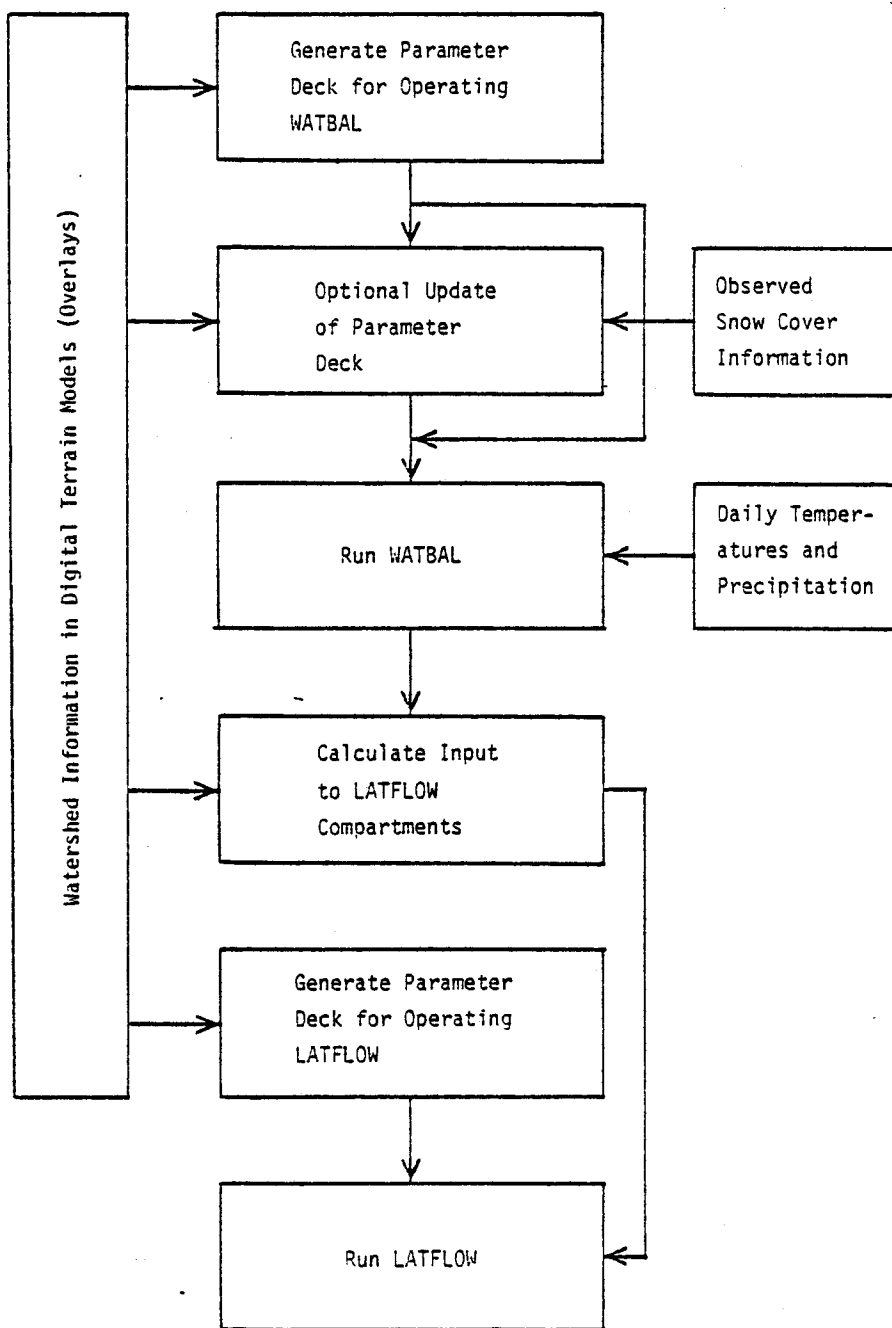
Figure 8.15. Flow Chart of Complete Simulation Run
Including the Update Option.

Snow-course measurements obtained in April during the late snow accumulation phase and Landsat imagery acquired during the later half of the snowmelt season have the greatest potential for improving the prediction of spring runoff from snowmelt.

Besides Landsat imagery and traditional snow course measurements lower resolution imagery from environmental satellites and data from aerial gamma surveys could be used as well for simulation update, once the data is properly formatted.

IX. SUMMARY AND CONCLUSIONS

This report presents a watershed information system designed for the analysis and simulation of hydrologic processes on mountain watersheds. The system is unique in that it utilizes a spatially variable data base and simulates hydrologic processes using this information.

The first step in the analysis procedure is to digitize watershed information using available data sources such as topographic maps, vegetation and soils maps, aerial photography, and remote sensing imagery. Data are digitized on a grid cell basis. For purposes of this study, of the Williams Fork Watershed in western Colorado, a grid cell size equivalent to 1 cm x 1 cm on a 1:24,000 USGS topographic map was selected. This covers an area of 5.76 ha. Other grid cell sizes can be used. However, it is necessary that the gridded maps correspond exactly. That is, a grid cell on one map should have an identical cell on all other maps.

Using Program INGRID, digitized data sets are read into the computer to establish files or overlays of computerized map data. Additional overlays can be created. For example, using a soil type overlay for the watershed and known characteristics of the various soil types, additional overlays displaying wilting point, field capacity, and water holding capacity can be created. Data sets or overlays required for hydrologic simulation include watershed physiography (slope, aspect, distance to stream), vegetation (type and density), and soils (type, characteristics). Overlays can be displayed as computer printed gray-maps.

To simplify calculations, grid cell elements are combined into homogeneous hydrologic response units (HRU's) based on slope, aspect, vegetation type and elevation zone. Hydrologic simulation is calculated on an HRU basis.

The second step is the hydrologic simulation using the spatial data system. Parameters to operate the model are derived automatically from the digital overlays using program PARAM. The main water balance subroutine (WATBAL) is a modified version of the Leaf-Brink Subalpine Watershed Model. This model does the water balance accounting as well as the snow accumulation and melt calculations. Output from the simulation includes daily snowmelt, snowpack water content, snowcover, snowpack temperature, etc. Output can also be displayed in a gray-map form.

Water from melting snowpack or rainfall is routed downslope, either as surface or subsurface flow, to the channel. The summation of all flow increments added to the channel equals the daily streamflow volume.

Options available to the users include an update capability. A simulation run can be interrupted and adjusted to account for new information. Update options include inputing snow course data or remote sensing snowcover data.

The spatial data system has several distinct advantages. First, hydrologic processes are simulated for a wide range of conditions occurring on the watershed. It is possible to compare snowpack characteristics on north and south slopes, or under dense forest versus open forest versus alpine tundra, since hydrologic processes are simulated for the full range of conditions existing on the watershed. Similarily, it is possible to predict the effect of a change in the watershed surface such as timber harvest or a fire, simply by changing the appropriate overlays to reflect the change.

Perhaps one of the most promising applications of the watershed information system is its ability to utilize remote sensing data in the simulation process. Since remote sensing imagery is also a spatially variable data set which may already be in a digital form, it is necessary only to superimpose an appropriate grid corresponding to the overlay grid base. Remote sensing imagery can, therefore, be used to provide basic overlay data (vegetation type, vegetation density, etc.) or to provide timely information for update purposes. The application of remote sensing technology is limited only by the limitations of existing sensors to provide appropriate information.

Based on the results of this study, the following conclusions can be made.

1. The watershed information system developed is potentially a highly useful tool for watershed management, snowmelt forecasting, and resource management decisions once the initial overlays have been prepared, repeated simulation and comparisons can be made with only a modest investment in computer time and data preparation.

2. The application of remote sensing to hydrologic simulation appears to have its chief utility as a source of information concerning watershed surface characteristics and as a means of providing timely information for remote watershed areas. Although remote sensing technology has advanced greatly in the past five years, it remains an important but secondary source of data rather than a primary source. The hydrologic simulations of this study were found to be highly sensitive to the quality of the driving data. In particular, precipitation amounts and distribution and air temperatures still must be measured on the ground for best results.

Papers, Reports, Thesis Originating from this Study

Striffler, W. D. and Diane Fitz, 1980. Application of remote sensing in hydrology. Final Report, Part I. Environmental Resource Center Completion Report No.   Colorado State University,   pp.

Thomsen, Anton G. and W. D. Striffler, 1980. A watershed information system. Final Report, Part II. Environmental Resources Center Completion Report No.   , Colorado State University   pp.

Thomsen, Anton G. and W. D. Striffler, 1979. Hydrograph simulation with spatially distributed input. Paper presented at American Geophysical Union Fall Meeting, December 1979 (Abstract Published in EOS 60(46): 819, November 13, 1979).

Thomsen, Anton G. and W. D. Striffler, 1980. A watershed information system. Proc. of Western Snow Conference, Laramie, Wyoming, April 15-17, 1980 (In Press).

Thomsen, Anton G. and W. D. Striffler, 1980. Spatial simulation of snow processes. Symposium on Watershed Management, Vol. I, p. 326-334. Sponsored by ASCE, Boise, Idaho, July 21-23, 1980.

Hogg, Susan E., Anton G. Thomsen and W. D. Striffler, 1980. A baseflow simulation model. Symposium on Watershed Management, Vol. II, p. 755-763, Sponsored by ASCE, Boise, Idaho, July 21-23, 1980.

Thomsen, Anton G. and W. D. Striffler, 1980. Spatial simulation of snow processes. Submitted to NORDIC HYDROLOGY.

Pernia, Jose, E., 1978. Hydrologic parameters from Landsat imagery for William Fork Watershed, MS Thesis, Department of Civil Engineering, Colorado State University, 124 pp.

Thomsen, Anton G., 1980, A watershed information system, Ph.D. Thesis Department of Earth Resources, Colorado State University, 160 pp.

Fitz, Diane C., 1980. Application of remote sensing in hydrology, Masters Paper, Department of Earth Resources, Colorado State University, 132 pp.

REFERENCES

Amidon, Elliot, L. Computer Mapping Systems for Integrated
    Resource Inventories. Paper presented at the National
    Workshop on Integrated Inventories of Renewable Natural
    Resources, Tucson, Arizona, January 18-21, 1978.

Barnes, J. C. and C. J. Bowley, 1979. The Evaluation of
    Satellite Snow Mapping with Emphasis on the Use of
    Landsat in the Snow ASVT Study Areas. Presented at
    the Workshop on Operational Applications of Satellite
    Snowcover Observations, Reno, Nevada, 1979.

Dillard, John P. and Charles E. Orwig. Use of Satellite Data
    in Runoff Forecasting in the Heavily Forested, Cloud-
    Covered Pacific Northwest. Presented at Final Workshop
    on the Operational Applications of Satellite Snowcover
    Operations. April 16-17, 1979, Sparks, Nevada.

Foyster, Angela M. Application of the Grid Square Technique to
    Mapping Evapotranspiration. Journal of Hydrology, 19(1973)
    205-226.

Frank, Ernest C. and Richard Lee, Potential Solar Beam Irradiation
    on Slopes. Tables for 30° to 50° Latitude. U.S.D.A. Forest
    Service, Research Paper RM-18, 1966. 116 pp.

Hillel, Daniel. Soil and Water: Physical Principles and Processes.
    Physiological Ecology, Academic Press, Inc., Second Printing,
    1972. 288 pages.

Horne, B.K.P. and B. L. Bachman, 1978. Using Synthetic Images to
    Register Real Images with Surface Models. Comm. ACM 21, 11
    914-924, November 1978.

Judson, Arthur, Climatological Data from the Berthoud Pass
    Area of Colorado, U.S.D.A. Forest Service, General Technical
    Report RM-42, October 1977, 94 pp.

Kirkby, M. J., Editor. Hillslope Hydrology. John Wiley and
    Sons. 1978. 389 pages.

Leavesley, George H. Dissertation: A Mountain Watershed Simulation
    Model. Colorado State University, December 1973, 174 pages.

Leaf, Charles F. and Glen E. Brink, Hydrologic Simulation Model of
    Colorado Subalpine Forest, U.S.D.A. Forest Service, Research
    Paper RM-107, May 1973. 23 pages.

Leaf, Charles F. and Glen E. Brink, Land Use Simulation Model of the Subalpine Coniferous Zone. U.S.D.A. Forest Service, Research Paper RM-135, February 1975. 42 pages.

List, R. S., Ed., Smithsonian Meteorological Tables, 6th Revised Ed. 1966. Smithsonian Institute, Washington, D. C., 527 pages.

Odegaard, H. A., 1979. Applications of Satellite Data for Snow Mapping in Norway. Presented at the Workshop on Operational Applications of Satellite Snowcover Observations. Reno, Nevada, April 1979.

Robinson, N., Solar Radiation, Elsivier Publishing Co., NY 1966, 347 pages.

Schneider, S. R., 1979. The NOAA/NESS Program for Operation Snowcover Mapping: Preparing for the 1980's. Presented at the Workshop on Operational Applications of Satellite Snowcover Observations. Reno, Nevada, April 1979.

U.S.D.A. Soil Conservation Service. Summary of Snow Course Unit Measurements for Colorado and New Mexico. Snow Survey SCS, Denver, Colorado.

Wymore, Ivan F., Dissertation: Water Requirements for Stabilization of Spent Shale. Colorado State University. August 1974. 137 pages.

Odegaard, H. A., 1979. Applications of Satellite Data for Snow Mapping in Norway. Presented at the Workshop on Operational Applications of Satellite Snowcover Observations. Reno Nevada, April 1979.